Deciphering tissue-specific signals and molecular mechanisms in control of T_H17 cells

Inaugural-Dissertation

to obtain the academic degree

Doctor rerum naturalium (Dr. rer. nat.)

submitted to the Department of Biology, Chemistry and Pharmacy

of Freie Universität Berlin

by

ANNA PASCUAL REGUANT, M.Sc.

from Manresa (Spain)

2016

March 2011 – March 2016

Supervised by Dr. Enric Esplugues / Prof. Dr. Anja Erika Hauser

Deutsches Rheuma-Forschungszentrum & Charité Universitätsmedizin

1rst Reviewer: Prof.Dr.Anja Erika Hauser

2nd Reviewer: Prof. Dr. Rupert Mutzel

Date of defense:18.07.2016

Acknowledgements

It is a pleasure for me to thank those who made this dissertation possible.

First of all, I am indebted to DRFZ and CCO, together with all the coworkers of both institutes, for creating a great working atmosphere and for providing help and support over the last five years.

I am heartily thankful to my former supervisor, Dr. Enric Esplugues, for giving me the possibility to start with him this exciting project and for encouraging me to develop passion and a proper understanding of the subject.

I owe my deepest gratitude to my current supervisor, Prof. Dr. Anja Erika Hauser, for her guidance and support during the last two years. This thesis would not have been done without her.

It is an honor for me to have Prof. Dr. Rupert Mutzel as a reviewer of my project and I am grateful to him for showing interest in my topic.

I would like to show my gratitude to my friends and former colleagues, Dr. Daniel Cirera-Salinas and Dr. Caterina Curato, for supporting me in a number of ways, for our fruitful discussions and for sharing with me amazing moments inside and outside the laboratory.

I cannot thank Dr. Jannike Bayat Sarmadi enough for our last two years working closely together and, especially, for challenging and enriching my ideas. I also want to thank Karo Pollock and Robert Günther for their precious help with the EAE experiments, as well as the rest of AG Hauser and AG Niesner, for the nice research atmosphere.

I will always be grateful to my parents and my sister for their unconditional love, for believing in me and for teaching me to be passionate and rigorous, which was essential for the completion of this project.

Lastly, my partner Adrian Leeland deserves a special mention for standing always by my side, for encouraging me to do my best and for pushing me forward, notwithstanding adversities and setbacks.

Directory

List of abbreviations

Ab	antibody
Ahr	aryl hydrocarbon receptor
APC	antigen-presenting cell
AP-1	activator protein 1
BSA	bovine serum albumin
CCL20	chemokine (C-C motif) ligand 20
CCR6	chemokine (C-C motif) receptor 6
CD3	cluster of differentiation 3
CD4	cluster of differentiation 4
CD11b	cluster of differentiation 11b (integrin alpha M, ITGAM)
CD45	cluster of differentiation 45 (protein tyrosine phosphatase receptor type C)
CD62L	L-selectin
CNS	central nervous system
Csf2	colony stimulating factor 2
CX_3CR1	CX_3C chemokine receptor 1
DCs	dendritic cells
EAE	Experimental Autoimmune Encephalomyelitis
EDTA	ethylenediaminetetraacetic acid
(e)GFP	enhanced green fluorescent protein
EpCAM	epithelial cell adhesion molecule
F4/80	EGF-like module-containing mucin-like hormone receptor-like 1
Fab	fragment antigen binding
FACS	fluorescence-activated cell sorting
Fc	fragment crystallizable
FcR	Fc-receptor
FCS	fetal calf serum
Fig	figure
Foxp3	forkhead box protein 3
FSC	forward scatter
GATA3	GATA binding protein 3
GM-CSF	granulocyte-macrophage colony stimulating factor
HBSS	Hanks' balanced salt solution
IBD	inflammatory bowel disease
IEC	intestinal epithelial cell
IEL	intraepithelial lymphocyte
IFN-γ	interferon γ
IHC	immunohistochemistry
Ikfz3	Ikaros family zinc finger protein 3
IL	interleukin
i.p.	intraperitoneal
Irf4	Interferon regulatory factor 4
i.v.	intravenous
LP	lamina propria
Ly6C	lymphocyte antigen 6C
MHC	major histocompatibility complex
MLN	mesenteric lymph node
MOG	myelin oligodendrocyte glycoprotein
mRNA	messenger ribonucleic acid
MS	Multiple Sclerosis

NaCL	sodium chloride
NK	natural killer (cell)
OSM	Oncostatin M
PBS	phosphate buffered saline
PECAM-1	platelet endothelial cell adhesion molecule-1
RA	rheumatoid arthritis
$RAG^{-/-}$	recombination activating gene
RFP	red fluorescent protein
RPMI	Roswell Park Memorial Institute (medium)
ROR-α	receptor-related orphan nuclear receptor α
ROR-γt	receptor-related orphan nuclear receptor γt
rT_H17	regulatory T helper 17
RT-PCR	reverse transcription polymerase chain reaction
SEM	standard error of the mean
SFB	segmented filamentous bacteria
SI	small intestine
SLOs	secondary lymphoid organs
SSC	sideward scatter
Tbx21	T-box 21
TCR	T cell receptor
T_H1/ T_H2/ T_H17	T helper 1/ 2/ 17 cell
TGFß	transforming growth factor ß
TNF-α	tumor necrosis factor α
Treg	regulatory T cell
U	Units
Wt	wild type

ZUSAMMENFASSUNG

T_H17-Zellen spielen eine große Rolle bei Entzündungen und sind in einigen Autoimmunerkrankungen involviert. Die Entzündungsreaktion im Gewebe ist eine protektive Antwort des Organismus auf Infektionen, kann allerdings, wenn sie fehlreguliert ist, auch zur Autoimmunität führen. Während einer Immunantwort ist der Austausch zwischen dem entzündlichen Gewebe und dem Immunsystem der Schlüssel, um die Gewebeintegrität zu erhalten und physiologische Prozesse aufrechtzuerhalten. Wie das inflammatorische Gewebe das Ausmaß der Immunreaktion durch die Kontrolle von proinflammatorischen T-Zellen reguliert, ist nicht genau charakterisiert. Zusätzlich sind einige Antigen-präsentierende Zellen (APCs) bekannt, die zum Rückgang einer Gewebeentzündung und zur Wiederherstellung der Homöostase durch deren Expression von antiinflammatorischen Mediatoren führen, und schließlich das Schicksal der T-Zellen beeinflussen. Hier konnten wir zeigen, dass intestinale Epithelzellen (IEC) die größte Quelle für das Alarmin Interleukin-33 (IL-33) nach einer T-Zell-abhängigen Inflammation ist und dass T_H17-Zellen den IL-33-Rezeptor (ST2) *in vivo* exprimieren. Daneben konnten wir zeigen, dass Monozyten, die die Lamina propria (LP) während des Rückgangs der Entzündung neu besiedeln, die Hauptquelle für Oncostatin (OSM) sind und dass T_H17-Zellen den OSM-Rezeptor (OSMRβ) exprimieren. IL-33 und OSM reduzieren beide die Expression von proinflammatorischen Genen (*Tbx21, Ifng* und *Csf2*) und induzieren die Expression des antiinflammatorischen Gens *Il10* in der Maus und in humanen T_H17-Zellen. *In vivo*-Experimente, die in *St2*$^{-/-}$-Mäusen durchgeführt wurden, zeigten, dass IL-33-Signale die proinflammatorischen Kapazitäten von T_H17-Zellen im Dünndarm nach akuter Entzündung limitieren, und somit den klinischen Verlauf positiv beeinflussen. Passend dazu zeigten *in vivo*-Experimente in Mäusen, in denen experimentelle autoimmune Enzephalomyelitis (EAE) induziert wurde, dass OSM auch die T_H17-Pathogenität eindämmt, und folglich die Schwere der Erkrankung reduziert. Schließlich zeigen wir, dass sich während der Antwort auf IL-33 und OSM proinflammatorische T_H17-Zellen entwickeln, die einen regulatorischen Phänotyp mit immunsuppressiven Eigenschaften aufweisen. Unsere Ergebnisse liefern neue Einblicke in den Mechanismus, wie IEC über die IL-33/ST-Achse und wie Monozyten über die OSM/OSMRβ-Achse proinflammatorische T_H17-Zellen im Dünndarm kontrollieren könnten, um die Homöostase aufrechtzuerhalten.

Abstract

T_H17 cells are major drivers of inflammation and are involved in several autoimmune diseases. Tissue inflammation is a beneficial host response to infection but, when deregulated, can also contribute to autoimmunity. The crosstalk between the inflamed tissue and the immune system during an inflammatory response is the key for preserving tissue integrity and to maintain physiological processes. However, how the inflamed tissue is able to regulate the magnitude of an immune response by controlling pro-inflammatory T cells is not well characterized. In addition, during the resolution of tissue inflammation several antigen presenting cells (APCs) with tolerogenic properties are known to further push the system back to homeostasis through the expression of anti-inflammatory mediators that ultimately influence T cell fate. Here, we show that intestinal epithelial cells (IEC) are the main source of the alarmin interleukin-33 (IL-33) upon T cell dependent intestinal inflammation and that T_H17 cells express the IL-33 receptor (ST2) *in vivo*. Also, we show that monocytes repopulating the lamina propria (LP) during the resolution of inflammation are the main source of Oncostatin (OSM) and that T_H17 cells express the OSM receptor (OSMRβ). Both IL-33 and OSM promote a reduced expression of pro-inflammatory genes (*Tbx21, Ifng* and *Csf2*) and induce the expression of the anti-inflammatory gene *Il10* in mouse and human T_H17 cells. *In vivo* experiments performed with *St2*$^{-/-}$ mice demonstrate that IL-33 signaling limits the pro-inflammatory capacity of T_H17 cells in the small intestine (SI) upon acute inflammation, thereby ameliorating the clinical course. Similarly, *in vivo* experiments performed with Experimental Autoimmune Encephalomyelitis (EAE)-induced mice demonstrate that OSM also restrains T_H17 pathogenicity, thereby attenuating disease severity. Finally, we show that pro-inflammatory T_H17 cells acquire a regulatory phenotype with immune-suppressive properties in response to both IL-33 and OSM. Our results provide new insights into the mechanisms by which IEC, via IL-33/ST2 axis, and monocytes, via OSM/OSMRβ axis, may control pro-inflammatory T_H17 cells in the small intestine in order to sustain homeostasis.

1 Introduction

1.1. T_H17 cells

1.1.1 Introduction

The adaptive immune system successfully fights against the distinct classes of existing pathogens by facilitating the differentiation of naïve $CD4^+$ T cells into distinct types of effector cells with particular immune functions*(1)*. Naive T cells recirculate through secondary lymphoid organs (SLOs) such as peripheral lymph nodes, spleen, and gut-associated lymphoid tissues in a strategy that maximizes their opportunity for antigen detection. However, upon activation, effector T cells couple differentiation with migration cues towards non-lymphoid tissues (preferential sites of infection for most pathogens) in order to coordinate function and localization and so contributing to infection control *(2)*. The migration of effector T cells from the circulation to specific tissue sites to exert their biological function relies on lymphocyte-endothelial recognition through adhesion molecules, as well as on different chemokine/chemokine receptor axis. Combinatorial association of chemokine and adhesion receptors allows for diversity of tissue and microenvironment-specific targeting *(3)*

Each effector T cell lineage is characterized by the expression of a specific master regulator, different surface markers and the production of a set of cytokines that confer them specific immune activities to protect the host. Following infection, innate immune cells that have encountered an antigen produce particular combinations of cytokines that, together with the triggering of the T cell receptor (TCR), promote the differentiation of naïve $CD4^+$ T cells *(4)*. Historically, naïve T cells were known to give rise to T_H1 cells to fight against intracellular bacteria and viruses or to T_H2 cells to fight against helminthes. While the first were characterized by the expression of the master regulator Tbx21 and the production of IFN-γ as a hallmark cytokine, the latter express GATA3 and produce IL-4, IL-5 and IL-13 *(5–7)*. Commitment to one of these lineages provides positive feedback to increase further differentiation of naïve cells to that lineage while inhibiting alternative commitment: Tbx21 and IFN-γ enforce their own expression (T_H1 development) at the same time that prevent T_H2 differentiation, and vice versa *(8, 9)*. However, each subset of T_H cells has not only been linked to protection against specific invading pathogens, but also to the development of different immune-related diseases. T_H1 cells are known to participate in organ-specific autoimmune disorders and chronic inflammatory pathologies, such as Crohn´s disease, sarcoidosis and atherosclerosis and T_H2 cells are involved in several allergic reactions *(10)*.

In an antagonistic way, suppression of immune responses and maintenance of peripheral tolerance was found to be provided by regulatory T cells (Tregs), characterized by the expression of the transcription factor Foxp3 *(11)*. Tregs are abundantly found in the periphery, particularly in the intestine *(12)*, where they exert suppressor functions. For that, Tregs require not only Foxp3 expression, but also cell-cell contact and secretion of IL-10 *(13)*, a potent anti-inflammatory cytokine with non-redundant roles in intestinal homeostasis. Treg differentiation from naive precursors depends on high concentrations of TGFβ, while Treg expansion depends on IL-2. Although Tregs play an important role in maintaining peripheral tolerance to self-antigens and in counteracting the inflammatory activity of effector T helper subsets, an excessive Treg suppression may facilitate tumorigenesis and can be used by pathogens to escape immune surveillance, thereby compromising the health of the host *(14)*.

1.1.2 Characteristics and functions of T_H17 cells

It was not until 2005 that the T_H17 lineage was described as a distinct subset of T helper cells *(15–17)*. T_H17 cells were characterized by the expression of the transcription factors ROR-γt and ROR-α and the production of IL-17A, IL-17F and IL-22, cytokines involved in neutrophilia, tissue remodeling and repair, and production of antimicrobial peptides *(18–20)*. As part of their differentiation program and linked to the expression of ROR-γt, T_H17 cells express the chemokine receptor CCR6 *(21)*. Its natural ligand is CCL20, a chemokine produced by inflamed tissues, thereby promoting attraction and recruitment of T_H17 cells to the inflammatory site *(22)*.

T_H17 cells are abundant at mucosal interfaces, where they contain infection with extracellular bacteria and fungi *(1, 23)* and confer coverage of some microbes that are not targeted in T_H1 or T_H2 responses, including *Mycobacterium tuberculosis*, *Bacterioides fragilis* and *Klebsiella pneumoniae (24)*. In the small intestinal lamina propria, T_H17 responses are particularly enriched and amplified by a specific priming microenvironment, composed of intestinal microbiota (a crucial component of which is *Segmented Filamentous Bacteria (25)*) and innate immune cells that guide the cytokine requirements for T_H17 development *(26–28)*. IL-6 was found to be essential for T_H17 differentiation, whereas IL-1β and IL-21 help to increase the efficiency of this process and IL-23, to further sustain T_H17-mediated effector functions and survival *(29–31)*. It is also remarkable that the role of TFGβ in T_H17 differentiation is dose-dependent: high doses of TGFβ suppress ROR-γt function through increasing Foxp3 and, thus, facilitating Treg development, while low doses of TGFβ cooperate with IL-6 to overcome Foxp3-mediated repression of ROR-γt in favor of T_H17 differentiation *(21, 32)*. Through their reciprocal development, T_H17 and Treg cells regulate the differentiation of one another to maintain

equilibrium, providing a mechanism to combine immune homeostasis and pathogen clearance at the intestinal mucosa, where the body has a permanent interplay with intestinal microbiota and potentially harmful pathogens *(1, 22)*. Moreover, the production of IFN-γ by T_H1, IL-4 by T_H2 cells and the Treg-expanding cytokine IL-2 has also been reported to restrain T_H17 cell commitment *(15)*.

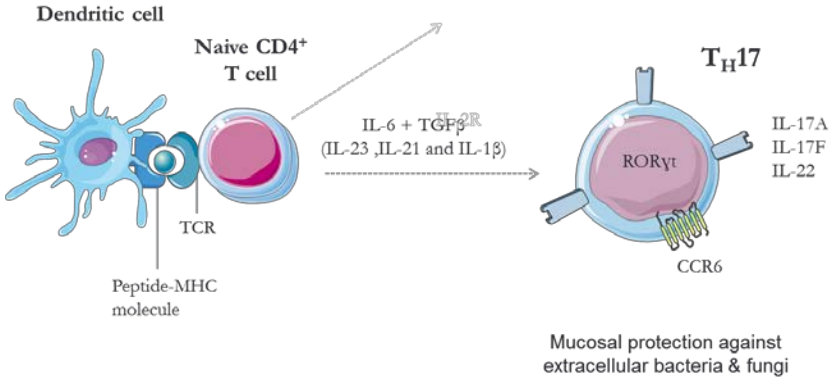

Schema 1. Characteristics and functions of T_H17 cells. T_H17 cells arise from naive lymphocytes that undergo functional differentiation upon encountering their cognate antigen displayed by activated APCs. T_H17 cells are characterized by the expression of ROR-γt as a master transcription factor, the chemokine receptor CCR6 that will guide their migration capacity and the production of IL-17A, IL-17F and IL-22, cytokines mediating granulopoiesis, neutrophil chemotaxis and production of anti-microbial peptides. Therefore, the role of T_H17 cells is the clearance of extracellular bacterial and fungal infections at mucosal barriers.

Similar to T_H1 and T_H2 subsets and despite the role of the T_H17 lineage in mucosal protection, these cells were also found to be highly pathogenic and essential for the establishment of tissue-specific inflammation *(17)*, becoming key drivers of several autoimmune disorders like multiple sclerosis (MS) *(33)*, rheumatoid arthritis (RA) *(34)*, psoriasis *(35)* and inflammatory bowel disease (IBD) *(36)*. Therefore, diverse clinical trials are currently focusing on targeting the T_H17 pro-inflammatory cell program and its signature genes *(37)*.

1.1.3 T_H17 cell plasticity

It was generally accepted that mature effector T cells showed a stable phenotype: once a $CD4^+$ T cell has committed to either the T_H1 or the T_H2 lineages, conversion to the other lineage doesn't occur *(22)*. This concept of a fixed phenotype and function was also initially applied to T_H17 cells, but it has been proven to be no longer valid. Recent studies provide strong evidence of a rather flexible and dynamic phenotype of the T_H17 subset, showing a high degree of functional plasticity that would allow these cells to shift to T_H1, T_H2 or Treg, depending on the prevailing environmental cues. In fact, an increasing body of data suggests that all $CD4^+$ T cell subsets may display remarkable plasticity *(13, 38, 39)*. This characteristic is thought to be

required to maintain immuno-competence after thymic involution in adulthood *(40)* and it would allow individuals to respond to environmental stimuli in a context-dependent manner *(13)*.

The existence of T_H17 cells capable of producing both IL-17A and IFN-γ (also expressing both ROR-γt and Tbx21 and named, therefore, T_H1/T_H17 cells) has been reported in patients with Crohn's disease (a form of IBD) *(41)*, type I diabetes mellitus*(42)* and arthritis *(43)*, where these IL-17A$^+$IFN-γ$^+$ double producing cells were shown to be highly pathogenic and to drive autoimmunity. IL-23 has been shown to induce this shift towards a T_H1/T_H17 phenotype *(44, 45)*. Moreover, in an inflammatory environment, they can further polarize to T_H1 cells through loss of ROR-γt and IL-17A expression and become main producers of IFN-γ together with the pro-inflammatory cytokine GM-CSF *(46)*. These pathogenic cells, also known as T_H1/exT_H17 cells, play an important role in the mouse model for MS, named experimental autoimmune encephalomyelitis (EAE) *(45)*, where they are also main producers of the pro-inflammatory cytokine TNF-α.

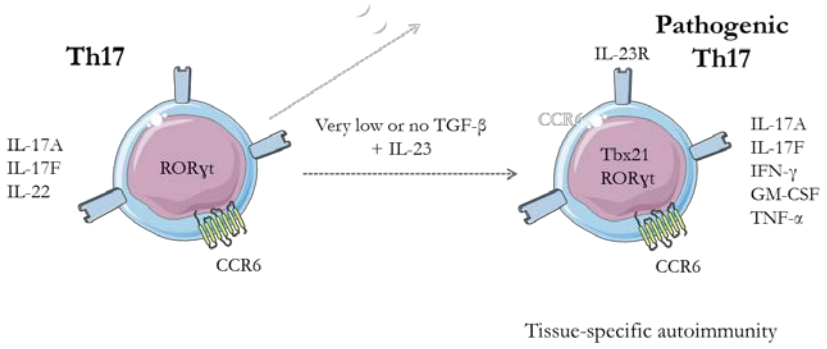

Schema 2. T_H17 cells shift to T_H1/T_H17 cells becoming highly pro-inflammatory and mediating autoimmune diseases. IL-17A$^+$IFN-γ$^+$ double producing cells may represent an intermediate state during T_H1 development from T_H17 precursors, in which Tbx21 and ROR-γt are co-expressed. T_H1/T_H17 cells have been associated with enhanced reactivity and pathological potential, promoting several autoimmune disorders.

On the other hand, T_H17 cells can go along a different path and switch into regulatory T cells that express the anti-inflammatory cytokine IL-10 independently of Foxp3, acquiring therefore regulatory functions both *in vitro* and *in vivo (47, 48)*. IL-10 itself, as part of a positive feedback loop, and TGFβ are two environmental cues known to induce this shift *(48, 49)*. IL-10$^+$ regulatory T cells generated from T_H17 cells are named regulatory T_H17 cells (rT_H17) in this study, as they express the master regulator ROR-γt in the absence of Foxp3 expression and still produce IL-17A. Interestingly, despite their differing functional properties, T_H17 cells and Tregs share common features. As previously mentioned, both populations are abundantly found in the intestine and share essential developmental cues, as both subsets are generated from naive T

cells under the influence of TGFβ and express high levels of aryl hydrocarbon receptor (Ahr), which integrates environmental stimuli consisting of both dietary and bacteria-produced ligands and promotes the induction of one or the other cell type in a ligand-specific fashion *(50)*. In fact, T_H17 and Tregs are not only present in a homeostatic balance, but they are even derived from a common precursor, since $Foxp3^+ROR\text{-}\gamma t^+$ double expressing cells exist during early T_H17 cell development *(13)* and have been found both in mice and humans *(51, 52)*. It is hypothesized that plasticity between Treg and T_H17 cells likely occurs in the context of dynamic changes in the intestinal inflammatory milieu: pro-inflammatory stimuli may promote conversion of immune-suppressive Tregs into pro-inflammatory T_H17 cells, while resolution of inflammation may trigger the alternate shift from pathogenic T_H17 to regulatory T cells *(53)*.

Given that T_H17 cells have emerged as a representative example of heterogeneous and flexible T lymphocytes, highlighting how cell plasticity plays a central role in keeping the balance between pathogenicity and tolerance *(54)*, it is of crucial importance to understand how the diverse functions of this T cell subset are regulated.

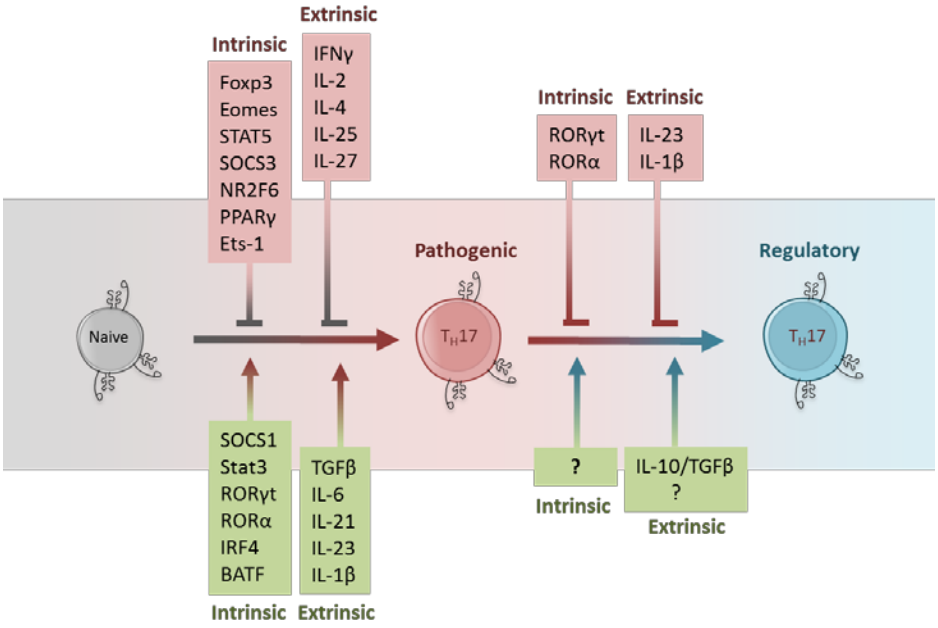

Schema 3. Factors controlling T_H17 cell plasticity. In the past few years, a lot of factors have been shown to positively or negatively regulate T_H17 cell development. Research has mainly focused on intrinsic and extrinsic signals controlling the development of pathogenic T_H17 cells, since these cells are key drivers of autoimmunity in several tissues. Cytokines that induce alternative T cell subsets, like IFN-γ, IL-2 and IL-4, as well as several transcription factors (Foxp3, STAT5, SOCS3, etc) effectively inhibit T_H17 development. On the contrary, cytokines like IL-1β and IL-23, and transcription factors like SOCS1 and ROR-γt, among others, are known to induce pathogenic T_H17 cells. However, very little is known about signals inducing the conversion from pathogenic to regulatory T_H17 cells.

1.1.4 Control of T_H17 cells occurs in the small intestine

T_H17 cells are particularly prevalent in the intestinal lamina propria. The gastrointestinal tract represents the largest surface area of the body that comes into direct contact with the external environment. Also, the intestine comprises the major single epithelial interface in the body, populated by the greatest number and diversity of resident microbes *(22)* that aids in digestion and markedly influences the development and function of the mucosal immune system *(55)*. The intestinal immune system, therefore, encounters more antigens than any other part of the body and it must discriminate between invasive pathogens and harmless antigens derived from food or commensal bacteria *(56)*. Thus, a fine-tuned regulation of the immune response is essential to protect the tissue from harmful cues, while keeping homeostasis to harmless antigens.

Key to the coexistence of commensal microbial communities and mucosal immune cells is the capacity to maintain the segregation between host and microorganism. The intestinal epithelium accomplishes this by forming a physical and biochemical barrier to commensal and pathogenic microorganisms. Furthermore, intestinal epithelial cells (IECs) can sense and respond to microbial stimuli to reinforce their barrier function and, more importantly, to participate in the coordination of appropriate immune responses, ranging from tolerance to inflammation *(55)*. Hence, IECs are considered immuno-competent cells that stablish a continuous dialogue with intestinal APCs and influence adaptive immune responses. At steady state conditions, IECs-derived TGFβ and retinoic acid, produced in response to commensal bacteria-derived signals, promote the development of DCs and macrophages with tolerogenic properties *(55)*. In that respect, $CD11c^+CD103^+$ DCs *(57)* and monocyte-derived CX_3CR1^+ macrophages *(58)* have risen special interest. The first act as migratory APCs that also imprint intestinal-homing properties on T cells in SLOs *(55)*. The latter are sessile, intestine-resident macrophages that have been shown to promote tolerance in the intestinal LP through the production of IL-10 and through the promotion of survival and local expansion of previously primed regulatory T cells *(55, 59)*.

Following priming by intestine-derived APCs in SLOs, T cells are recruited to the intestine, where they settle in the LP and become subject to the direct influence of IECs and resident APCs *(55)*. Depending on the signals received, LP T cells exert their regulatory or inflammatory effect on the local environment. Specialized T cells known as intraepithelial lymphocytes (IELs) also exist in close contact with the IEC layer and bidirectional interactions exist between the two in order to maintain intestinal barrier functions *(60)*. Because IELs contain granzyme granules with cytolytic activities, they are often described as cytotoxic cells *(61, 62)*.

In 2011 Esplugues *et al*. showed how pathogenic T_H17 cells are controlled in the small intestine (SI) in order to avoid exacerbated immune responses (Schema 4). By using a model of systemic tolerance induced by injections of CD3-specific antibody, they showed that the subsequent increase of IL-6 and TGFβ production by peripheral APCs led to the differentiation and proliferation of T_H17 cells in the periphery. These newly generated peripheral T_H17 cells expressed IL-17A, together with pro-inflammatory cytokines, such as TNF-α. The combination of IL-6 and TGF-β is indeed a well-known cytokine cocktail for the generation of T_H17 cells *(see section 1.1.2)* and the concentration of both cytokines occurred to be increased in the periphery upon anti-CD3 treatment. The secretion of IL-17A by newly generated T_H17 cells induced the expression of the chemokine CCL20 in IECs, facilitating therefore the migration of T_H17 cells specifically to the SI via the CCR6/CCL20 axis. As described in *section 1.1.2,* T_H17 cells express the chemokine receptor CCR6, which natural ligand is CCL20 and in line with that, CCR6-deficient mice failed to recruit T_H17 cells in the SI upon anti-CD3 treatment. Esplugues *et al* also demonstrated that once in the SI, T_H17 cells are controlled by two different mechanisms: they are eliminated via the intestinal lumen and, simultaneously, T_H17 cells remaining in the lamina propria acquire a regulatory phenotype, linked to their ability to produce IL-10. Interestingly, LP rT_H17 cells were shown to actively proliferate in the SI and were able to effectively suppress the proliferation of naive T cells *in vitro* and ameliorate the clinical course of EAE in adoptive transfer experiments, demonstrating their stable regulatory functions *in vivo (47–49)*. The acquisition of a suppressive phenotype by T_H17 cells is dependent on their recruitment to the SI, since splenic T_H17 cells of CCR6-deficient mice after anti-CD3 treatment, which are unable to migrate to the SI, showed a rather pro-inflammatory phenotype both *in vitro* and *in vivo*. The accumulation of T_H17 cells in the SI and the local acquisition of regulatory properties also occurred after influenza A viral infection (H1N1) and after intravenous (i.v.) injection of Staphylococcus aureus (used as a sepsis model). Hence, it was hypothesized to be a general mechanism to counteract most strong immune responses that result in T_H17 differentiation and T_H17-driven inflammation, which is beneficial in clearing infection, but immuno-pathogenic in excess.

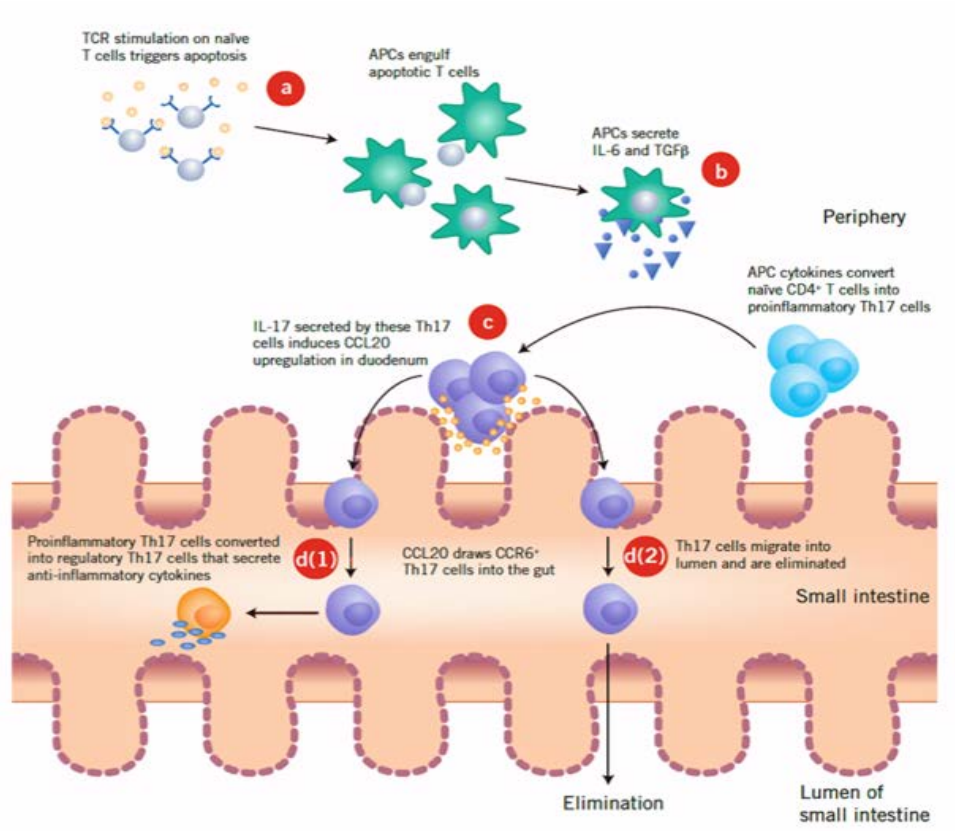

Schema 4. Control of T_H17 cells occurs in the SI. Upon strong and policlonal TCR activation that mimics antigen, naive T cells in the periphery undergo cell death. APCs encounter and phagocyte the apoptotic cells and start a massive but transient cytokine release, mainly composed of TGFβ and IL-6, a cytokine milieu that promote the generation of T_H17 cells. Because they secrete high amounts of IL-17A and other pro-inflammatory cytokines, they are described as pathogenic T_H17 cells. Via CCR6/CCL20 axis, T_H17 cells are recruited to the SI, where part of them are eliminated via feces while the ones that remain in the LP shift their phenotype: they down-regulate pro-inflammatory genes and express high amounts of IL-10, a potent-anti-inflammatory cytokine that confers these cells immune-suppressive functions (adapted from *(63)*).

Recently, it has also been reported that after respiratory influenza virus infection, IFN-γ producing, lung-derived $CD4^+$ T cells are recruited to the SI, where the number of pro-inflammatory T_H17 cells rapidly increases, inducing intestinal immune injury *(64)*. This study proofed why an infectious respiratory disease is often accompanied by gastroenteritis-like symptoms and, together with the work of Esplugues *et al.* and others, identified the SI as a major regulatory organ not only for local, but also for systemic immune function. It is the specific micro-environment found in the SI together with the expression of co-stimulatory molecules, which influence T cell plasticity and determine the outcome of T cell differentiation, the fine-tuned phenotype and the transcription and cytokine profile of intestinal $CD4^+$ T cells *(65, 66)*.

1.1.5 Anti-CD3 treatment as an *in vivo* model of tolerance that expands regulatory T_H17 cells in the SI.

The results from Esplugues *et al* mentioned above were obtained by the use of an antibody specific for mouse CD3, named 145-2C11, which was also used in many other experimental settings. The first mouse monoclonal antibody specific for human CD3, known as OKT3 (Ortho Biotech), was the first Food and Drug Administration approved monoclonal antibody for treatment in acute transplant rejection after kidney, heart or liver transplantation, back in the early 1980s *(67)*. It was engineered as a biological agent that efficiently promotes immune tolerance by targeting the functionally relevant receptor complex TCR-CD3 expressed by T cells, becoming the first successful tolerogenic therapy in humans.

Anti-CD3 treatment leads to two distinct phases in the subsequent immune response. The first phase covers the period of antibody administration (short-term effect or phase) in which reactive T cells disappear from the periphery. The second phase evolves after the end of the treatment (long-term effect or phase), leading to active immunological tolerance mediated by regulatory T cells. The short-term effect is due to the action of CD3-specific antibodies on T cells through three distinct non-mutually exclusive mechanisms: (1) antigenic modulation of the TCR–CD3 complex, followed by its internalization or shedding from the cell surface, (2) induction of apoptosis via activation-induced cell death that preferentially affects activated or auto-reactive T cells and/or (3) induction of anergy in T cells *(68)*. Preferential depletion of activated or auto-reactive T-cell in the periphery is thought to leave behind “space” for the homeostatic reconstitution that favors selective induction, survival and expansion of regulatory T cells, which establishes long-term tolerance *(68, 69) (see Schema 4).* Based on this, the anti-CD3 treatment appeared as a promising tool for the treatment of autoimmunity.

However, both OKT3 and 145-2C11 antibodies have unaltered Fc portions that can interact with Fc-receptors present on phagocytes and natural killer cells. This interaction occurs during the short-term phase of the anti-CD3 treatment and leads to a large-scale release of cytokines, mainly IL-6, IL-1β and TGFβ that causes strong side-effects and stems from the mitogenic capacity of CD3-specific antibodies *(67)*. The above-mentioned side-effects are known as the “flu-like” syndrome, which is characterized by fever, nausea, vomiting and diarrhea. These symptoms are linked to acute intestinal inflammation *(70–73)* and T-cell dependent small intestinal injury *(74)*. Esplugues *et al* also demonstrated that the acute intestinal inflammation observed upon anti-CD3 treatment was in fact dependent on the recruitment of T_H17 cells from the periphery to the duodenum via CCR6/CCL20 axis, as $CCR6^{-/-}$ mice not only failed to recruit T_H17 cells but did also not show signs of intestinal inflammation. Nevertheless, the cytokine

release is only transient and the syndrome, therefore, self-limiting. It resolves with the complete restoration of the tissue and systemic homeostasis *(75)* by the fifth day of treatment *(76)*, corresponding to the long-term phase.

Recently, new strategies meant to prevent or minimize unwanted side-effects, led to the design of humanized CD3-specific antibodies that were engineered to prevent binding to Fc-receptors, while retaining their full therapeutic activity. Anti-CD3 treatment based on non-FcR-binding antibodies is currently under clinical studies for treatment of autoimmune diseases such as type I diabetes (Otelixizumab and Teplizumab, in phase III clinical trials), ulcerative colitis and Crohn's disease (both Visilizumab).

Although non-FcR-binding antibodies have less severe side-effects, the antibody 145-2C11 is still being used as a treatment in mouse models for tissue-specific autoimmune diseases, such as type 1 diabetes *(77)*, rheumatoid arthritis *(78)* and lupus nephritis *(79)*. This antibody also has protective effects when administered during the course of EAE, since MOG-specific T_H17 cells are then recruited to the duodenum of the CD3-specific treated animals, preventing therefore the accumulation of these pro-inflammatory cells in the CNS *(47)*. In the present study, the 145-2C11 antibody was used according to Esplugues *et al*. as an *in vivo* model to induce systemic immune tolerance at the expense of an acute, transient and local SI inflammation that resolves together with the expansion of rT_H17 cells (Schema 5).

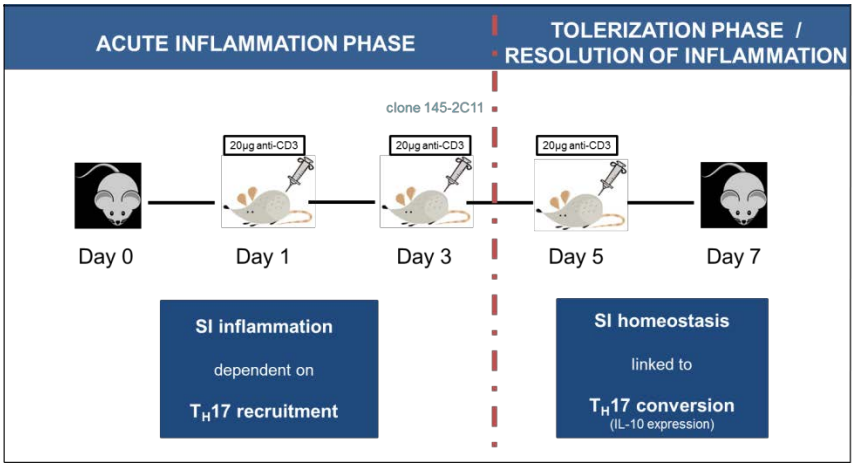

Schema 5. Anti-CD3 treatment as an *in vivo* model of tolerance that expands regulatory T_H17 cells in the SI. The administration regime of the anti-CD3 treatment is based on three injections of 20µg of CD3-specific monoclonal antibody (clone 145-2C11) every 48 hours. 4 hours after the first injection (day 1), pathogenic T_H17 cells start to accumulate in the LP and first signs of intestinal inflammation are observed. On day 5 the system goes back to homeostasis, tissue is completely restored and T_H17 cells gain the ability to produce IL-10, which confers these cells regulatory properties and suppressive functions both *in vitro* and *in vivo*.

Esplugues *et al*. showed how the SI controls overwhelming T_H17 responses. However, specific SI cell types and signals governing the conversion of pathogenic T_H17 cells towards a regulatory phenotype have not yet been fully understood. The fact that rT_H17 cells have only been found in the duodenum upon strong TCR activation, such as after anti-CD3 treatment, indicates that cellular and molecular changes occurring locally, in a tissue-specific manner, are in control of T_H17 pathogenicity. Hence, preliminary studies performed in the laboratory aimed to assess the differential gene expression profile of several immuno-competent cells in the SI and spleen (used as SLO), comparing both tissues upon anti-CD3 treatment and in homeostatic conditions. Among others, in this analysis two genes popped-up that drew our attention and that are subject of the present study: Interleukin-33 (IL-33) and Oncostatin (OSM).

1.2. IL-33

IL-33 is a member of the IL-1 cytokine family *(80)*, mainly expressed in the nuclei of endothelial and epithelial cells at mucosal interfaces *(81–83)*. It has dual roles, acting as a transcription factor in control of gene expression (intracellular IL-33) and acting as a cytokine when it is released (extracellular IL-33). Generally, IL-1 family members are considered as pro-inflammatory cytokines that locally orchestrate acute inflammatory processes. They have pleiotropic functions in innate responses and participate in shaping adaptive immunity by skewing the differentiation of naive T lymphocytes and by directly affecting the effector functions of different subsets *(84)*.

IL-33 is also known to function as an alarmin, a molecule indicating tissue damage upon injury or infection *(85, 86)*. Although it has been linked to various inflammatory and allergic processes and autoimmune diseases *(80, 87–89)*, recent studies have described the role of IL-33 in the regulation of tissue homeostasis, injury and repair, especially in the intestine *(90)*. The emerging picture is that IL-33 participates in maintaining barrier function by inhibiting gene expression in endothelial and epithelial cells in steady state. In parallel, nuclear IL-33 functions as a stored alarmin that is released when barriers are breached to coordinate immune defense and repair mechanisms, while initiating differentiation of T_H cells as the adaptive immune response is triggered *(84)*.

IL-33 signals through a receptor complex that consists of the subunit IL-1R4 (also named ST2) and the accessory protein IL-1R3 (also known as IL-1RAcP). In this study, IL-33 receptor will be referred as ST2. ST2 was found to be abundantly and constitutively expressed by mast cells and T_H2 cells under the control of GATA3; thereby contributing to the conception of IL-33 as cytokine that favors immune responses with a T_H2 bias. Accordingly, early studies stablished the role of

IL-33 in T_H2 development and diseases associated with type 2 responses, such as allergic asthma *(91)*. However, ST2 is also known to be expressed by multiple non-hematopoietic and hematopoietic cells, including epithelial and endothelial cells, fibroblasts, dendritic cells, innate lymphoid cells type 2, T_H1 cells and Tregs, among others. Interestingly, ST2 is not normally expressed in some of these cell types (this is the case for T_H1 cells), but reports exist showing that after stimulation a transient up-regulation of ST2 occurs and has important cellular functional implications *(87)*. Similarly, surface expression of ST2 is known to be subject to down-regulation rapidly upon IL-33 binding *(92)*.

The wide distribution of ST2 and the interplay between basal and induced expression of IL-33 and also of its receptor point to a key role of the IL-33/ST2 axis in both inflammation and homeostasis. A deeper knowledge of the tissue- and cell- specific mechanisms by which the IL-33/ST2 axis governs both processes in the intestine remains an important area for further exploration.

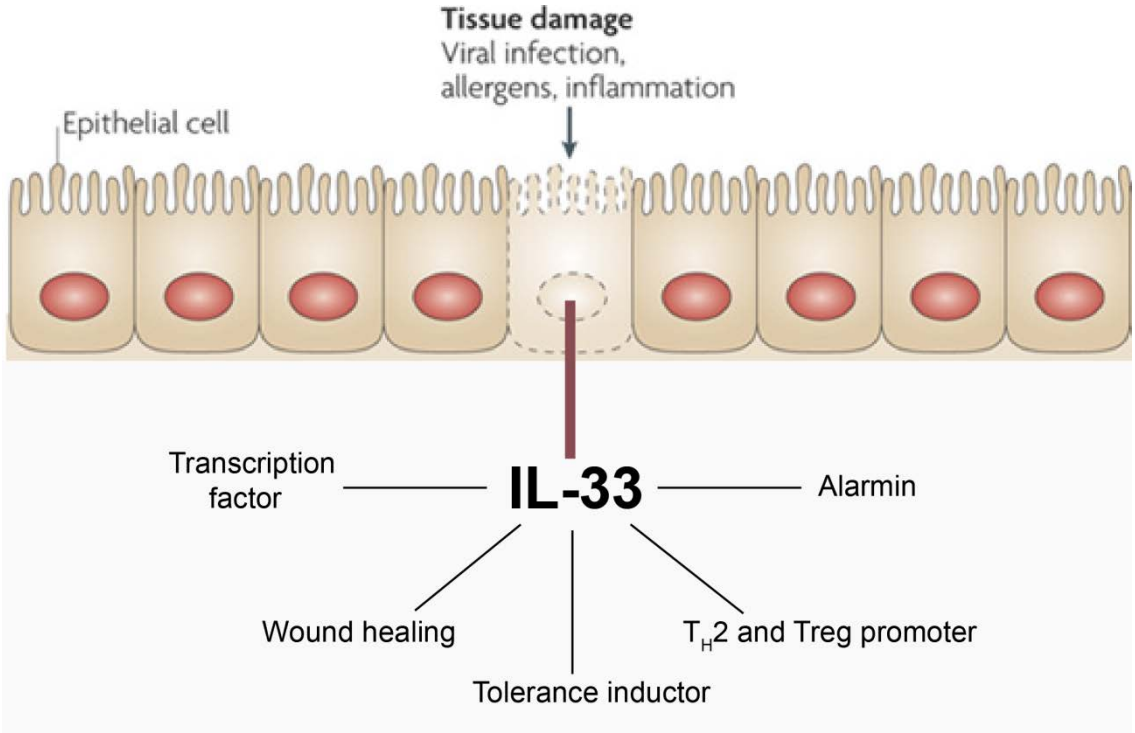

Schema 6. IL-33 in mucosal immunology. Origin and diverse functions of IL-33 in mucosal barriers, such us the lungs and the intestine. Adapted from *(84, 91, 93)*

1.3. OSM

OSM is a cytokine that belongs to the IL-6 (or gp130) family. It has pleiotropic functions in differentiation, cell proliferation, hematopoiesis and inflammation. Primary sources of OSM are activated monocytes and macrophages, although OSM production by DCs, neutrophils and T cells has also been described *(94)*. Generally, OSM systemic levels are low in chronic inflammatory conditions and levels at local sites of inflammation are more indicative of potential functions in chronic disease *(95)*. Although some studies argue for a pro-inflammatory role of OSM in autoimmune diseases such as psoriasis *(96)* and RA *(97)*, a greater body of evidence suggest that OSM is rather an anti-inflammatory meditator with potent effects on cytokine regulation. It has a range of anti-inflammatory properties *in vitro* that include the down-regulation of pro-inflammatory cytokines like GM-CSF, TNF-α and IL-8, the up-regulation of anti-inflammatory mediators and the decrease in the production of proteases, which directly contribute to tissue destruction *(98)*. OSM has also been shown to reduce inflammation in mouse models of RA, EAE *(99)* and colitis (a form of IBD) *(100)*, to promote intestinal barrier functions *(101)* and to attenuate acute inflammatory reactions *in vivo (102)*. Moreover, OSM has raised special interest among neuro-immunology researchers in the past few years and several neuroprotective roles have been attributed to this cytokine *(103–105)*. Thus, OSM has become nowadays a promising therapeutic candidate to limit CNS damage in MS, but not only that, a collective picture of OSM is emerging that suggests a natural role for the cytokine in the attenuation of the inflammatory response and in the wound healing process. However, little is known about the effects of this cytokine on T cells mediating tissue-specific inflammatory conditions.

1.4. Aims of this work

Esplugues *et al.* and others showed that after administration of the CD3-specific antibody 145-2C11, pathogenic or auto-reactive T_H17 cells from the periphery were recruited to the SI, where they were converted to IL-10-secreting, rT_H17 cells with *in vitro* and *in vivo* immune-suppressive functions *(47–49)*. However, cell types, signals and molecular mechanisms governing this conversion have not yet been fully elucidated. Because neither peripheral T_H17 nor SI T_H17 cells in steady state mice produce IL-10 or exert suppressive functions, it is hypothesized here that the specific micro-environment found in the SI during anti-CD3 treatment controls T_H17 cell plasticity in favor of a regulatory phenotype. The local tissue response upon injury and the tissue-specific accumulation of T_H17 cells makes of the anti-CD3 treatment a good model to study the interactions between an inflamed tissue and the subsequent modulation of the ongoing T-cell response.

In consideration of the evidence pointing to the intestine as a crucial immune organ, where tolerance is strictly and efficiently maintained to avoid unwanted immune responses to self-, dietary or flora antigens *(54, 106–108)*, it is of great interest to comprehend the tissue-specific mechanisms by which the SI is capable of inducing tolerance in T_H17 cells. Deciphering these mechanisms may help to develop new therapeutic strategies to control pathogenic T_H17 cells and, thus, help fighting prevalent autoimmune diseases, such us MS, RA, psoriasis and IBD.

Therefore, the aims of this study are:

1- **To identify tissue-specific signals and molecular mechanisms involved in the conversion from pathogenic T_H17 cells towards r T_H17 cells, occurring in the SI.**

2- **To identify the SI cellular sources of the above mentioned signals in control of T_H17 cells**

2 Materials and Methods

2.1 Buffers, media and reagents

Name	Ingredients	Source
PBS pH 7.2 (phosphate buffered saline)	137 mM NaCl	Merck
	2.7 mM KCl	Merck
	10 mM Na2HPO4	Merck
	2 mM KH2PO4	Merck
PBS/BSA pH 7.2 (bovine serum albumin)	PBS	
	0.5% (w/v) BSA	PAA Laboratories
PBS/BSA/EDTA pH 7.2 (ethylenediaminetetraacetic acid)	PBS	
	0.5% (w/v) BSA	PAA Laboratories
	2 mM EDTA	Sigma-Aldrich
Erythrocyte lysis buffer pH 7.3	H_20	
	0.83% (w/v) NH_4Cl	Sigma-Aldrich
	0.1 mM EDTA	Sigma-Aldrich
	10 mM $NaHCO_3$	Sigma-Aldrich
Digestion mix for preparation of intestinal single cell suspension	RPMI 1640 Medium	Life Technologies
	Collagenase type IV (100 U/ml)	Sigma-Aldrich
RPMI 1640 medium, serum-free		Life Technologies
RPMI 1640 medium with serum (preparation medium)	RPMI 1640 Medium	Life Technologies
	10% FCS (fetal calf serum)	Sigma-Aldrich
Fixation/permeabilization buffer (Foxp3 staining buffer kit)	Fixation/permeabilization diluent	eBioscience
	25% (v/v) Fixation/permeabilization concentrate	eBioscience
Washing buffer (Foxp3 staining buffer kit)	H_2O	
	10% (v/v) permeabilization buffer	eBioscience
1% formaldehyde solution	PBS	
	5% (v/v) of 20% formaldehyde solution	Science Services
Saccharose solution	PBS	Roth
	10%, 20% or 30% (w/v) saccharose	Roth
Washing and staining solution (histology)	PBS	
	1% (w/v) BSA	PAA Laboratories
	0.1% (v/v) Tween	Sigma-Aldrich
	(v/v) Triton-X 100 (optional, for nuclear stains)	Sigma-Aldrich
Blocking buffer (histology)	PBS	
	10% (v/v) rat serum	Sigma-Aldrich

Prolong Gold antifade reagent Invitrogen		Invitrogen
OCT Medium		Sakura
LP lymphocytes isolation buffer	Hanks' balanced salt solution (HBSS) without calcium and magnesium	Gibco
	5% (v/v) EDTA	Sigma-Aldrich
Anesthetics solution	0.9% sterile NaCl solution	B. Braun
	Ketamine (50 mg/ml)	Inresa Arzneimittel GmbH Freiburg
	Xylazin (Rompun, 20 mg/ml)	Bayer Healthcare
0.9% sterile NaCl solution		B. Braun
Rat serum		Sigma-Aldrich
Goat serum		Sigma-Aldrich
Rabbit serum		Sigma-Aldrich
Mouse serum		Sigma-Aldrich
Fetal calf serum (FCS)		Sigma-Aldrich
Ethanol (96%)		Roth
2-Methylbutan		Roth
Trizol reagent		Life Technologies
Percoll		GE Healthcare
Anti-Biotin MicroBeads		Miltenyi Biotec
CD4 (L3T4) MicroBeads		Miltenyi Biotec

Table 1**. Buffers, media and reagents**

Specificity	Clone	Conjugate	Source
CD3	145-2C11	-	DRFZ
CD44	IM7	APC	eBioscience
CD62L	MEL-14	FITC	eBioscience
CD25	PC61.5	PE	eBioscience
CD8a	53-6.7	biotin	Miltenyi Biotech
CD25	7D4	biotin	Miltenyi Biotech
CD28	37.51		Miltenyi Biotech
CD3	145.2C		Miltenyi Biotech
CD4	RM4-5	APC-eFluor 780 PE-Cy7	eBioscience
CD4	GK1.5	PE	BioLegend
CD3	145-2C11	Alexa Fluor 647, Digoxigenin	DRFZ
CD3	17A2	FITC, BV 650	BioLegend
TCRβ	H57-597	PE-Cy7	BioLegend
CD11c	N418	Alexa Fluor 647, Digoxigenin	DRFZ
CD11c	N418	BV 650	BioLegend

CD11b	M1/70	Pacific Blue	BioLegend
MHCII	M5/114.15.2	PE	DRFZ
MHCII	M5/114.15.2	PE-Cy7	eBioscience
Ly6C	HK1.4	PE-Cy7	eBioscience
CD45.2	104	BV 785 APC	BioLegend eBioscience
CD45.1	A20	PE	eBioscience
CD45	30-F11	V450	BD Biosciences
EpCAM	G8.8	Alexa Fluor 488	BioLegend
EpCAM	G8.8	PerCP-eFluor 710	eBioscience
PECAM-1	MEC13.3	Alexa Fluor 647	BioLegend
Ror-γt	B2D	PerCP-eFluor 710	eBioscience
Ror-γt	104	PE	BD Biosciences
T-bet	4B10	Pacific Blue	Biolegend
Foxp3	FJK-16s	FITC	eBioscience
IL-17A	TC11-18H10.1	FITC	Biolegend
IFN-γ	XMG1.2	Pacific Blue	EBioscience DRFZ
TNFα	MP6-XT22	PerCP	Biolegend
CCR6	11A9	PE	BD Biosciences
CCR4	1G1	PE	BD Biosciences
CXCR3	1C6/CXCR3	APC	BD Biosciences
CD45RA	HI100	FITC	BD Biosciences
CD25	B1.49.9	FITC	Immunotech
CD8	B9.11	PC5	Immunotech
IL-33	polyclonal	Alexa Fluor 594	R&D Systems, labeled with APEX-Kit (Invitrogen)
GFP	polyclonal	Alexa Fluor 488	Rockland, labeled at DRFZ
FcgRII/III	2.4G2	-	DRFZ
IL-4	11B11		DRFZ

Table 2**. Primary antibodies**

Specificity	Clone	Host species/ isotype	Conjugate	Source
Digoxigenin	polyclonal	Sheep,Fab-fragments	Alexa Fluor 647, Alexa Fluor 594	DRFZ
hamster IgG	polyclonal	goat, IgG	-	BioLegend

Table 3**. Secondary antibodies**

Reagent	Source
Fixable viability dye eFluor 780	eBioscience
CFSE	eBioscience
DAPI	DRFZ
Hoechst	eBioscience

Table 4**. Viability dyes and other fluorescent dyes**

Name	Source
IL-6	R&D Systems
IL-2	R&D Systems
TGF-β1	R&D Systems
OSM	R&D Systems
IL-33	R&D Systems

Table 5**. Cytokines**

2.2 Mice

Wild-type C57BL/6 and congenic B6.SJL-*Cd45.1* mice were purchased from Charles River. *St2*$^{-/-}$ mice *(109)* and IL17A-eGFPxFoxp3-mRFP reporter mice *(47)* on a C57BL/6 background were bred and housed under specific pathogen-free conditions in the animal facility of the Charité with a 12 h light–dark cycle. Mice were age and sex-matched and 8-12 weeks old when used in experiments. The mice had free access to food and water. Protocols for animal experiments were approved in accordance with institutional, state and federal guidelines (Landesamt Für Gesundheit und Soziales, Berlin, Germany).

2.3 Induction of EAE

IL17A-eGFPxFoxp3-mRFP reporter female mice, aged 8-10 weeks, were immunized subcutaneously in the base of the tail with 250 µg MOG_{35-55} peptide in CFA and 400 ng pertussis toxin in PBS was administered i.p. on day 0 and day 2. The mice were randomized in two groups: the OSM-treated group received 10 µg of OSM in PBS / day at days 7 to 12 and the control group received vehicle alone for the same period of time. The mice were weighed daily and scored for clinical signs of EAE until they were euthanized (day 21 post-immunization).

Clinical disease was scored in a blinded fashion as follows:

Score	Description
0	No signs of impairment
1	Complete tail paralysis
1,5	Complete tail paralysis Righting reflex impaired
2	Complete tail paralysis Righting reflex impaired Weak paralysis hint legs
3	Complete tail paralysis Righting reflex impaired Complete paralysis hint legs
4	Complete tail paralysis Righting reflex impaired Complete paralysis hint legs Complete paralysis front legs
5	Moribund

Table 6. Clinical scores for EAE

2.4 *In vivo* T cell stimulation and intestinal lymphocyte isolation

Mice were injected with anti-CD3 antibodies (20 µg) i.p. 1–3 times at an interval of 2 days between injections and sacrificed 4 hours (or 24 hours, where indicated) after the final injection. For the controls, isotype control or PBS was injected. LP intestinal lymphocytes were isolated as described in *(47)* with minor modifications. In brief, small intestines were removed, opened longitudinally and then cut into strips 1 cm in length. Tissues were washed twice in PBS and incubated with Hank's Buffered Saline (5% FCS) in the presence of 2 mM of EDTA at 37ºC for 30 min on a shaker to release intraepithelial lymphocytes. The remaining tissues were further digested with complete RPMI medium supplemented with 100 U/ml of collagenase type IV at 37ºC for 30-40 min on a shaker. The LP cells were then layered on a Percoll gradient and the lymphocyte enriched population was recovered after centrifugation (400 *g*, 20 min) at the 40/75% interface.

2.5 Cell counts

To determine absolute numbers of intestinal or CNS T cells for an individual mouse, viable $CD45^+$ cells were counted in a defined volume of the respective sample using the MACSQuant analyzer cytometer and the resulting cell counts were then used to calculate absolute numbers for the total volume of the sample. Also, the frequency of the subset of interest amongst viable $CD45^+$ cells was measured by flow cytometry and this frequency was then used to calculate the absolute cell number of this subset from total viable $CD45^+$ cells.

2.6 Intracellular cytokine staining

In order to stain T cells from spleen and small intestine of IL17A-EGFPxFoxp3-RFP reporter mice before and after CD3-specific antibody treatment, SI cell suspension were obtained as described above and smashed and filtered splenocytes were incubated with erythrocyte lysis buffer (ACK). Single cell suspensions were then incubated with an FC-blocking antibody to prevent non-specific binding and stained with anti-CD45-Pacific Blue, anti-CD4-BV785, anti-TCRβ-PECy7 anti-CCR6-BV605, Live-dead-eF780 and anti-ST2 conjugated to digoxigenin. A second incubation with anti-DIG-PE, followed by two rounds of Faser kit-PE according to manufacturers' protocol was performed. For cytokine detection, cells were re-stimulated with PMA (5 ng/ml) and Ionomycin (500 ng/ml) for 5 h with addition of Brefeldin A and Monensin (5 µg/ml) at 30 min, followed by fixation in 2% formaldehyde. Intracellular staining was performed in PBS/0.2% BSA containing 0.05% saponin with anti-IL-17A-FITC anti- IFN-γ-Pacific Blue and anti-TNFα-PerCP T-bet, Roryt, c-maf and Foxp3 protein amounts were analyzed using the Foxp3 staining buffer set according to the manufacturer's instructions. Briefly, cells were stained with antibodies against CD4 and CD45.2 and then fixed with Fixation/Permeabilization buffer, followed by intracellular staining with Pacific Blue-conjugated anti–T-bet, PE–conjugated anti–Rorγt and FITC-conjugated anti-FoxP3 in permeabilization buffer. The following antibodies were used for FACS sorting of human PBMC: anti-CCR6-PE or biotinylated anti-CCR6 followed by streptavidin-Pacific blue, anti-CCR4-PE, anti-CXCR3-APC, anti-CD45RA-FITC, anti-CD25-FITC, anti-CD8-PC5.

2.7 Flow cytometry and FACS sorting

Mouse peripheral T cells were obtained from spleen and lymph nodes of 8- to 12-week old mice and $CD4^+CD62L^+CD25^-CD44^-$ T cells (naïve T cells) were sorted by FACSAria II (BD). Human $CCR6^+CCR4^+CXCR3^-CD45RA^-CD25^-CD8^-$ T_H17 cells were sorted according to *(110)*. Single cell suspensions were analyzed on a Becton Dickinson Fortessa or LSRII and data analyzed with FlowJo software (Tree Star).

2.8 Histopathology

Small intestines were removed and fixed immediately in 10% neutral-buffered formalin in PBS for >24 h, embedded in paraffin and cut into 5-7µm sections. The sections were deparaffinized and stained with hematoxylin and eosin (H&E) to determine histological changes. Tissues were graded semi-quantitatively from 0 to 5 in a blinded fashion as described *(111)*:

Score	Description
0	No changes observed
1	minimal scattered mucosal inflammatory cell infiltrates
2	mild scattered to diffuse inflammatory cell infiltrates, sometimes extending into the submucosa and associated with erosions
3	moderate inflammatory cell infiltrates that were sometimes transmural, often associated with ulceration, with moderate epithelial hyperplasia and mucin depletion
4	marked inflammatory cell infiltrates that were often transmural and associated with ulceration, with marked epithelial hyperplasia and mucin depletion
5	marked transmural inflammation with severe ulceration and loss of intestinal glands

Table 7. Clinical scores for intestinal inflammation

2.9 Immunofluorescence microscopy

Small intestines and spleen were removed from wild type or IL17A-EGFPxFoxp3-RFP reporter mice before and after CD3-specific antibody treatment *in vivo*. Tissues were fixed in 1% paraformaldehyde (PFA) at 4°C over night. Subsequently PFA was replaced with 30% sucrose solution and incubated at 4°C for 6-8 hours. After that, samples were washed and placed in oct filled cryomolds. For freezing, the cryomolds were placed in chamber filled with 2-methylbutane, which was subsequently placed in dry ice submerged with ethanol. After freezing, the samples were stored at -80ºC. Cryosections were cut at 7 mm on a Leica CM1850 freezing microtome, transferred onto Superfrost Plus Gold slides (Fisher Scientific) and air dried. For immunohistological staining, sections were surrounded with a PAP pen (Zymed Laboratories) and submerged with PBS for 20 min. After that, sections were blocked for 20 min at room temperature with 10% rat serum in PBS. For immunofluorescent staining, antibodies were diluted in staining buffer and incubated at room temperature for 60 min. The following antibodies were used for staining: anti-CD11c-Alexa Fluor 64), anti-PECAM-Alexa Fluor 647, anti-IL-33-Alexa Fluor 59), anti-EpCAM-Alexa-48), Hoechst 33342 or DAPI (as indicated) and anti-GFP-Alexa-48). Nuclear stains were added after washing once with PBS for 5 min and incubated for 10 minutes at room temperature. After staining, samples were washed 3 times by immersing in PBS for 5 minutes and mounted with ProLong gold mounting medium. Sections were analyzed by confocal microscopy using a Zeiss LSM 710 microscope with 20x/0.5 NA (air) objective at room temperature.

2.10 T_H17 differentiation *in vitro*

Splenocytes from wild-type C57BL/6 mice were incubated with CD4-microbeads and then positively selected through LS columns (Miltenyi Biotec). After enrichment, naive cells ($CD4^+CD25^-CD62L^{hi}CD44^{low}$) were FACS-sorted as mentioned above. $CD4^+$ naive T cells were

cultured for 5 days at 10^6 cells/ml with plate bound anti-CD3 (3 µg/ml) and soluble anti-CD28 (2 µg/ml) in RPMI Media 1640 supplemented with 10% Fetal Calf Serum, 2 mM L-glutamine, 100 U/ml penicillin, 100µg/ml streptomycin, 5 mM 2-β-mercaptoethanol under T_H17 conditions: TGF-β (2 ng/ml) and IL-6 (25 ng/ml). Neutralizing anti-IFN-ɣ and anti-IL-4 were each used at 5 µg/ml. Where indicated, IL-33 (20ng/ml) was added to the culture.

For the human cultures, healthy leukapheresis blood and buffy coats were randomly obtained from the Charité Blood Bank and Deutsches Rotes Kreuz (DRK). Ethics approval was obtained from the Institutional Review Board of the Charité-Universitätsmedizin Berlin, Germany (EA1/221/11, EA1/293/12). All work was carried out in accordance with the Declaration of Helsinki for experiments involving humans. Human peripheral blood mononuclear cells (PBMC) were isolated using Ficoll-Paque Plus (GE Healthcare) and T cells were isolated with CD4 microbeads (Miltenyi Biotech), followed by the above mentioned sorting strategy.

2.11 Suppression assay

CFSE (5µg/ml) labeled $CD4^+CD25^-$ T cells (responder cells) were cultured in 96-well round bottom plates at $2x10^4$ or $1x10^4$cells/well with $8x10^5$ irradiated APCs (splenocytes MACS depleted for $CD4^+$, $CD8^+$ and $CD25^+$ T cells) as feeder cells in the presence of $2x10^4$ cells/well of FACS sorted $CD4^+$IL-17A$^-$Foxp3$^+$ (Tregs) or $CD4^+$IL-17A$^+$Foxp3$^-$ T cells (T_H17), previously cultured for 4 days in the presence or absence of IL-33 (20ng/ml). Cell cultures were stimulated with 0,1 µg/ml of anti-CD3 antibody. After 4 days, cells were harvested, stained and the CFSE signal was analyzed by flow cytometry.

2.12 RT-PCR

Mouse tissues were withdrawn immediately after sacrifice and washed in ice-cold Hank´s balanced solution prior to the addition of 1ml of Trizol. Samples were flash-frozen in liquid nitrogen and stored at -80°C. RNA was extracted according to the manufacturers' protocol (Rneasy, Qiagen) and its concentration and integrity were measured using NanoDrop 2000 (Thermo Scientific). Complementary DNA was synthesized from 1µg RNA using Taqman RT reagents (Applied Biosystems), following the manufacturers protocol. Quantitative real-time PCR was performed in triplicate using TaqMan Gene Expression Assays (Applied Biosystems) for the respective genes on StepOnePlus Real-Time PCR System (Applied Biosystems). mRNA levels were normalized to HPRT as a housekeeping gene for mouse samples and to GAPDH for human samples and differences were calculated using the $2^{\Delta Ct}$ method.

2.13 Gene expression analysis

Total RNA extracted (100 ng; RNeasy, Qiagen) from intestinal $CD45^-$ cells from CD3-specific antibody-treated or untreated animals and total RNA extracted from splenic and intestinal $CD11b^+$ cells from CD3-specific antibody-treated mice were used to perform a genome-wide transcriptional profiling assay (GeneChip Mouse 2.0 ST Array, Affymetrix). Data was analysed with GeneSpring GX 11 (Agilent Technologies).

2.14 Statistical analysis

Where appropriate, Student's *t*-test was used. For the comparison of more than two groups a one-way ANOVA followed by Bonferroni multiple comparison test was performed. All statistical analysis was calculated in Prism (GraphPad). Differences were considered to be statistically significant when $P < 0.05$.

3 Results

3.1 IL-33 in control of T_H17 cells

3.1.1 Epithelial cells in the proximal part of the SI are the major source of the alarmin IL-33 upon anti-CD3 treatment

As previously mentioned in section 1.1.5 and in order to identify tissue-derived signals involved in the control of pathogenic T_H17 cells occurring in the SI upon anti-CD3 treatment, we performed a gene expression analysis of non-hematopoietic cells. Briefly, we compared the SI $CD45^-$ fraction (non-hematopoietic cells) of mice injected with CD3 specific antibody against the SI $CD45^-$ population of untreated mice (steady state). The results of the microarray showed a significant up-regulation of *Il33*, among others, in $CD45^-$ cells from the inflamed SI of anti-CD3 treated mice compared to the SI of steady state animals (Fig. 1A). Because IL-33 is an alarmin reported to play a crucial role in mucosal immunity and intestinal homeostasis *(112–114)* it was considered as a candidate for further analysis. To confirm the transcriptome data, mRNA levels of *Il33* were analyzed by RT-PCR. The results also showed a significant up-regulation of *Il33* in the $CD45^-$-cell fraction isolated from CD3-specific antibody treated animals compared to non-immunocompetent cells from untreated mice (Fig. 1B).

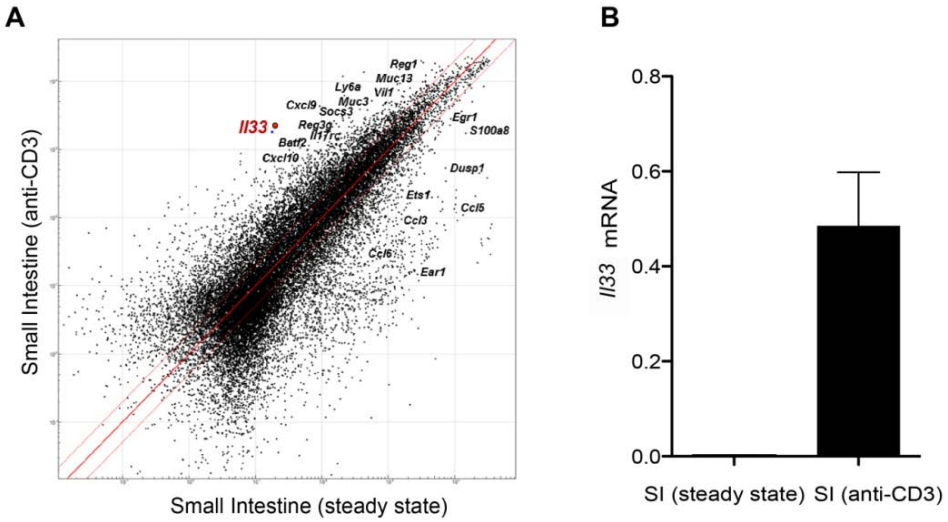

Figure 1. Il33 is highly expressed in non-hematopoietic cells from the SI of anti-CD3 treated mice. C57BL/6 mice were injected i.p. with 20µg anti-CD3. (A) Gene expression analysis comparing non-hematopoietic cells ($CD45^{neg}$) isolated from the SI of CD3-specific antibody treated and control mice. (B) Il33 mRNA expression after anti-CD3 treatment (mean ± S.E.M..; n=4).. Data are representative of at least two independent experiments.

Once we determined that *Il33* was induced by anti-CD3 treatment in SI non-hematopoietic cells, we wanted to investigate the specific cellular source of the alarmin. It has been previously described that epithelial and endothelial cells at mucosal barriers are the main producers of IL-33 *(115, 116)*. To confirm these sources in our experimental model, immunofluorescence staining of tissue sections from steady state mice and from anti-CD3 treated animals was performed in collaboration with Dr. Bayat Sarmadi from our group (Fig. 2A). The tissues under study were the duodenum, as the proximal part of the SI, and the spleen and mesenteric lymph nodes (MLN), as peripheral lymphoid tissues. IL-33 expression in the duodenum of steady state mice was only detected in some isolated; rare cells, positive for the endothelial marker PECAM-1. IL-33^{+}PECAM-1^{+} cells were located in the LP; specifically in the basis of the villi, around the crypt. Although upon CD3-specific antibody injection, a weak IL-33 staining could still be observed in some isolated PECAM-1^{+} endothelial cells in the same region, a bright IL-33 staining was also extensively detected in cells positive for the epithelial cell marker EpCAM, in the apical part of the villi. Histological analysis in peripheral lymphoid tissues (Fig. 2B) revealed lower levels of IL-33, especially in the spleen, where IL-33 staining was very weak, almost non-detectable. In both tissues, IL-33 was found in or attached to CD45^{+}, PECAM-1^{+} or fibronectin^{+} structures, indicating that IL-33 in this tissues may come from a quite heterogeneous population, including lymphocytes, endothelial cells and stromal cells. But more importantly, in both spleen and MLN, no significant differences on IL-33 expression were found upon treatment, neither in signal intensity nor in specific cellular localization.

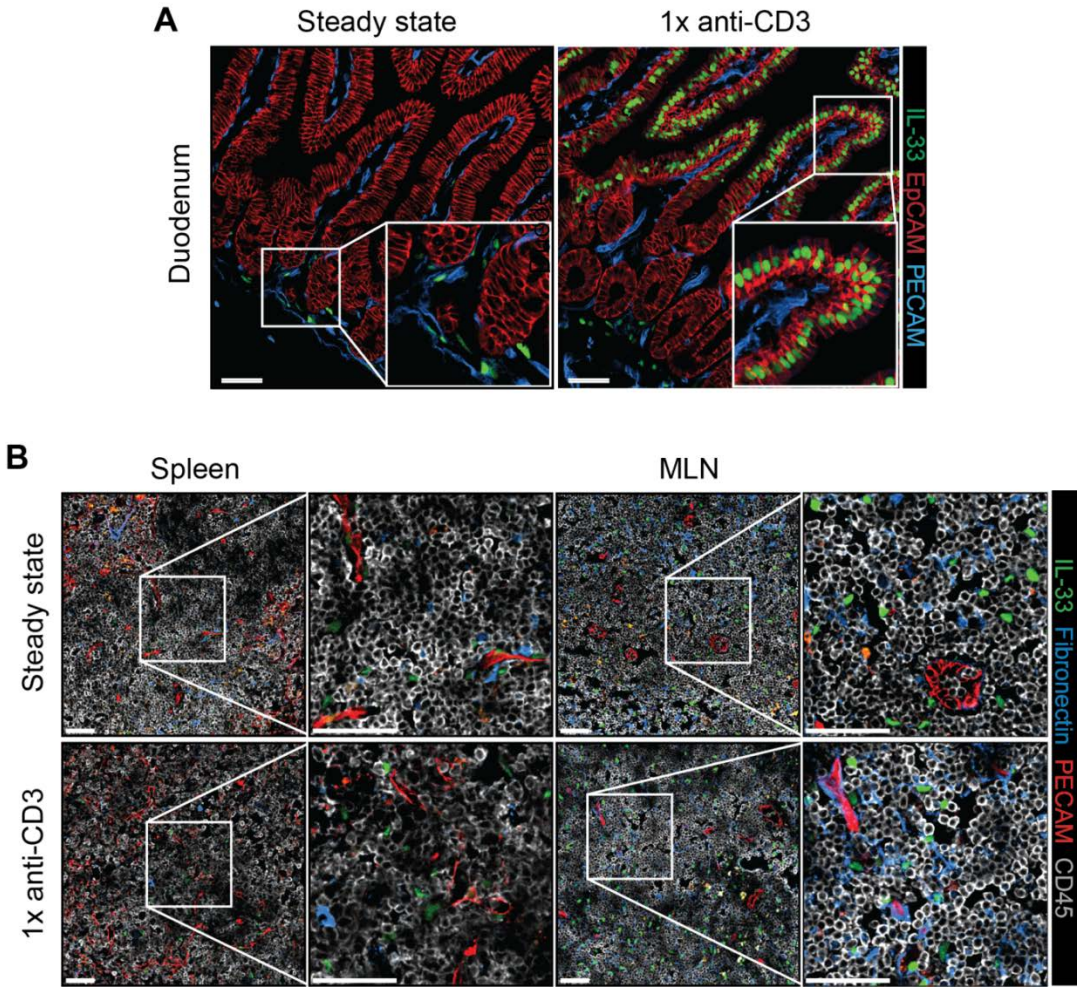

Figure 2. IL-33 production is drastically increased in IECs upon anti-CD3 injection. C57BL/6 mice were injected i.p. with 20µg anti-CD3 and after four hours, the duodenum and the spleen and mesenteric lymph nodes (control tissues) were isolated. (A) Histological analysis of IL-33 (green), EpCAM (red) and PECAM (blue) in the duodenum is shown at steady state and after injection of anti-CD3 antibody. (B) Histological analysis of IL-33 (green), Fibronectin (blue), PECAM (red) and CD45 (white) in the spleen and mesenteric lymph nodes is shown in steady state mice and upon anti-CD3 injection. Scale bar = 50µm. In collaboration with Dr. Bayat Sarmadi.

These results suggest that IL-33 is a local, tissue-specific signal induced in the SI upon anti-CD3 treatment and show that endothelial cells represent the basal source of IL-33 in homeostatic conditions, while IECs represent the major source of the alarmin IL-33 upon T-cell dependent inflammation.

To further analyze the spatial and temporal distribution of IL-33 expression in the distinct parts of the intestine (duodenum, jejunum, ileum and colon), IL17A-eGFPxFoxp3-mRFP double reporter mice were injected intraperitoneally (i.p.) with CD3-specific antibody on days 1, 3 and 5 and the tissues were analyzed 4h after each injection and compared to steady state conditions. The time-course analysis of the *Il33* transcript (Fig. 3A) showed that *Il33* expression levels were 450-fold up-regulated right after the first injection with CD3-specific antibody (day 1), decreasing rapidly afterwards. *Il33* expression was mainly restricted to the

duodenum and, to a lesser extent, to the jejunum. By immunofluorescence microscopy performed in collaboration with Dr. Bayat-Sarmadi, the spatial distribution of IL-33^{+} IECs along the intestine of anti-CD3 treated mice was visualized and the results of the gene expression analysis were confirmed (Fig 3.B). IL-33 was strongly induced in IECs in the proximal part of the SI upon anti-CD3 treatment, decreasing towards the distal parts in a gradient-like fashion. Few IL-33^{+} IECs were found in the ileum and non in the colon.

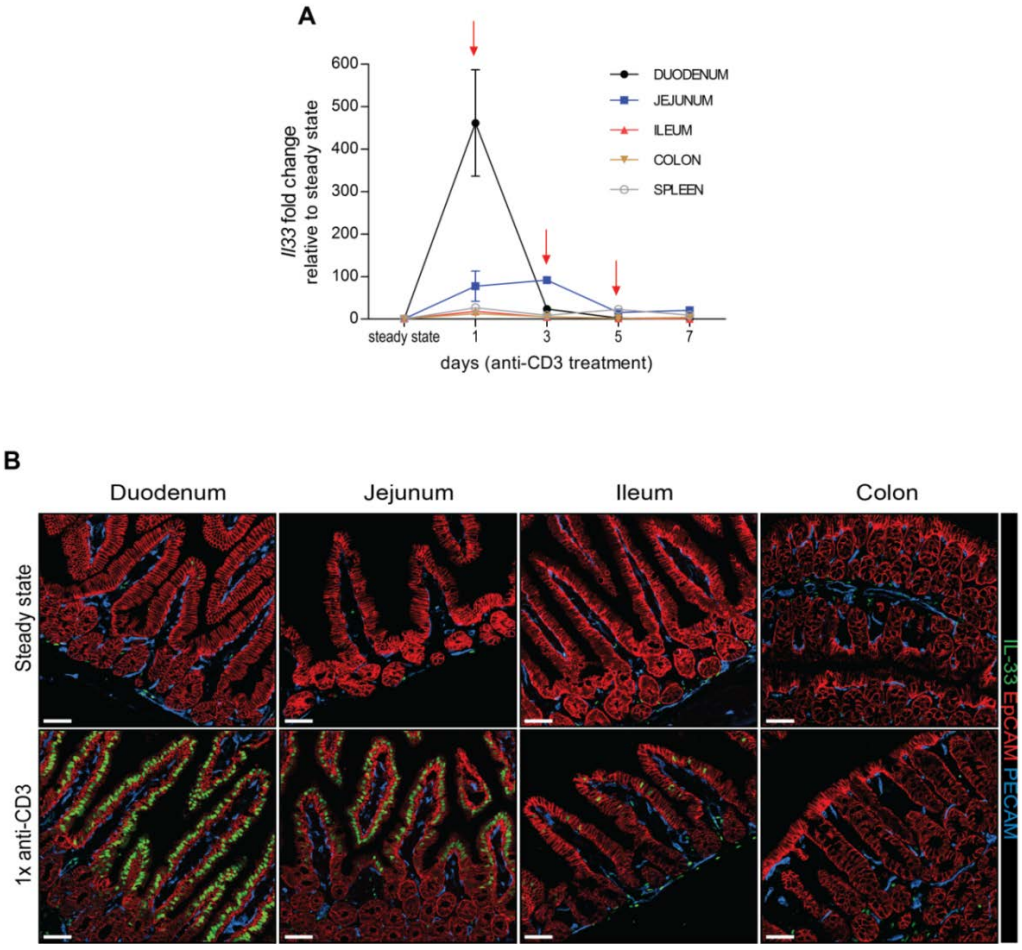

Figure 3. IL-33 expression is mainly restricted to the duodenum and decreases in a gradient-like fashion towards the distal parts of the SI. C57BL/6 mice were injected i.p. with 20µg anti-CD3 at day 1, 3 and 5. Four hours after each injection, the different parts of the intestine were isolated, as well as the spleen (control tissue). (A) Quantitative PCR analysis (qPCR) of Il33 mRNA was performed for each tissue at every time-point. Red arrows indicate anti-CD3 injections. Data are presented as mean ± S.E.M. and normalized to the values in steady state. (B) Immunohistochemistry (IHC) analysis of IL-33 (green), EpCAM (red) and PECAM (blue) localization in the different parts of the SI in steady state and during anti-CD3 treatment. Data are representative of ≥ 3 independent experiments (n=4animals/group). Scale bar = 50µm. Immunohistochemistry performed in collaboration with Dr. Bayat-Sarmadi.

Next, we wanted to explore in depth the kinetics of *Il33* specifically in the duodenum, where its highest levels were observed. Thus, the tissue was analyzed at 4h and 24h after each injection (days 1-7). Indeed, the peak of *Il33* was again observed 4 hours after the first injection (day 1), after which the levels decreased to a value six-fold less (Fig. 4A). However,

the *Il33* transcript was up-regulated within 4h after every additional injection (day 3 and 5), but only reaching a two-fold value. The acute and time-limited expression of *Il33* in the inflamed SI supported and emphasized its role as alarmin. The kinetics of IL-33 was also confirmed by immunofluorescence staining of duodenal sections (Fig. 4B), in which IL-33 expression was highly induced in IECs 4h after each CD3-specific antibody injection (days 1, 3 and 5). The histological analysis of the duodenum also showed that, upon anti-CD3 treatment, IECs-derived IL-33 expression was concurrent to the recruitment of T_H17 cells in the LP (Fig. 4B) and these observations were determinant to further investigate whether IL-33 could have an effect on the T_H17 cells accumulating there.

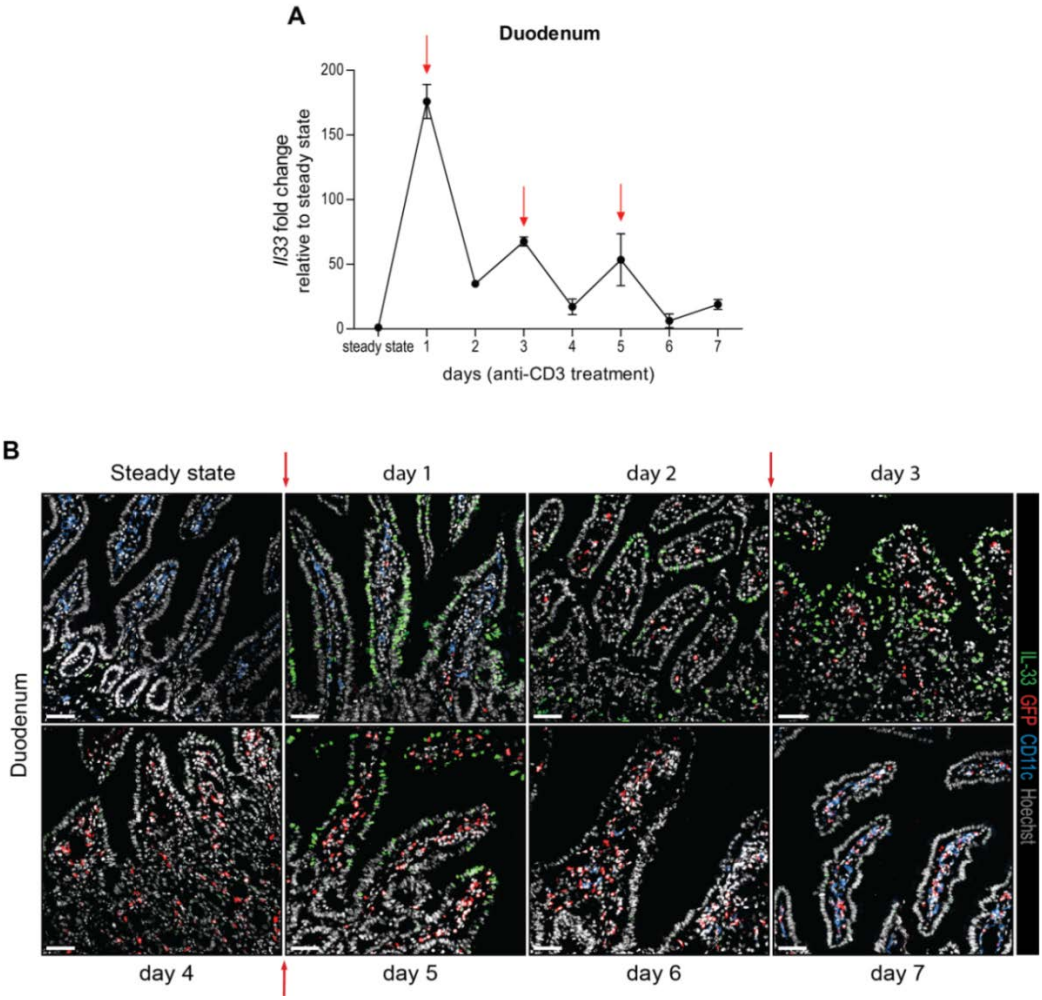

Figure 4. IL-33 peak occurs 4h after the first injection of anti-CD3 specific antibody. IL17A-eGFPxFoxp3-mRFP reporter mice were injected i.p. with 20µg anti-CD3 at day 1, 3 and 5. (A) Duodenal Il33 mRNA was measured by qPCR 4 hours and 24 hours after each injection. Data are presented as mean ± S.E.M. and normalized to the values in steady state. (B) IHC of the duodenum at the indicated time-points, showing the localization of IL-33 (green), IL-17A (red, GFP), CD11c (Blue) and Hoechst (white, nuclear counterstaining). Red arrows indicate anti-CD3 injections. Data are representative of ≥ 3 independent experiments (n=4 animals/group). Scale bar = 50µm. IHC performed in collaboration with Dr. Bayat Sarmadi.

3.1.2 T_H17 cells express ST2 upon anti-CD3 treatment

IL-33 mediates its function via ST2, a plasma membrane receptor that has been described to be expressed in various T-cell subsets including T_H2 *(117)*, T_H1 *(87)* and Treg cells *(118)*. However, it was not known whether T_H17 cells express ST2 and could subsequently respond to IL-33. Because the anti-CD3 treatment model promoted not only IL-33 induction in IECs, but also T_H17 cell accumulation in the proximal parts of the SI *(47)*, this model was suitable to address this question. Therefore, CD3-specific antibodies were injected at day 1, 3 and 5 in IL17A-eGFPxFoxp3-mRFP double reporter mice. Lymphocytes were analyzed by flow cytometry and identified by their forward scatter (FSC) and side scatter (SSC) properties, doublet exclusion and further gating on live and $CD45^+CD4^+$ T cells (Fig. 5A).

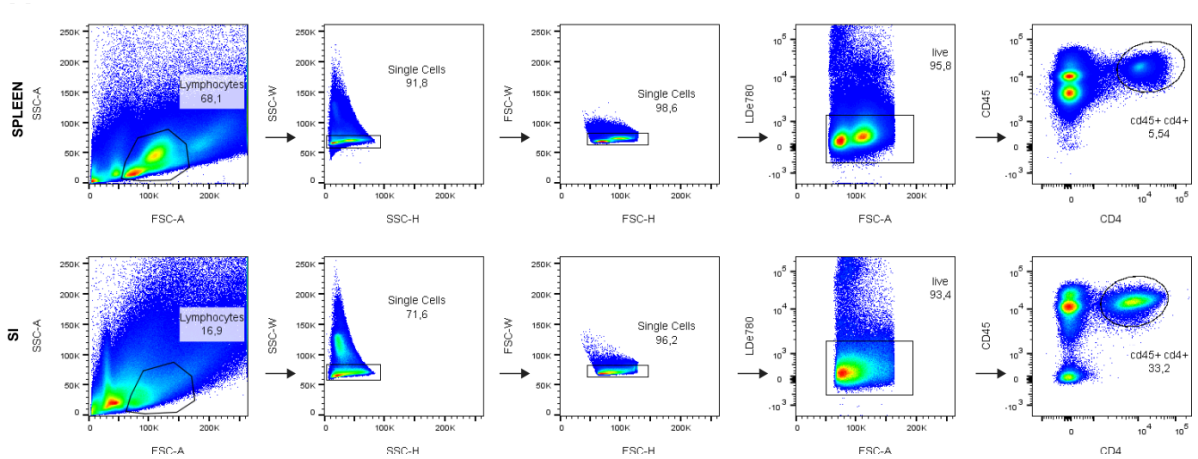

Figure 5. . Identification of lymphocytes by flow cytometry in IL17A-eGFPxFoxp3-mRFP double reporter mice for further analysis. Identification of lymphocytes from single cell suspensions by their scatter properties, exclusion of doublets and dead cells and gating on $CD45^+CD4^+$ T cells. Dot plots show the gating strategy to identify splenic and SI lymphocytes at steady state conditions. The analysis of T cell populations at the different time-points upon anti-CD3 treatment depicted in the next figure is based on this same gating strategy.

As shown in Fig. 6A and similar to previous reports *(47)*, the anti-CD3 treatment resulted in a specific increase in the frequency of T_H17 cells in the SI, a 14-fold increase at day 5, while the frequency of Tregs decreased 2,6-fold in the same tissue and time-frame. The absolute numbers of T_H17 cells were also significantly increased in the SI after anti-CD3 treatment when compared to Tregs, while the number of T_H17 cells did not significantly change in the spleen. Absolute numbers of Tregs in the same organ were even diminished (Fig. 6A).

ST2 expression was determined in IL-17A-$eGFP^+$Foxp3-$mRFP^-$ population (T_H17) and in IL-17A-$eGFP^-$Foxp3-$mRFP^+$ population (Tregs). The latter, known to be $ST2^+$ in the colon *(118)*, served as a positive control. T_H17 cells isolated from the spleen and SI of untreated mice did not express ST2, while a significant proportion of $Foxp3^+$ cells expressed ST2 in both organs (Fig. 6B). After anti-CD3 treatment, only a small fraction of T_H17 cells (~4%)

was found to express ST2 in the SI. However, around 30% of splenic T_H17 cells expressed ST2 at day 5, thus representing a frequency three times higher than the frequency observed in splenic Tregs (Fig. 6B). Splenic T_H17 cells express CCR6, a chemokine receptor known to re-direct T_H17 cells towards the SI, where high amounts of CCL20, the CCR6 natural ligand, are released by IECs during anti-CD3 treatment *(47)*. Indeed, around 90% of splenic T_H17 cells expressed CCR6 after treatment and, interestingly, ST2 expression in this subset was largely restricted (89%) to CCR6-expressing cells. On the contrary, ST2 expression in Tregs was mainly restricted (84%) to the $CCR6^-$ population (Fig. 6B). Together, these data show that ST2 expression is strongly and specifically induced in splenic $CCR6^+$ T_H17 cells, a population that has previously been shown to migrate to the SI via the CCR6/CCL20 axis *(47)*.

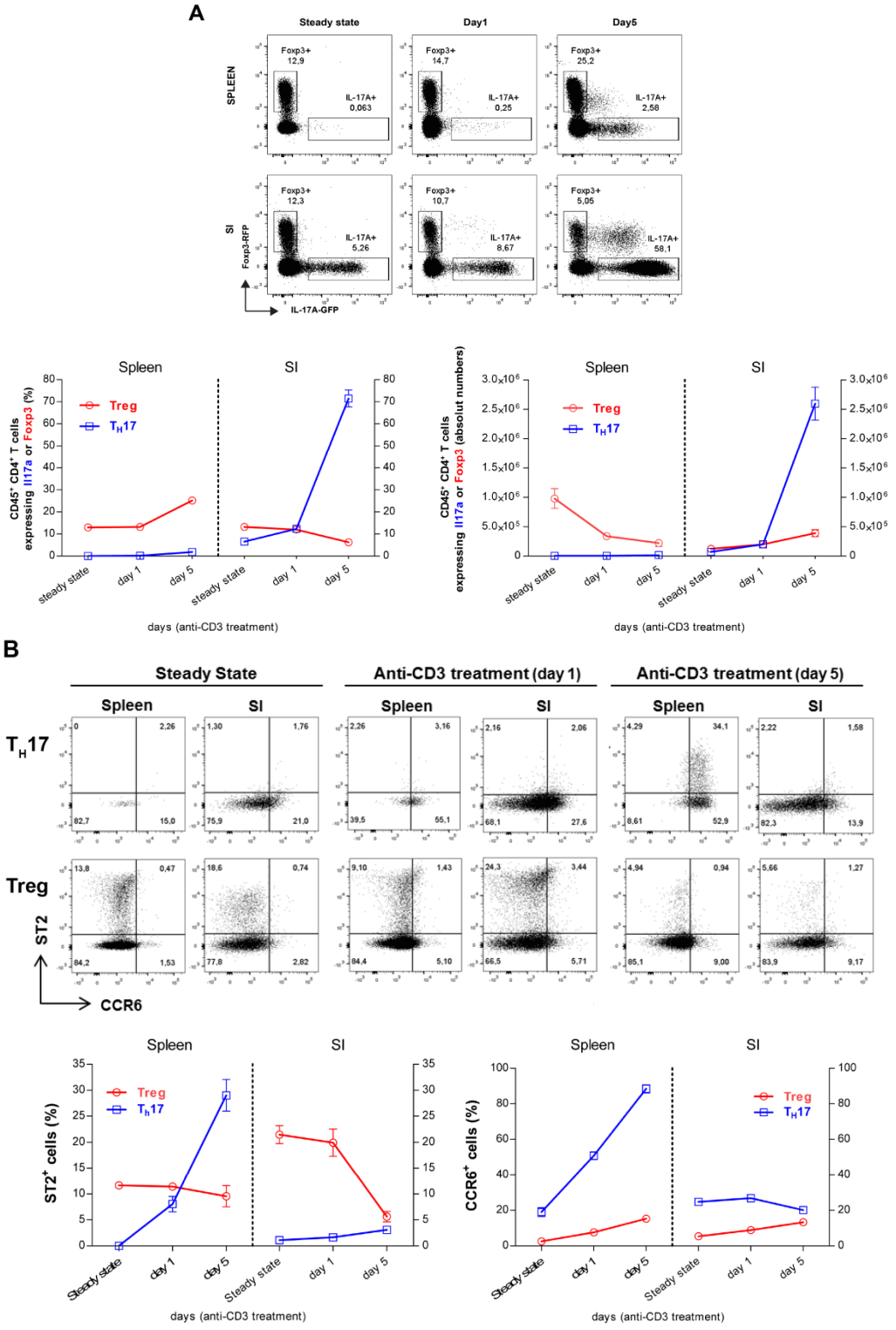

Figure 6. Flow cytometric analysis of T_H17 and Treg cell populations in the SI during anti-CD3 treatment. IL17A-eGFPxFoxp3-mRFP double reporter mice were injected i.p. with anti-CD3 antibody at days 1,3 and 5. Frequencies and absolute numbers of IL-17A-GFP$^+$ cells (T_H17 cells) and Foxp3-RFP$^+$ cells (Tregs) gated as in Fig. 5 are shown in (A): Frequencies of ST2$^+$ and CCR6$^+$ cells in the T_H17 and the Treg cell compartment (B) were determined at steady state and at day 3 and 5 of anti-CD3 treatment. Data are shown as a representative dot plot for each tissue and time point and the mean ± S.E.M.. Data are representative of two independent experiments with n= 5 animals/time-point.

3.1.3 Absence of ST2 mediated signaling enhances the pro-inflammatory capacity of T_H17 cells that accumulate in the SI upon anti-CD3 treatment

In light of the finding that T_H17 cells express ST2 *in vivo*, our next aim was to assess the role that the IL-33/ST2 signaling pathway plays in these cells. For that, CD3-specific antibody was injected i.p. on days 1, 3 and 5 in *St2*$^{-/-}$ mice and wild-type control littermates. Flow cytometric analysis of splenic and intestinal T cells was performed at steady state and at the above mentioned time-points. Lymphocytes were identified by their forward scatter (FSC) and side scatter (SSC) properties, doublet exclusion and further gating on live and TCRβ$^+$CD45$^+$CD4$^+$ T cells (Fig.7).

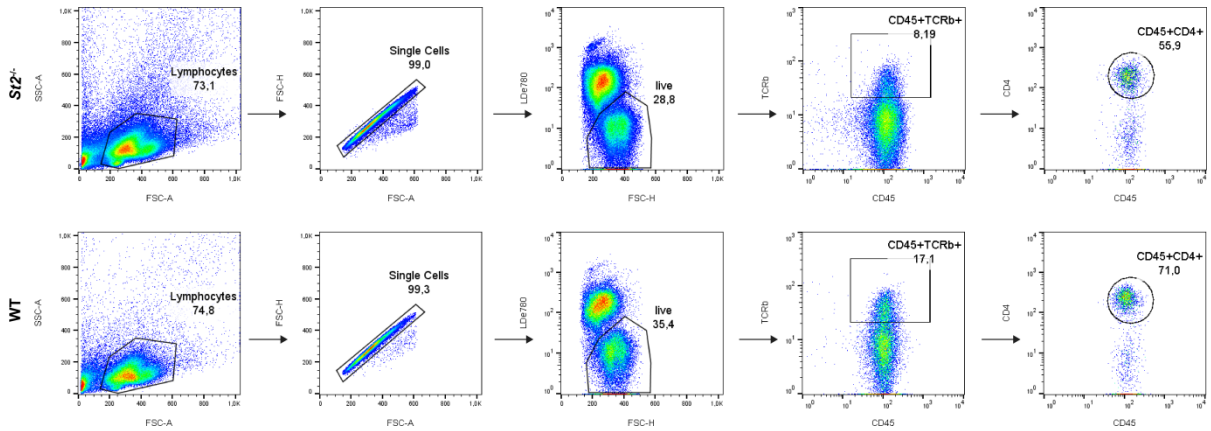

Figure 7. Identification of lymphocytes by flow cytometry in *St2* $^{-/-}$ and wild type mice for further analysis. Identification of lymphocytes from single cell suspensions by their scatter properties, exclusion of doublets and dead cells and gating on TCRβ$^+$CD45$^+$CD4$^+$ T cells. Dot plots show the gating strategy to identify splenic lymphocytes in each animal group at steady state conditions. The analysis of T cell populations at the different time-points upon anti-CD3 treatment depicted in the next figures is based on this same gating strategy.

Because the strongest up-regulation of *Il33* was found at day 1 (Fig.3A), the greatest differences between *St2*$^{-/-}$ and control mice were expected at this time-point and it was therefore chosen for further analysis. At day 1, the frequencies of splenic T cells were significantly decreased in *St2*$^{-/-}$ mice (Fig. 8A), while ROR-γt$^+$, Foxp3$^+$ and ROR-γt$^+$/Foxp3$^+$ cell frequencies were significantly increased in the spleen of these mice compared to control littermates (Fig. 8B).

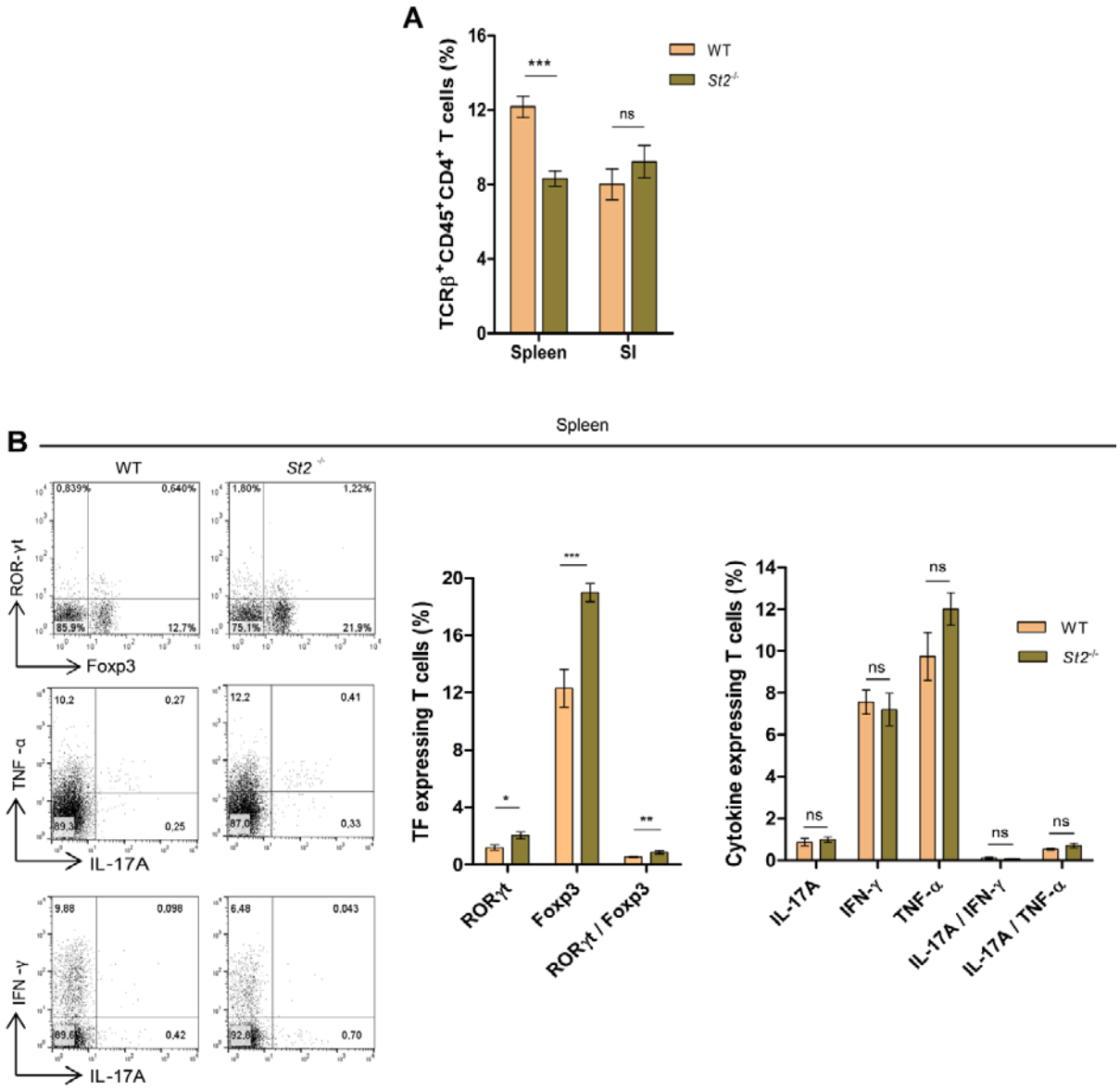

Figure 8. *St2* $^{-/-}$ mice show impaired T cells frequencies in the spleen at day 1 of the anti-CD3 treatment. *St2* deficient (*St2*-/-) and wild-type C57BL/6 (wt) mice were injected i.p. with 20µg anti-CD3 and flow cytometry analysis (FACS) of spleen and SI was performed 4 hours after the injection. (A) Frequencies of splenic and intestinal T cells, gated as in (Fig.6) comparing *St2*$^{-/-}$ and wt mice. A representative FACS dot plot from each animal group and the frequencies of TF and cytokine expressing T cells isolated from the spleen gated as in (Fig. 6) are shown in (B). Results are shown as mean ± S.E.M. and are representative of 2 independent experiments with n= 4 animals/group. * P < 0,05, **P < 0,01, ***P<0,005 as calculated by paired Student's *t*-test. ns, not significant.

Although T cell frequencies in the SI did not change between groups (Fig. 8A), we observed a selective enrichment, both in frequencies and total numbers, of ROR-γt-expressing cells in the SI of *St2*$^{-/-}$ mice (Fig. 9A,B). By contrast, frequencies of intestinal Foxp3- expressing cells and Foxp3/ROR-γt- double expressing cells were unaffected by ST2 deficiency (Fig. 9A). Interestingly, elevated frequencies and total numbers of IL-17A^{+} T cells were also found in the SI in the absence of *St2* (Fig. 9A,B). Although no significant differences were observed in IFN-γ or TNF-α production by T cells, the percentage of T cells co-expressing these pro-

inflammatory cytokines together with IL-17A was also increased in the SI of *St2*$^{-/-}$ compared to the WT mice (Fig. 9A).

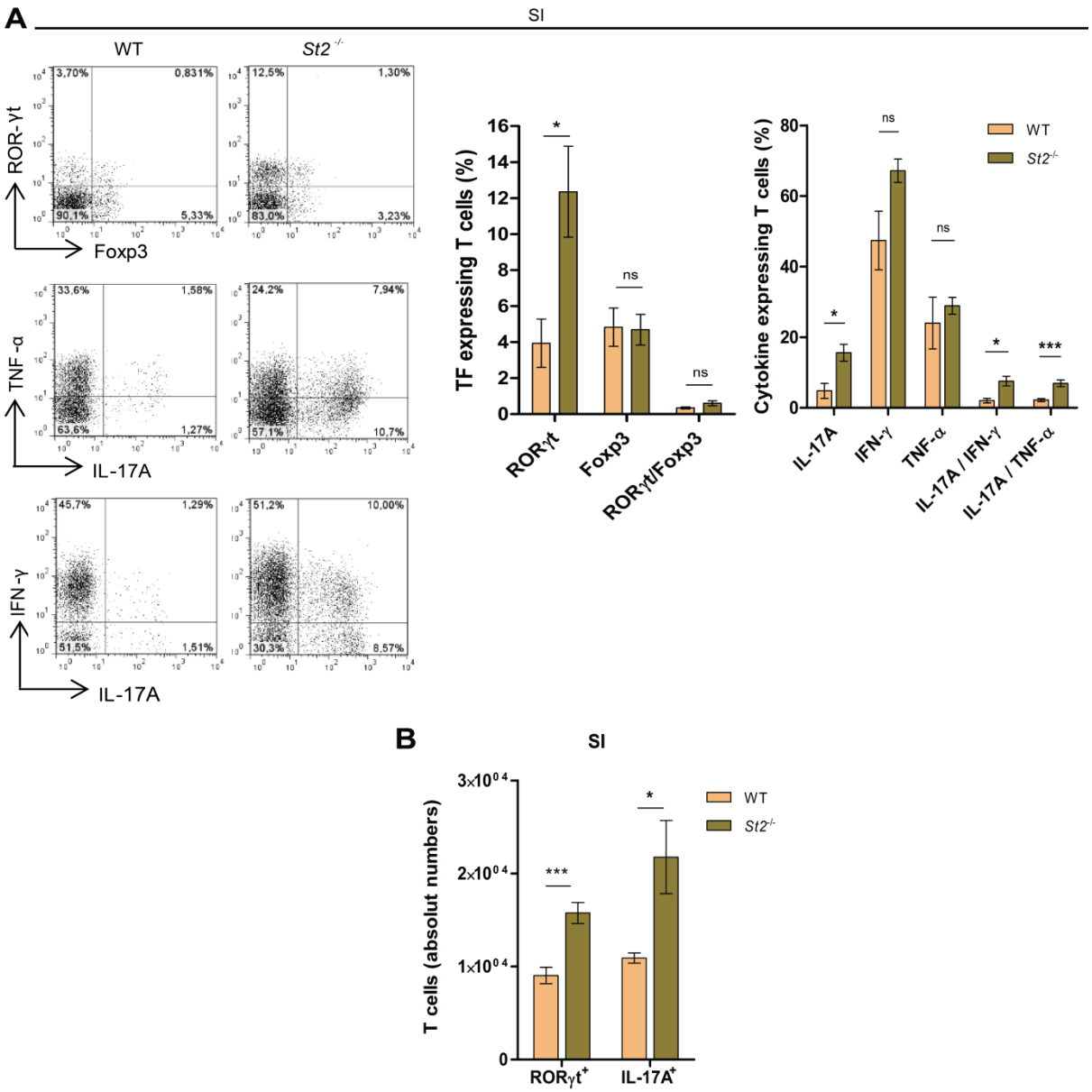

Figure 9. *St2* $^{-/-}$ mice show a specific increase of pathogenic T_H17 cells in the SI at day 1 of the anti-CD3 treatment. *St2* deficient (*St2*-/-) and wild-type C57BL/6 (wt) mice were injected i.p. with 20µg anti-CD3 and flow cytometry analysis (FACS) of SI was performed 4 hours after the injection. A representative FACS dot plot from each animal group and the frequencies of TF and cytokine expressing T cells isolated from the SI and gated as in (Fig. 6) are shown in (A). (D) Absolut numbers of ROR-γt^{+} and IL-17A^{+} T cells in the SI. Results are shown as mean ± S.E.M.and are representative of 2 independent experiments with n= 4 animals/group.* P < 0,05, **P < 0,01, ***P<0,005 as calculated by paired Student's *t*-test. ns, not significant.

As expected, the analysis at day 3 showed milder differences between groups. T cell frequencies were also found reduced in the spleen of *St2*$^{-/-}$ mice at this time point (Fig. 10A), while frequencies of IL-17A-producing T cells were increased (Fig. 10B). Although frequencies of IL-17A/IFN-γ- and IL-17A/TNF-α- double producing T cells were also increased in the spleen of mice lacking *St2* (Fig. 10B), they represented a very small proportion of T cells in the periphery (0,1-0,5%), which would probably have only minor impact on the overall immunological response. There was a slight but not significant increase in the frequency of IFN-γ^{+} cells and TNF-α^{+} cells in the spleen of *St2*$^{-/-}$ mice (Fig. 10B) and there was also a tendency for the frequencies of SI T_H17 cells in the *St2* deficient mice to be increased. However, these differences did not reach statistical significance (Fig. 10C).

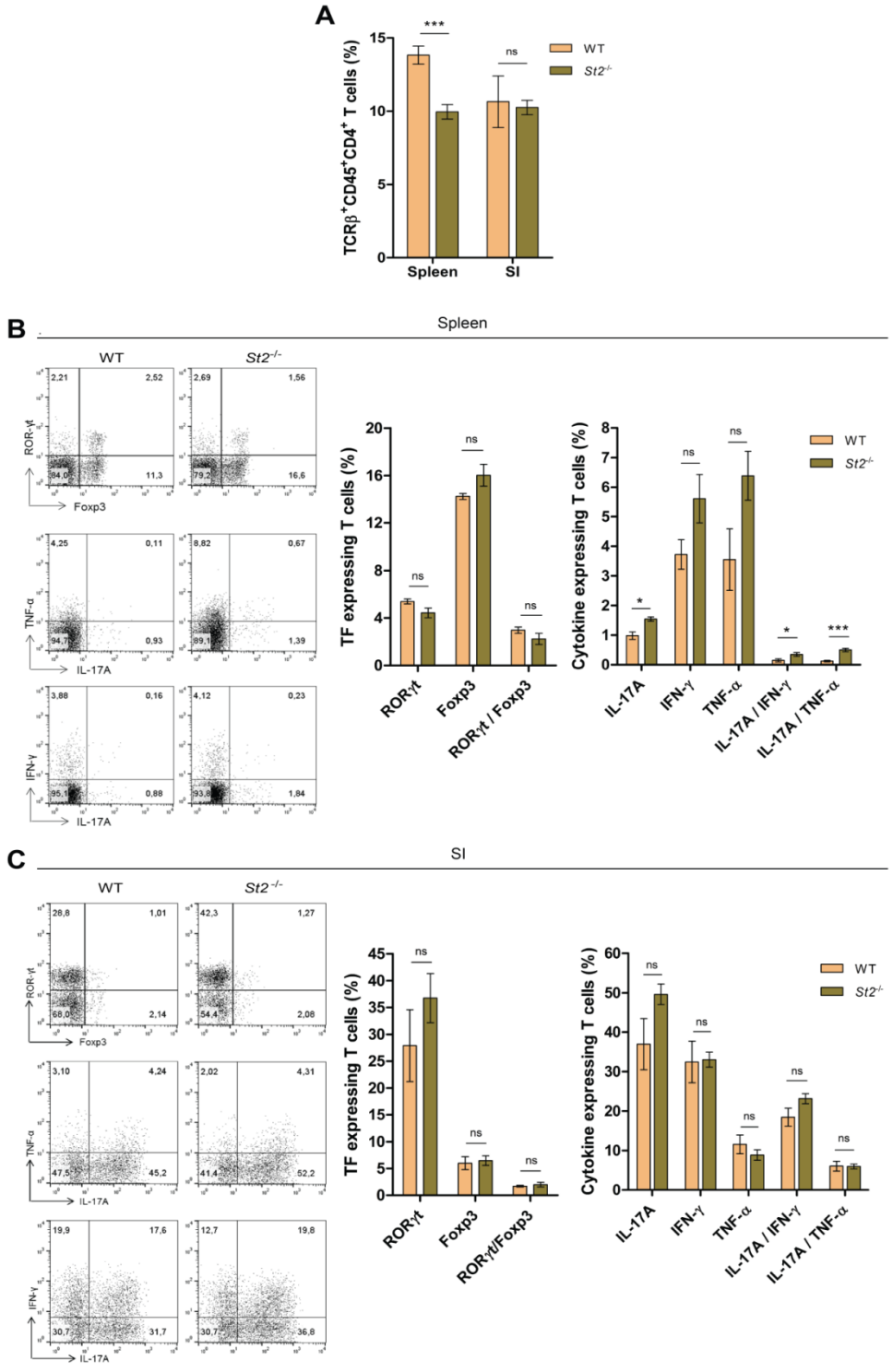

Figure 10. *St2* $^{-/-}$ mice and control littermates show a comparable T_H17 cell population in the SI at day3 of the anti-CD3 treatment. *St2* deficient (*St2*$^{-/-}$) and wild-type C57BL/6 (wt) mice were injected i.p. with 20µg anti-CD3 at day 1 and 3 and flow cytometry analysis (FACS) of spleen and SI was performed 4 hours after the second injection. (A) Frequencies of splenic and intestinal T cells, gated as in Fig. 6 comparing *St2*$^{-/-}$ and wt mice. A representative FACS dot plot from each animal group and the frequencies of TF and cytokine expressing T cells isolated from the spleen (B) and from the SI (C), gated as in (A). Results are shown as mean ± S.E.M. and are representative of 2 independent experiments with n= 4 animals/group.* P < 0,05, **P < 0,01, ***P<0,005 as calculated by paired Student's *t*-test. ns, not significant.

As previously described, the anti-CD3-treatment leads to a recovery phase (day 5-7), characterized by the resolution of inflammation in the SI and the complete recovery of the individuals. In line with this, no differences were found in the spleen or the SI between *St2* deficient mice and control littermates at day 5 (Fig. 11). T cell frequencies were similar in both animal groups in the spleen, as well as in the SI (Fig. 11A). No significant differences between groups were found in the spleen regarding the expression of transcription factors (Foxp3 and ROR-γt) or cytokines (IL-17A, TNF-α and IFN-γ) (Fig. 11B). The FACS analysis of the SI also yielded similar results in the $St2^{-/-}$ compared to wt mice, concerning transcription factors and cytokines secreted by T cells at day 5 (Fig. 11C). These results suggest that the role of the IL-33/ST2 axis is prominent during the acute inflammation phase, but not during resolution of inflammation.

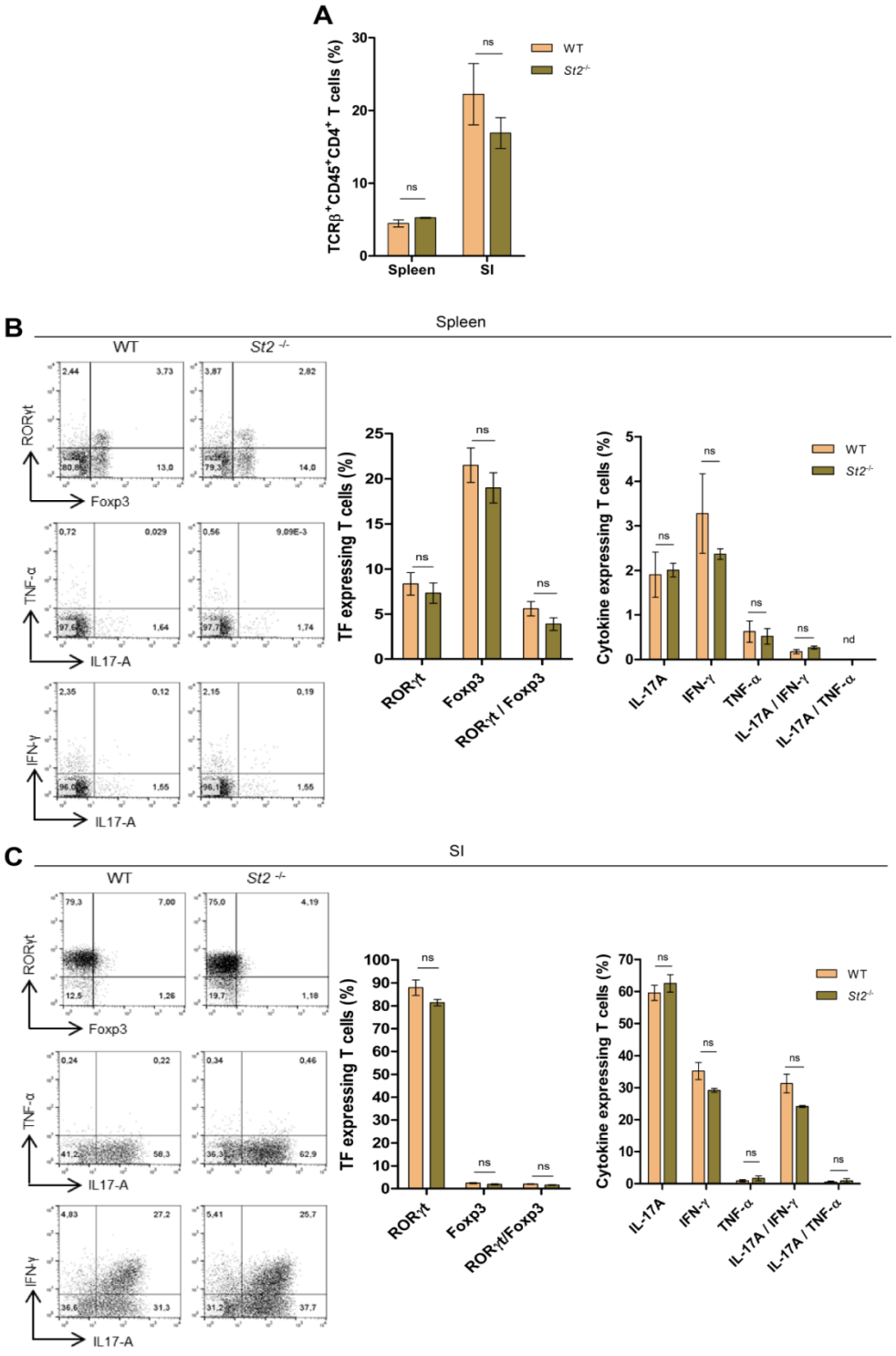

Figure 11. *St2* $^{-/-}$ mice and control littermates show no differences in spleen or SI at day 5 of the anti-CD3 treatment. *St2* deficient (*St2*$^{-/-}$) and wild-type C57BL/6 (wt) mice were injected i.p. with 20µg anti-CD3 at day 1, 3 and 5 and flow cytometry analysis (FACS) of spleen and SI was performed 4 hours after the third injection. (A) Frequencies of splenic and intestinal T cells, gated as in Fig. 6 comparing *St2*$^{-/-}$ and wt mice. A representative FACS dot plot from each animal group and the frequencies of TF and cytokine expressing T cells isolated from the spleen (B) and from the SI (C), gated as in (A). Results are shown as mean ± S.E.M. and are representative of 2 independent experiments with n= 4 animals/group.* P < 0,05, **P < 0,01, ***P<0,005 as calculated by paired Student's *t*-test. ns, not significant. nd, not detectable.

We next aimed to compare frequencies of T cells and cytokine expression between the two cohorts in homeostatic conditions, since without such analysis any observed differences upon anti-CD3 treatment could be due to differences at steady state. Splenic T cell frequencies were found reduced in mice lacking *St2* (Fig. 12A), but no differences on cytokine expression were found between groups in the spleen (Fig. 12B). More importantly, we could not find any difference in the SI between steady state $St2^{-/-}$ mice and control littermates (Fig. 12A, C). Hence, the differences observed in the SI after the first injection with CD3-specific antibody were induced by the treatment itself, which speaks for the importance of the IL-33/ST2 axis in the ongoing acute inflammatory response.

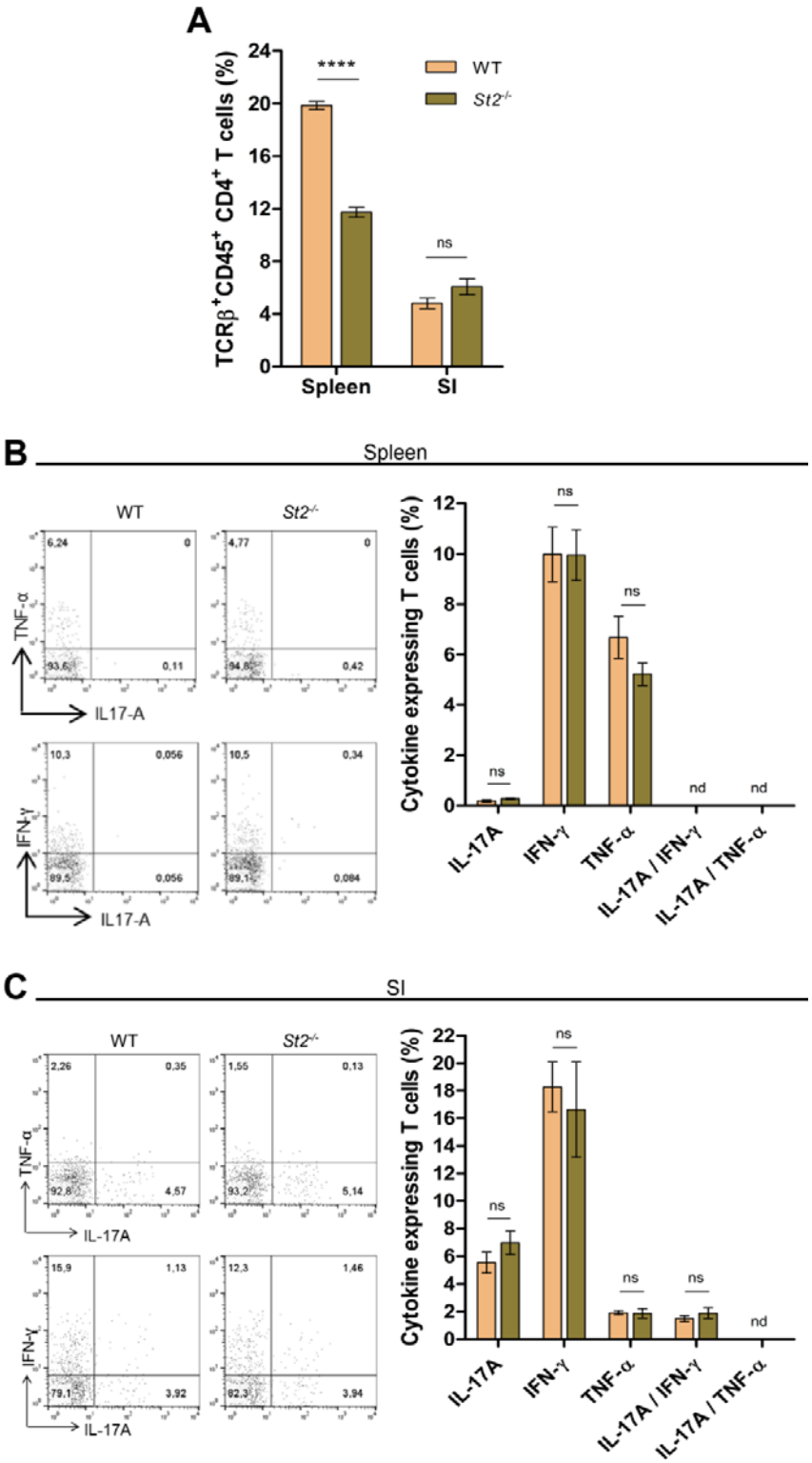

Figure 12. *St2* $^{-/-}$ mice show lower splenic T cell frequencies at steady state, but comparable levels of cytokine expression. *St*2 deficient (*St2*$^{-/-}$) and wild-type C57BL/6 (wt) mice were analyzed by flow cytometry analysis (FACS) of spleen and SI at steady state conditions. (A) Frequencies of splenic and intestinal T cells, gated as in Fig. 6 comparing *St2*$^{-/-}$ and wt mice. A representative FACS dot plot from each animal group and the frequencies of cytokine expressing T cells isolated from the spleen (B) and from the SI (C), gated as in (A). Results are shown as mean ± S.E.M. and are representative of 2 independent experiments with n= 4 animals/group.* P < 0,05, **P < 0,01, ***P<0,005 as calculated by paired Student's *t*-test. ns, not significant. nd, not detectable.

Altogether, the results point to a skewed distribution of T-cell subsets in the periphery of mice lacking ST2 signaling. More importantly, they clearly suggest that the IL-33/ST2 axis specifically restrains the pro-inflammatory capacity of T_H17 cells that accumulate in the SI upon inflammation.

To further study if the increased T_H17 cell pathogenicity observed in *St2*$^{-/-}$ mice upon anti-CD3 treatment had any clinical implications, intestinal inflammation was assessed in both animal groups. Mice lacking *St2* showed a more severe body weight loss (Fig. 13A), presented a higher degree of intestinal inflammation (Fig. 13B) and more severe duodenal injury as assessed by histology (Fig. 13C) compared to WT mice. Levels of *Il17a*, *Ifng* and *Tnf* in the duodenum were also quantified and found up-regulated in the mice lacking ST2 signaling (Fig. 13D), suggesting an exacerbated inflammatory cytokine milieu in the treated intestines of the *St2*$^{-/-}$ mice, in line with the results found on T cell populations. Thus, these data emphasize that the increased pro-inflammatory capacity of T_H17 cells found in mice lacking *St2* leads to a more severe clinical course during anti-CD3 treatment, mainly associated with tissue destruction, diarrhea and the consequent loss of body weight.

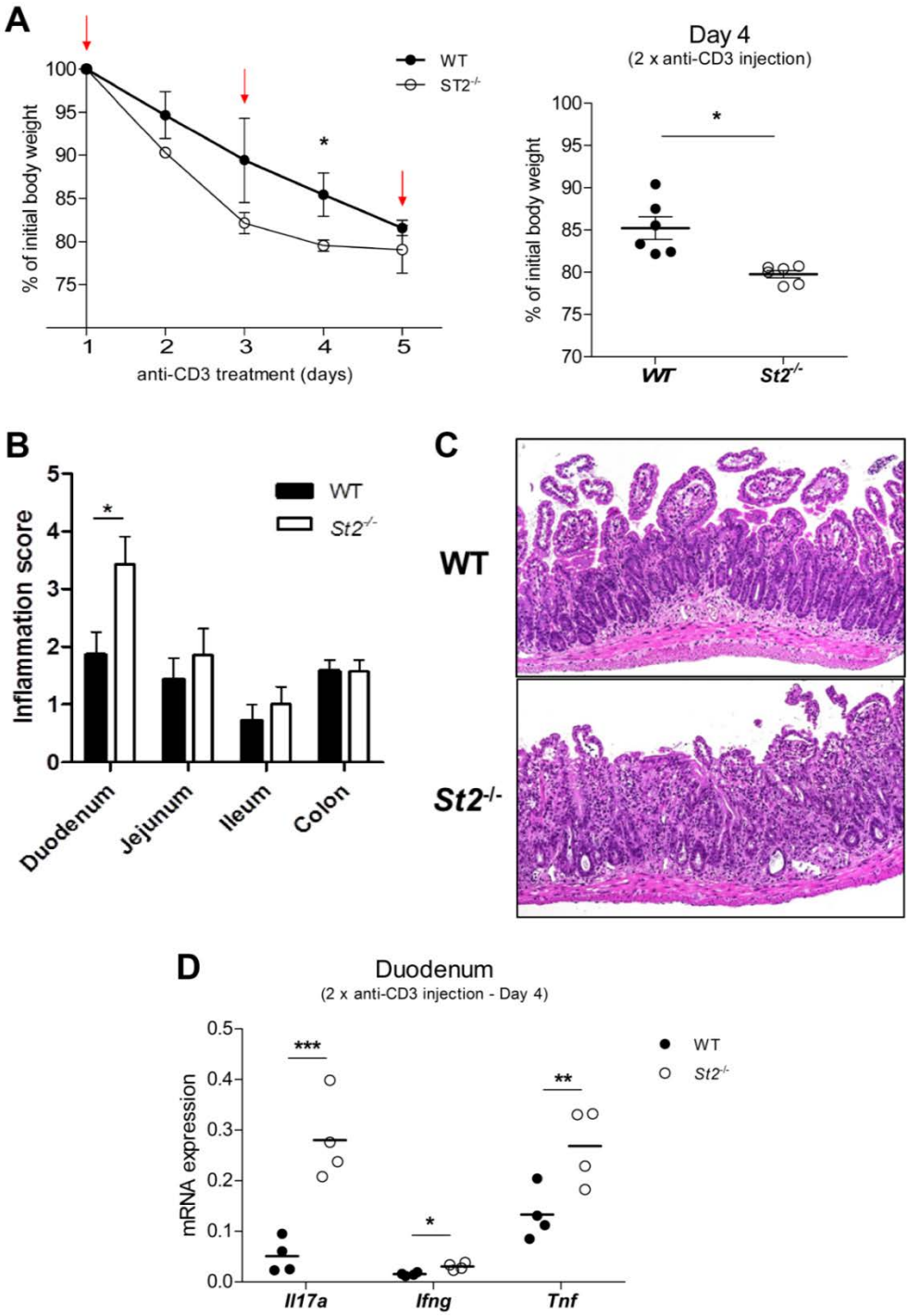

Figure 13. *St2*$^{-/-}$ mice show exacerbated inflammation in the SI during anti-CD3 treatment. *St2* deficient (*St2*$^{-/-}$) and wild-type mice (wt) were injected i.p. with 20µg anti-CD3 at day 1, 3 and 5. Body weight was monitored during the anti-CD3 treatment in 6 animals per group (A). Intestinal inflammation was assessed at day 4 after anti-CD3 treatment for the different parts of the intestine (n=7 animals/group) by H&E staining of histological sections. Histological scores describing the intestinal inflammation in WT versus *St2*$^{-/-}$ mice are depicted in (B) and one representative image from the duodenum of a WT and a *St2*$^{-/-}$ mouse is shown in (C). The levels of the pro-inflammatory genes *Il17a*, *Ifng* and *Tnf* were quantified by RT-PCR in the same tissue and the same time-point (D) (n=4 animals/group). Red arrow indicates anti-CD3 injection. Results are shown as mean ± S.E.M. and are representative of two independent experiments. *P < 0.05, ** P < 0.01, *** P < 0.001 as calculated by two-way ANOVA with Bonferroni post-test.

3.1.4 IL-33 induces changes in the gene expression profile of mouse and human T_H17 cells in favor of an immunosuppressive phenotype

To further elucidate specific and direct effects of IL-33 on mouse T_H17 cells, we moved to *in vitro* settings. Because naïve T cells are known to respond to IL-33 *in vitro (119)* and Tregs are known to express ST2 *(118)*, ST2 expression in T_H17 cultures was quantified and compared to both naïve T cells and Tregs. Indeed, *in vitro* differentiated murine T_H17 cells expressed ST2 (Fig. 14.A) and we therefore hypothesized that they could respond to IL-33. T_H17 cells were then cultured for 5 days and the changes in gene expression were quantified upon IL-33 addition (Fig. 14B). *Il17a* expression was induced in the presence of IL-33, as well as *Il10*, which was induced 4-fold. The increase in *Il10* expression in IL-33-stimulated T_H17 cells was accompanied by a reduction in the expression levels of the pro-inflammatory genes *Tbx21, Ifng* and *Csf2*.

Differences may exist between mouse and human T_H17 cells and our next goal was to decipher the effects of IL-33 on the human counterparts. Interestingly, human T_H17 cells responded similarly to IL-33 stimulation. *IL17A* and *IL10* were up-regulated in the presence of IL-33, while *TBX21* levels were remarkably reduced (Fig. 14C). At the protein level, IL-10 production in human T_H17 cells was also induced by IL-33 (Fig. 14D) compared to untreated cells and to cells treated with IL- 1β, a reported inhibitor of IL-10 in human T_H17 cells *(110)*. As expected, the maximum IL-10 production was found in T_H17 cells treated with IL-27, a cytokine known to strongly induce IL-10 *(120)*. Notably, IL-33 also dampened the production of GM-CSF, a cytokine associated with a pro-inflammatory phenotype, in human T_H17 cells (Fig. 14D). Thus, our data indicate that IL-33 is capable of inducing changes in the genetic profile of murine and human T_H17 cells by reducing the expression of pro-inflammatory genes and promotes the secretion of the anti-inflammatory cytokine IL-10 in human T_H17 cells.

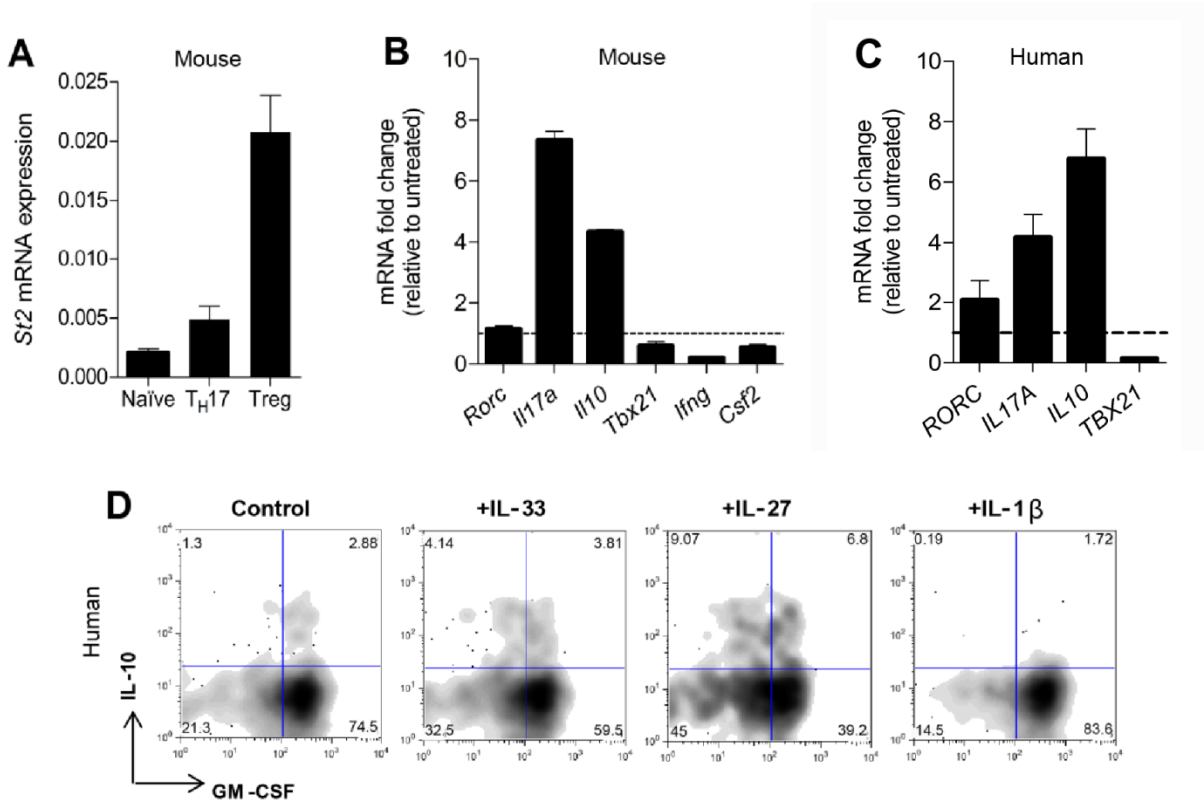

Figure 14. Mouse and human T_H17 cells respond to IL-33 *in vitro*. (A) Mouse naïve sorted $CD4^+CD25^-CD62L^+CD44^-$ T cells were stimulated *in vitro* with anti-CD3/CD28 and grown under T_H17 or Treg conditions for 5 days. *St2* expression was analysed by qPCR and compared to naïve cells (mean ± S.D. of 3 independent experiments). (B) Mouse T_H17 cells were treated with 20ng/ml IL-33 during the differentiation process (as in A). *Rorc*, *Il17a*, *Il10*, *Tbx21*, *Ifng* and *Csf2* expression levels were quantified by qPCR (dotted line at 1 indicates the value of control untreated T_H17 cells). Data are presented as mean ± S.E.M. of at least 3 independent experiments. (C) Fresh *ex vivo* sorted human $CCR6^+CCR4^+CXCR3^-CD45RA^-CD25^-CD8^-$ T_H17 cells were stimulated with CD3 and CD28 mAbs for 48h and expanded for another 3 days in the presence of 20ng/ml IL-33. *RORC*, *IL17A*, *IL10* and *TBX21* expression levels were quantified by qPCR (dotted line at 1 indicates value of non-treated T_H17 cells). Human T_H17 cells were also stimulated with PMA/Ionomycin for 5 hours to detect intracellular levels of IL-17A, IL-10 and GM-CSF by FACS. One representative dot plot out of 3 independent experiments of flow cytometry analysis of IL-10 and GM-CSF assessed on T_H17 cells (gated on $IL17A^+$ $CD4^+$ T cells) is shown in (D).

To elucidate the molecular mechanisms mediating *Il10* induction upon IL-33 stimulation, we performed an analysis of the transcription factors known to induce *Il10* expression in T cells. *Ahr (48)*, *Ikzf3 (121)*, *Jun* and *Irf4 (122)*, all known to be IL-10-related genes, were found to be up-regulated by IL-33 in T_H17 cells, together with *Il10* (Fig. 15A). Importantly, expression of *Ahr* was also found to strongly correlate with *Il10* expression in T_H17 cell cultures (Fig. 15B), suggesting that the transcription factor Ahr may be involved in the induction of *Il10* downstream of IL-33/ST2 signaling. Although *Maf* is a reported inducer of *Il10* in T_H17 cells *(123)*, it was not up-regulated upon IL-33 signaling (Fig. 15A). Nevertheless, expression of *Maf* was found to correlate with *Il10* expression in T_H17 cell cultures (Fig. 15A.), indicating a

link between both transcripts, but not with IL-33. The transcription factor AP-1, encoded by *Jun,* showed the highest fold change upon IL-33 stimulation in the cultures in which *Il10* was also induced (Fig. 15A).

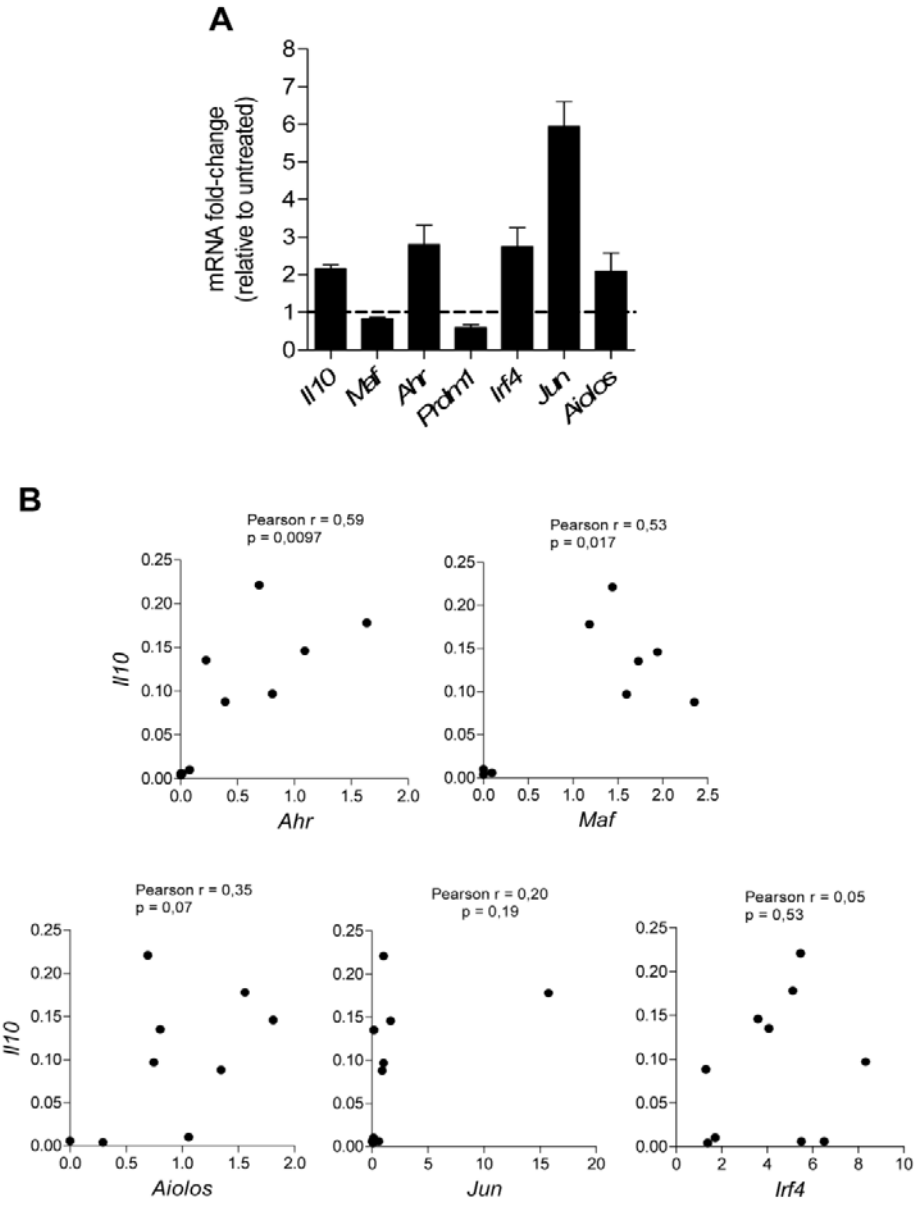

Figure 15. Molecular mechanisms mediating *Il10* induction upon IL-33 stimulation. (A) Mouse naïve sorted $CD4^+CD25^-CD62L^+CD44^-$ T cells were stimulated *in vitro* with anti-CD3/CD28 and grown under T_H17 conditions and treated with 20ng/ml IL-33 for 5 days. *Il10, Maf, Ahr, Prdm1, Irf4, Jun* and *Aiolos* expression levels were quantified by qPCR (dotted line at 1 indicates the value of control untreated T_H17 cells). Data are presented as mean ± S.E.M. of 5 independent experiments. (B) Correlation between *Il10* and *Ahr, Maf, Irf4, Jun* and *Aiolos* expression in T_H17 cells as measured by qPCR and analyzed by Pearson test (n=10).

Once shown that IL-33 acts directly on T_H17 cells and induces IL-10 production *in vitro,* we aimed to further evaluate the scope of IL-33 effects in this T-cell subset. In order to analyze this in an *in vivo* setting, the anti-CD3 treatment model was again used. Because the highest

frequency of ST2$^+$CCR6$^+$IL-17A$^+$ T cells was found at day 5 (Fig. 6B), this time point was selected for further analysis. CD3-specific antibody was injected at day 1, 3 and 5 to IL17A-eGFPxFoxp3-mRFP reporter mice and splenic IL-17A-eGFP$^+$RFP$^-$ cells (T_H17) and Foxp3-RFP$^+$GFP$^-$ cells (Tregs) were FACS-sorted. After 24 hours in culture with different concentrations of IL-33, the expression levels of selected genes of interest were quantified (Fig. 16.A). The expression of the master regulators for each subset, *Rorc* and *Foxp3*, showed only minor changes upon IL-33 stimulation (Fig. 16B). On the contrary, *Il10* expression was induced by IL-33 in a dose-dependent manner in T_H17 cells, while its levels were only marginally, non-significantly increased in the Treg cultures. Furthermore, the expression of *Ifng* was efficiently down-regulated by IL-33 in the T_H17 cell culture, even at low doses (Fig. 16C). These results demonstrate that activated, splenic T_H17 cells respond to IL-33 *ex vivo* by down-regulating the expression of *Ifng* and up-regulating *Il10*.

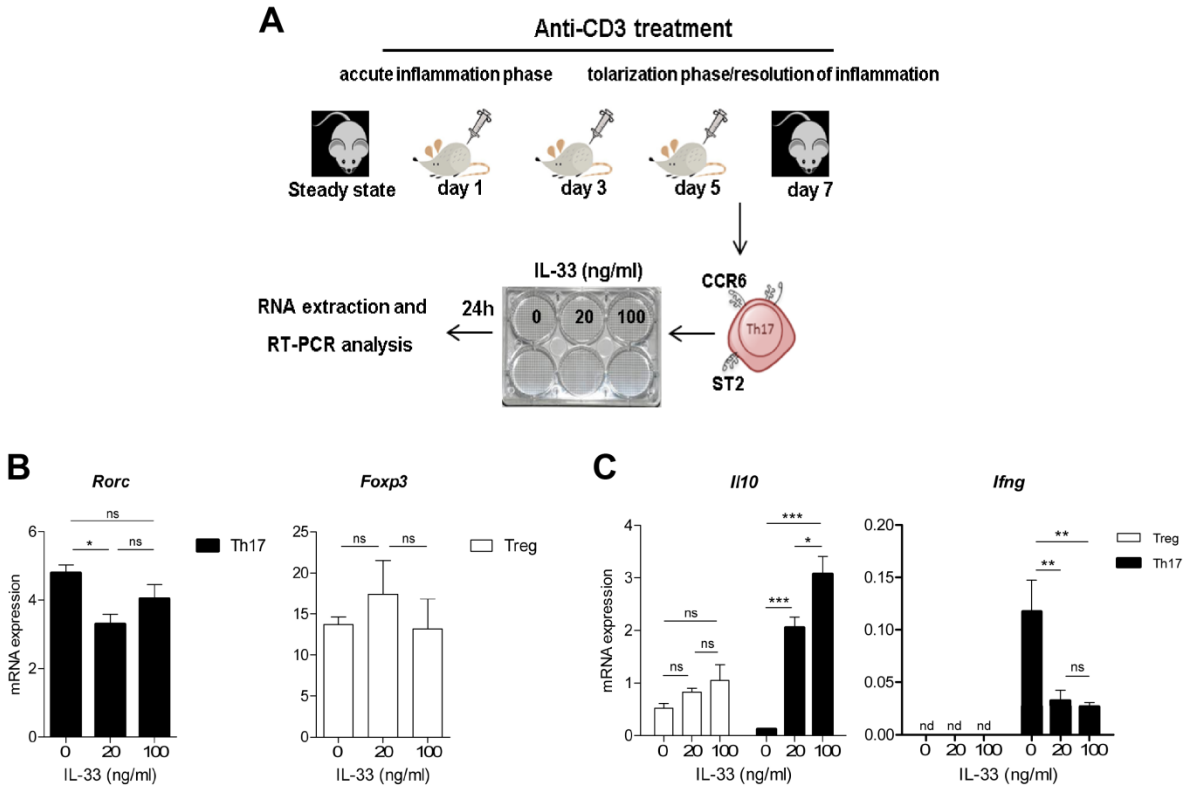

Figure 16. IL-33 up-regulates *Il10* and down-regulates *Ifng* expression in T_H17 cells *ex vivo*. (A) IL17A-eGFPxFoxp3-mRFP reporter mice (n=7) were injected i.p. with 20µg anti-CD3 at day 1, 3 and 5. Splenic T_H17 cells (CD45$^+$CD4$^+$IL-17A-GFP$^+$Foxp3-RFP$^-$) and Treg cells (CD45$^+$CD4$^+$IL-17A-eGFP$^-$ Foxp3-mRFP$^+$) were sorted 4h after the last injection. Sorted cells were cultured in the presence of 0, 20 or 100ng/ml of IL-33 for 24h. mRNA expression levels of *Rorc* and *Foxp3* (B) and mRNA expression levels of *Il10* and *Ifng* (C) were measured by qPCR. Results are presented as mean ± S.E.M. and are representative of 2 independent experiments.* P<0,05, ** p<0,005, *** p<0,0001 as calculated by one-way ANOVA with Bonferroni post-test. ns, not significant. nd, not detectable.

Tregs are a subset of T cells that have the ability to suppress harmful immunological reactions to self or foreign antigens by inhibiting the proliferation of effector (or responder) T cells. Therefore, the regulatory function of T cells can be analyzed *in vitro* by a so-called suppression assay. For this purpose, Tregs are co-cultured with $CD4^+$ responder T cells in the presence of a polyclonal stimulus, in this case APCs and anti-CD3/anti-CD28. Responder T cells alone without stimulus show a hypo-proliferative response (anergy) and responder T cells alone with stimulus show a proliferative response. Co-culture of Tregs together with responder cells in the presence of the stimulus results in reduced proliferation of responder T cells. In this assay, the CFSE dye is used to monitor cell proliferation, since live cells are covalently labeled with this bright, stable dye and every generation of cells appears as a different peak on a flow cytometry histogram. Based on this, and to assess whether IL-33 stimulation affected not only the genetic and cytokine profile of T_H17 cells, but also T_H17 cell functions, the *in vitro* suppressive capacity of IL-33-stimulated T_H17 cells was compared to untreated T_H17 cells (non-suppressive) and to professional Tregs (Fig. 17A). As expected, Treg cells inhibited T-cell proliferation to the greatest extent. Nevertheless, addition of IL-33 significantly enhanced murine T_H17 suppressor functions in the various suppression assays performed (Fig. 17B).

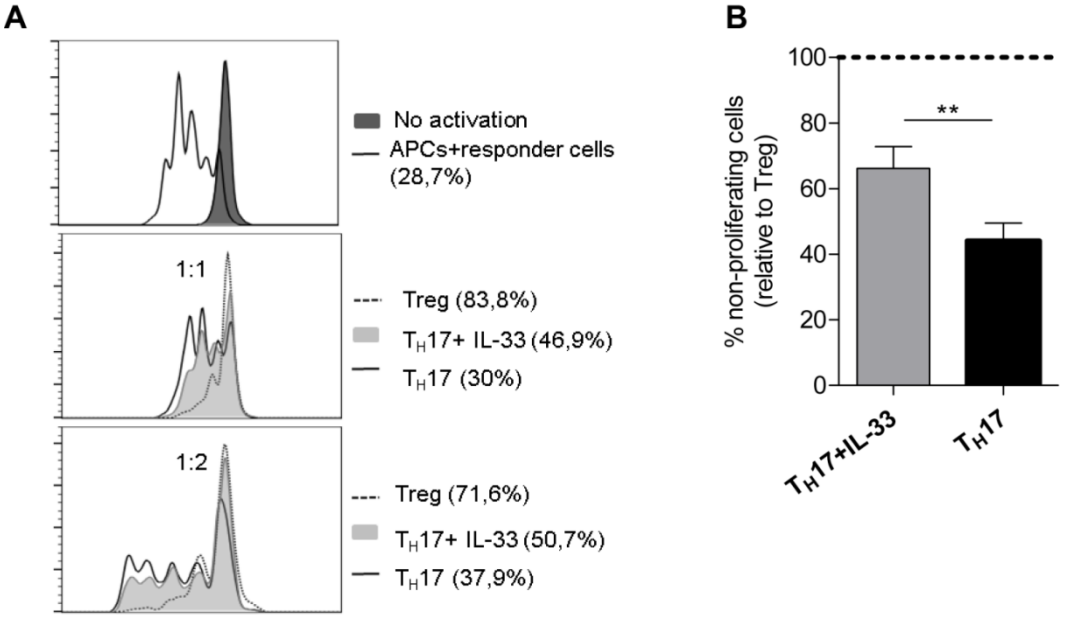

Figure 17. IL-33 promotes regulatory functions in T_H17 cells *in vitro*. Suppression assay in a mouse T cell culture was performed by using MACS enriched $CD25^+$ Treg cells and *in vitro* generated T_H17. T_H17 treated or not with 20ng/ml of IL-33 were sorted at day 4 for $CD4^+IL17eGFP^+FoxP3mRFP^-$.(A) After 3 days of co-culture, percentages of non-proliferating responder CFSE-labelled $CD4^+CD25^-$ T cells were quantified by FACS. (B) Bar histogram summarized frequencies of non-proliferating responder cells obtained in all the different assays relative to professional Tregs (100% suppression ability, dotted line). Data are shown as mean ± S.E.M. of 6 independent experiments. **p<0,005 as calculated by paired Student's *t*-test.

Collectively, the data indicates that the changes in the T_H17 cell cytokine profile observed *in vivo* after anti-CD3 treatment were due, at least in part, to the binding of IL-33 to its receptor in this subset, leading to an increase in *Il10* and a decrease in *Ifng* expression and promoting the acquisition of a proper regulatory phenotype by T_H17 cells.

3.2 OSM M in control of T_H17 cells

3.2.1 *Osm* is highly expressed in SI monocytes upon anti-CD3 treatment

As described in *section 3.1* we identified a tissue-specific, local factor in control of T_H17 cells. This factor is IL-33 and it is produced by IECs, which are immuno-competent cells of non-hematopoietic origin. Nevertheless, a huge population of hematopoietic cells resides in the LP and it is well known to influence T cell responses in the SI *(see section 1.1.4)*. In fact, prominent candidates for controlling T_H17 cells in the LP are APCs of myeloid origin, such as DCs and macrophages. Consequently, $CD11b^+$ cells, which include both populations of APCs, were sorted from spleen and the SI of anti-CD3 treated animals and their transcriptome data was compared. The results of the microarray showed a significant up-regulation of *Osm* in SI $CD11b^+$ cells (Fig. 18A) compared to the spleen. OSM is a multifunctional cytokine that has been shown to reduce inflammation and tissue destruction in murine models of RA, MS *(99)* and IBD *(100)*, diseases linked to a deregulated functionality of T_H17 cells. Therefore, OSM was investigated in further studies. To confirm the transcriptome data, a time-course analysis of the *Osm* transcript was performed during anti-CD3 treatment in the different parts of the intestine and the spleen, which was again used as a SLO. The results showed a specific up-regulation of *Osm* in the duodenum of the treated animals, compared to the other tissues analyzed (Fig. 18B). In the duodenum, *Osm* levels increased during the treatment, reaching the highest value at day 5 and decreasing afterwards to values comparable to those found in steady state mice. On the contrary, *Osm* expression in the spleen remained at basal levels during the treatment.

To decipher the specific cellular source of OSM in the SI and based on previous reports showing that activated monocytes and macrophages are the main producers of this cytokine *(124, 125)*, different subsets of $CD11b^+$ APCs were sorted by flow cytometry from the SI. DCs, macrophages and monocytes from steady state mice and monocytes from anti-CD3 treated mice at day 5 were sorted by specific cell surface markers and subsequently analyzed for *Osm* expression. After the treatment no macrophages can be found in the SI, explaining the absence of this subset in the analysis performed. While *Osm* levels were non-detectable in DCs, both macrophages and monocytes expressed the transcript.

Nevertheless, *Osm* levels were greatly up-regulated in CX_3CR1^+ monocytes isolated from the SI after anti-CD3 treatment (Fig. 18C).

Altogether, these data suggest that OSM is a local, tissue-specific factor induced in the SI during the phase of resolution of inflammation after anti-CD3 treatment, the main sources of which are LP CX_3CR1^+ monocytes that are known to have tolerogenic properties (*see section 1.1.4*).

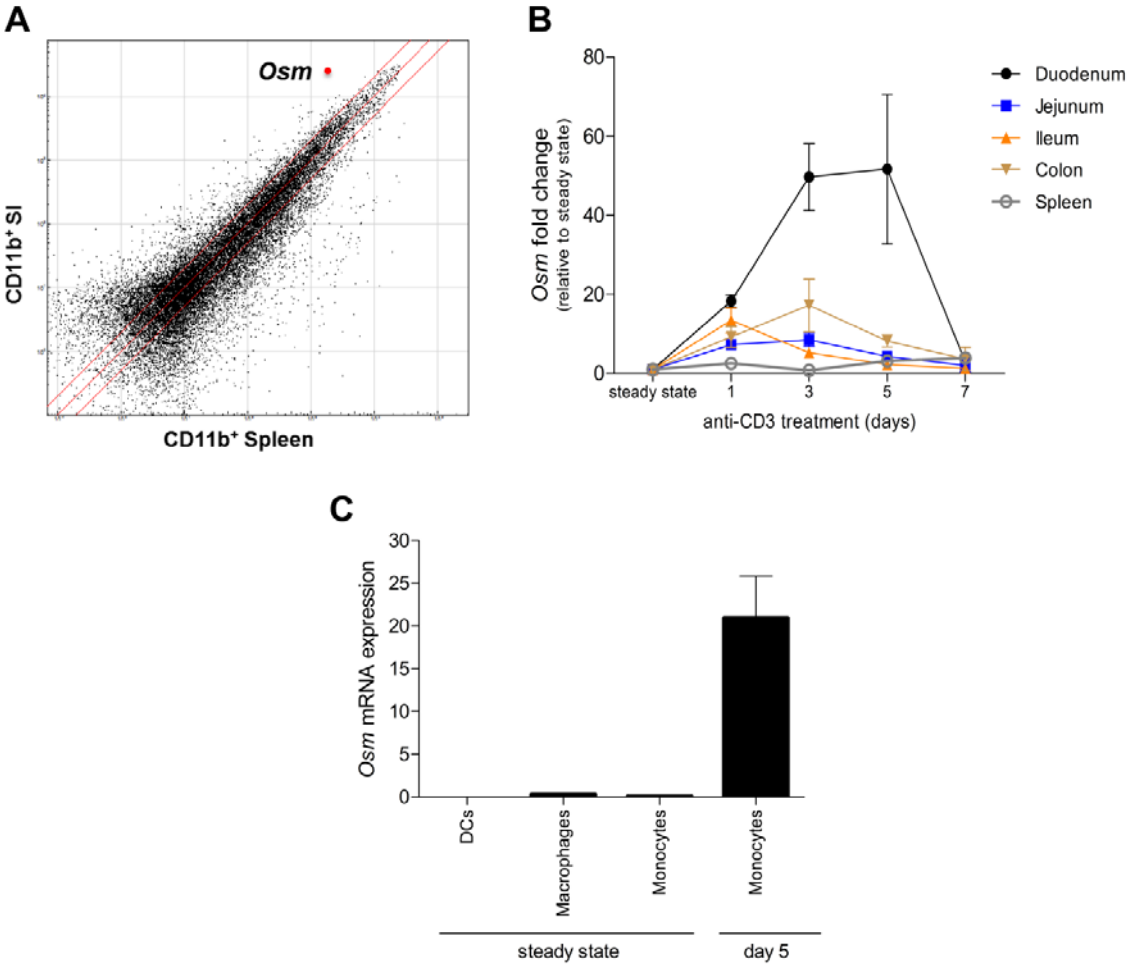

Figure 18. Monocytes in the SI are the main producers of *Osm* during anti-CD3 treatment. C57BL/6 mice were injected i.p. with 20µg anti-CD3 at days 1, 3 and 5. (A) Gene expression analysis comparing $CD11b^+$ myeloid cells isolated from the SI and from the spleen (control tissue) of CD3-specific antibody treated mice at day 5. (B) Time-course analysis of *Osm* mRNA expression by RT-PCR during anti-CD3 treatment in the different parts of the intestine and the spleen of treated mice, relative to steady state control mice. (C) *Osm* mRNA expression quantified by RT-PCR in different sorted $CD11b^+$ APCs isolated from the SI of mice at steady state (DCs: $CD11c^+MHCII^+CX_3CR1^-$, macrophages: $CD11c^+MHCII^+Ly6C^-CX_3CR1^+$, monocytes: $CD11c^+Ly6C^{+/-}CX_3CR1^+$) and treated mice at day 5 (monocytes: $CD11c^+Ly6C^{+/-}CX_3CR1^+$). Data are depicted as mean ± S.E.M. (n=4) and are representative of at least two independent experiments.

3.2.2 OSM M induces changes in the gene expression profile of mouse and human T_H17 cells in favor of a regulatory phenotype

OSM has been shown to play an important role in cytokine regulation, dampening pro-inflammatory mediators and inducing anti-inflammatory cytokines *(98, 102, 126)*. Because *Osm* showed a great up-regulation upon anti-CD3 treatment specifically in the SI, where T_H17 cells are known to accumulate, the effects that OSM may exert on T_H17 cells needed to be explored. *Osmr* expression in naïve T cells, T_H17 and Treg cells was quantified and T_H17 cell cultures showed the highest levels of the receptor (Fig. 19A). Therefore, T_H17 cells were stimulated with OSM and the changes in gene expression related to untreated cells were quantified. While the expression levels of *Rorc*, the master transcription factor for T_H17 cells, did not change, *Il17a, Tbx21* and *Csf2* expression were reduced in the OSM-stimulated cultures (Fig.19B). On the contrary, *Il10* expression was drastically increased. Human T_H17 cells responded similarly to OSM stimulation. *IL10* was up-regulated in the presence of OSM, while *IL17A* and *TBX21* levels were remarkably reduced (Fig. 19C). At the protein level, IL-10 production in human T_H17 cells was also induced by OSM (Fig. 19D) compared to untreated cells and to cells treated with IL- 1β, a reported inhibitor of IL-10 in human T_H17 cells *(110)*. As expected, the maximum IL-10 production was found in T_H17 cells treated with IL-27, a cytokine known to strongly induce IL-10 *(120)*. Notably, OSM also dampened the production of the pro-inflammatory cytokine GM-CSF by human T_H17 cells (Fig. 19D). Thus, our data indicate that OSM is capable of inducing changes in the genetic profile of murine and human T_H17 cells by decreasing the expression of pro-inflammatory genes and promotes the secretion of the anti-inflammatory cytokine IL-10 by human T_H17 cells.

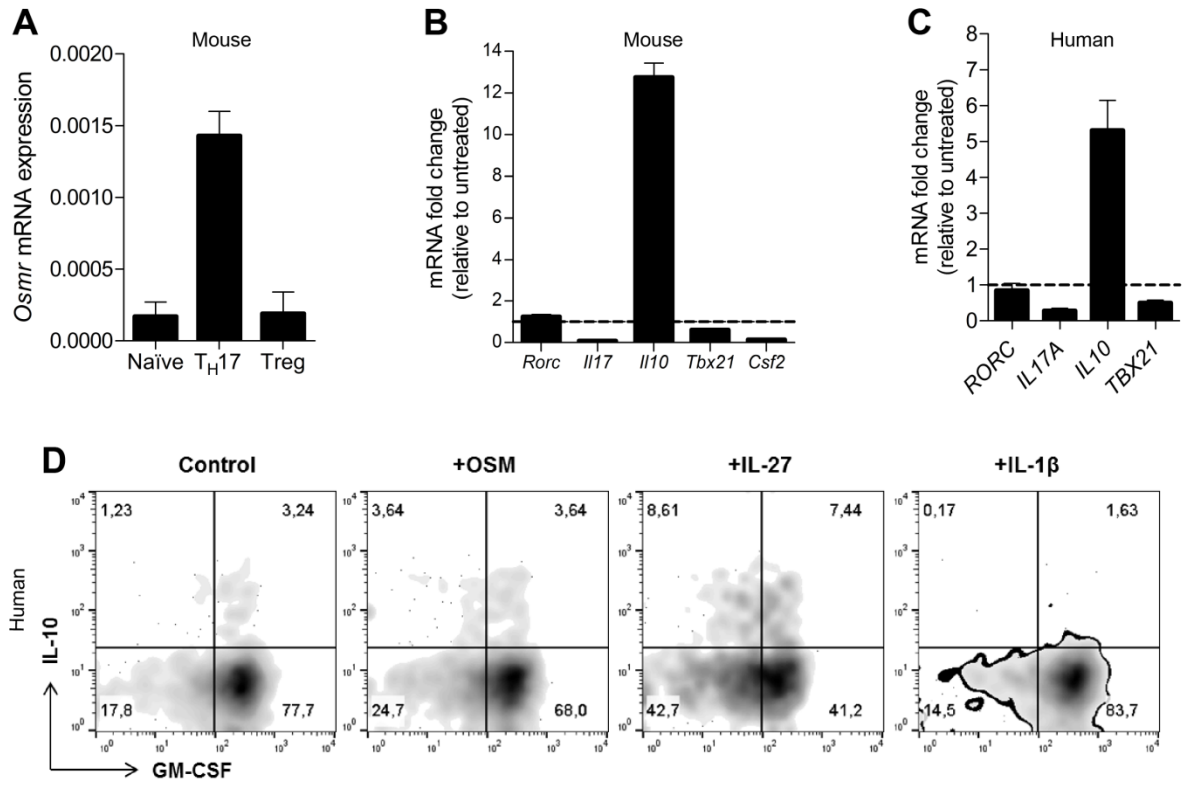

Figure 19. Mouse and human T_H17 cells respond to OSM *in vitro.* (A) Mouse naïve sorted $CD4^+CD25^-CD62L^+CD44^-$ T cells were stimulated *in vitro* with anti-CD3/CD28 and grown under T_H17 or Treg conditions for 5 days. *Osmr* expression was analyzed by qPCR and compared to naïve cells (mean ± S.D. of 3 independent experiments). (B) Mouse T_H17 cells were treated with 50 ng/ml OSM during the differentiation process (as in A). *Rorc*, *Il17a*, *Il10*, *Tbx21* and *Csf2* expression levels were quantified by qPCR (dotted line at 1 indicates the value of control untreated T_H17 cells). Data are presented as mean ± S.E.M. of at least 3 independent experiments. (C) Fresh *ex vivo* sorted human $CCR6^+CCR4^+CXCR3^-CD45RA^-CD25^-CD8^-$ T_H17 cells were stimulated with CD3 and CD28 mAbs for 48h and expanded for another 3 days in the presence of 50 ng/ml OSM. *RORC*, *IL17A*, *IL10* and *TBX21* expression levels were quantified by qPCR (dotted line at 1 indicates value of non-treated T_H17 cells). Human T_H17 cells were also stimulated with PMA/Ionomycin for 5 hours to detect intracellular levels of IL-17A, IL-10 and GM-CSF by FACS. One representative dot plot out of 3 independent experiments of flow cytometry analysis of IL-10 and GM-CSF assessed on T_H17 cells (gated on $IL17A^+$ $CD4^+$ T cells) is shown in (D).

Finally, to evaluate the scope that the changes observed in the gene expression profile of OSM-treated T_H17 cells may have in the functionality of these cells, an *in vitro* suppression assay was again performed. The suppressive capacity of OSM-stimulated T_H17 cells was compared to untreated T_H17 cells and to professional Tregs (Fig. 20A). As expected, professional Treg cells inhibited T-cell proliferation to the greatest extent. Nevertheless, addition of OSM significantly enhanced murine T_H17 suppressor functions in the various suppression assays performed (Fig. 20B).

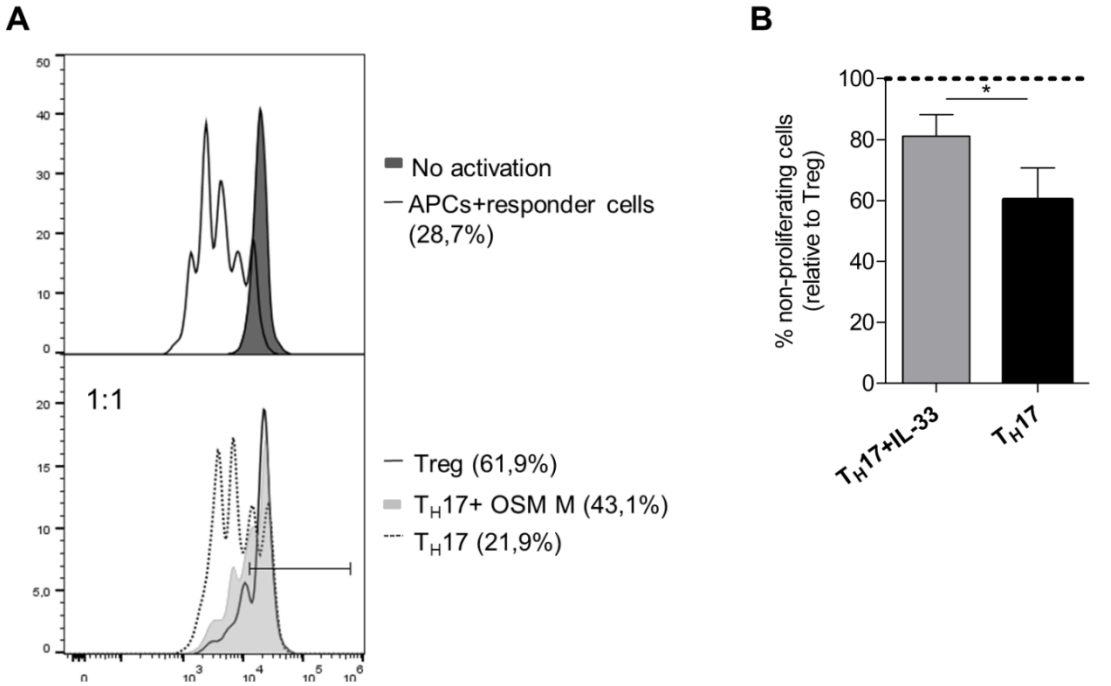

Figure 20. OSM promotes regulatory functions in T_H17 cells *in vitro.* Suppression assay in a mouse T cell culture was performed by using MACS enriched $CD25^+$ Treg cells and *in vitro* generated T_H17. T_H17 treated or not with 50ng/ml of OSM were sorted at day 4 for $CD4^+IL17eGFP^+FoxP3mRFP^-$.(A) After 3 days of co-culture, percentages of non-proliferating responder CFSE-labelled $CD4^+CD25^-$ T cells were quantified by FACS. (B) Bar histogram summarized frequencies of non-proliferating responder cells obtained in all the different assays, relative to professional Tregs (100% suppression ability, dotted line). Data are shown as mean ± S.E.M. of 4 independent experiments. *p<0,05 as calculated by paired Student's *t*-test.

Altogether, the results indicate that OSM exerts effects on both mouse and human T_H17 cells; it promotes a down-regulation of pro-inflammatory genes, an up-regulation of the anti-inflammatory cytokine IL-10 and it induces suppressive functions on T_H17 cells.

3.2.3 OSM attenuates EAE by restraining the inflammatory capacity of infiltrating T cells

EAE is the mouse model for MS, which is a demyelinating disease of the central nervous system (CNS) orchestrated by infiltrating auto-reactive T cells and endogenous glia *(127)*. T_H17 cells are known to infiltrate the CNS during the course of EAE and promote brain inflammation *(128)*. Anti-CD3 treatment attenuates EAE by re-directing to the SI MOG-specific T_H17 cells, meant to otherwise infiltrate the CNS *(47)*. In the SI, auto-reactive T_H17 cells convert to rT_H17 in response to the specific micro-environment composed of specialized cells with tolerogenic properties. We found OSM to be highly produced by tolerogenic monocytes of the SI LP during the phase of resolution of inflammation after anti-CD3 treatment *(see section 3.2.1)*. Thus, we hypothesized that OSM could be a SI-specific factor contributing to the conversion of T_H17 cells towards a regulatory phenotype. Indeed, OSM restrained T_H17 pathogenicity *in vitro* (*see section 3.2.2*). In addition, OSM has been

shown to be neuro-protective *(103)* and to positively affect the clinical symptoms in EAE *(99)*. However, the scope of OSM on infiltrating T cells has not yet been evaluated. Consequently, we next wanted to test if direct administration of OSM had protective effects on EAE-induced mice by modulating T_H17 responses. To address that question, IL17A-eGFPxFoxp3-mRFP double reporter mice were immunized with myelin oligodendrocyte glycoprotein (MOG) $_{35-55}$ peptide and treated before the onset, from day 7 to 12 post-immunization, with 10µg/day of OSM. Control mice were treated with vehicle during the same period of time. First clinical symptoms were observed on day 10 in control mice (15,4±1,4), whereas OSM treatment resulted in a later onset of the disease (18,5±1,1) and significantly lower disease severity (Fig. 21A). The control group experienced weight loss during the onset of EAE, while the OSM-treated group didn´t (Fig. 21B). Disease incidence in control mice was 80% at day 21, compared to 50% in OSM-treated mice (Fig. 21C). Taken together, these data suggested that although OSM-treated mice were also susceptible to EAE, OSM treatment resulted in reduced severity and attenuated clinical symptoms in MOG_{35-55} _immunized mice.

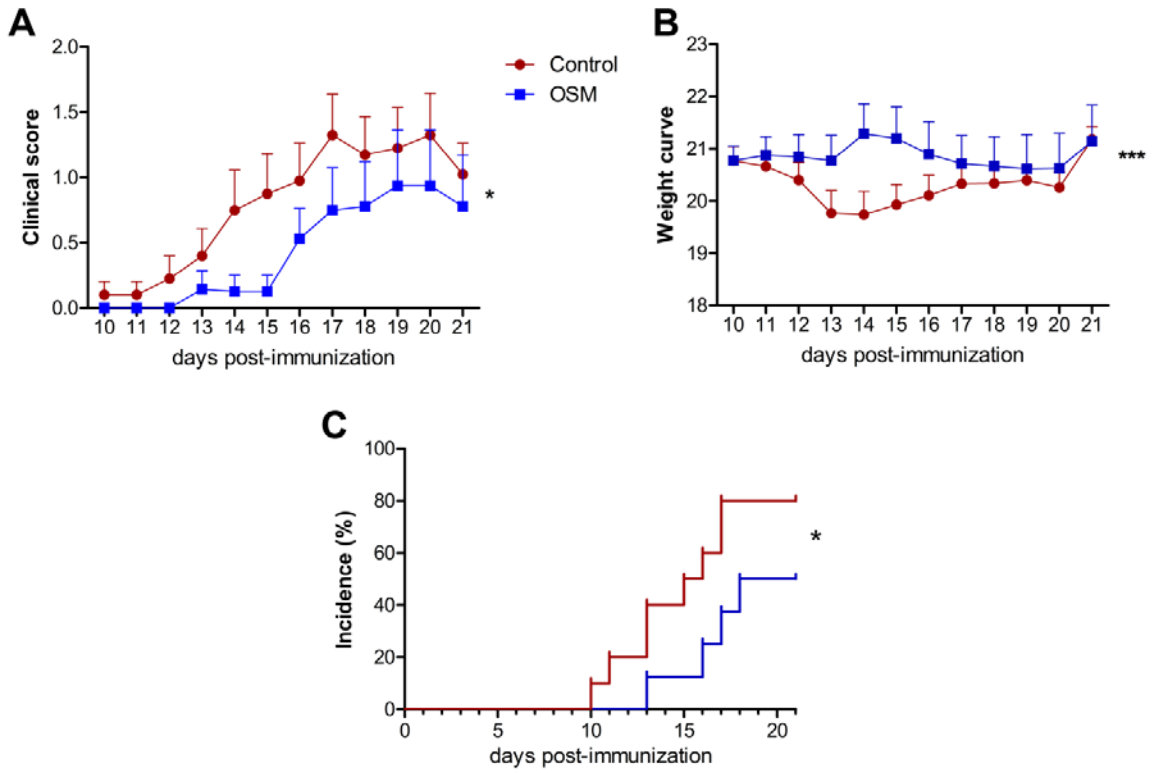

Figure 21. OSM treatment ameliorates EAE. IL17A-eGFPxFoxp3-mRFP double reporter mice were immunized with MOG_{35-55} peptide and treated on days 7 to12 with 200µl/day of isotonic NaCl solution (control group; n=10) or with 10µg/day of OSM (OSM-treated group; n=8).Mice were monitored daily for clinical symptoms of EAE. Clinical scores for both groups are shown in (A), weight curves are shown in (B) and the incidence in each group is shown in (C). Data are shown as mean ± S.E.M. and are representative of 2 independent experiments. A and B: *p<0,05 and ***p<0,005 as calculated by Mann-Whitney U-test. C:*p<0,05 as calculated by Gehan-Breslow-Wilcoxon test and Mantel-Cox test.

Accumulation of infiltrating inflammatory cells in the CNS is a hallmark of EAE. To assess whether the differences observed in the clinical course of EAE between groups were due to the effect of OSM on infiltrating T cells, both spleen (as a SLO) and CNS were isolated from each mouse on day 21 post-immunization and single cell suspensions were obtained. $CD45^+CD4^+$ T cells were quantified for each tissue and mouse and total numbers were compared between groups. A slight, but not significant decrease was found in total splenic T cell numbers (Fig. 22A), while absolute numbers of T cells were significantly reduced in the CNS of the OSM-treated group (Fig. 22B), indicating less tissue infiltration. The balance between T_H17 and Treg cells plays an important role in the development of MS and EAE *(129)*. Thus, the effect of OSM on the number of T_H17 and Treg cells was also evaluated by flow cytometry. The percentage of splenic IL-17-secreting T_H17 cells in EAE mice was similar in both animal groups, while the frequency of splenic Tregs was significantly lower in OSM-treated mice (Fig. 22C). However, no differences between groups were observed on frequencies of T_H17 and Treg cells in the CNS (Fig. 22D). These results indicated that OSM treatment restrained the accumulation of infiltrating T cells without changing the proportion between T_H17 cells and Tregs in the CNS.

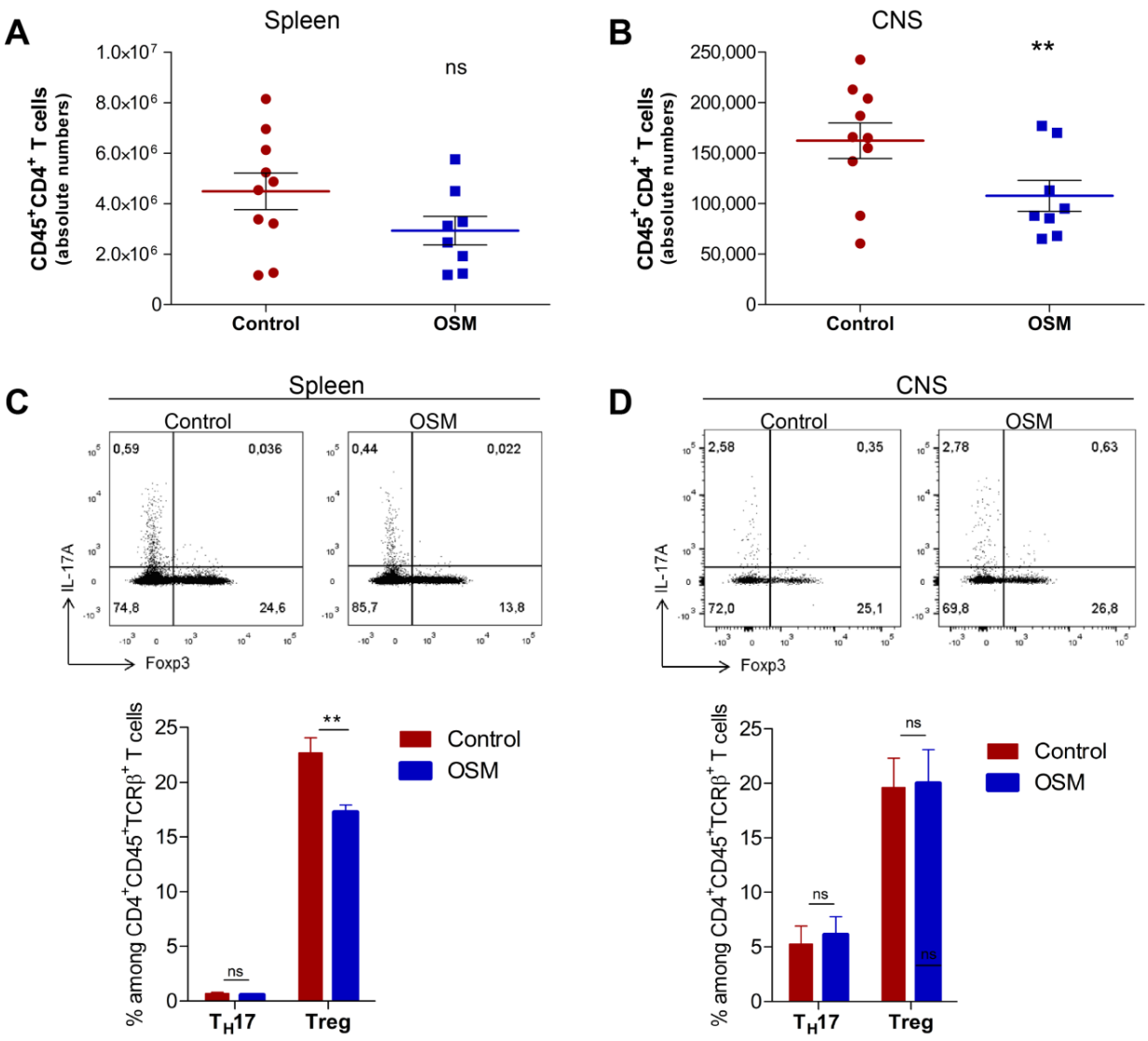

Figure 22. OSM-treated mice show reduced numbers of infiltrating T cells infiltrating. On day 21 post-immunization IL17A-eGFPxFoxp3-mRFP double reporter mice (control group, n=10 and OSM-treated group, n= 8) were sacrificed. Single cell suspensions were obtained from each mouse and total T cell numbers from spleen (A) and CNS (B) were quantified by MACSQuant (each dot represents one mouse). Frequencies of IL-17A-eGFP$^+$ cells (T_H17) and Foxp3-mRFP$^+$ cells (Tregs) from the spleen (C) and the CNS (D) were analyzed by FACS and are shown as a representative dot plot of each tissue and animal group and as mean ± S.E.M. Data are representative of 2 independent experiments. **p<0,01 as calculated by unpaired Student's *t*-test. ns, not significant.

IFN-γ and GM-CSF derived from over-reactive T cells are considered two key pro-inflammatory cytokines mediating neuro-inflammation *(128, 130–132)*. To determine whether the protective function of OSM in EAE was also associated with modulation of inflammatory cytokines derived from infiltrating T cells, frequencies of IFN-γ$^+$ and GM-CSF$^+$ T cells were analyzed by flow cytometry. OSM treatment resulted in similar production of IFN-γ and GM-CSF by splenic T cells (Fig. 23A), but, interestingly, reduced levels of T cell derived-IFN- γ were found in the CNS of OSM-treated animals (Fig. 23B).

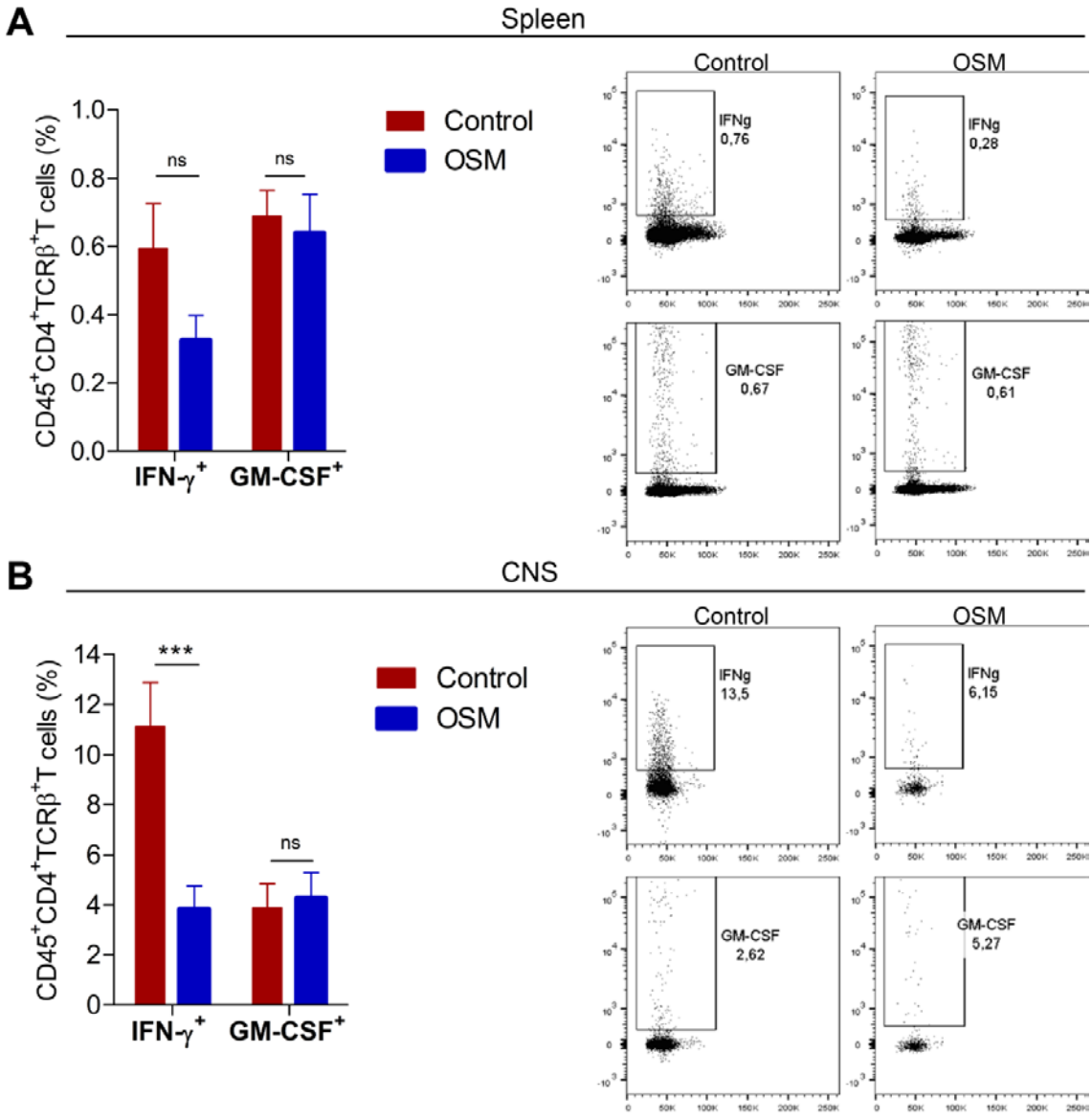

Figure 23. OSM-treatment limits the production of IFN-γ by T cells infiltrating the CNS. On day 21 post-immunization IL17A-eGFPxFoxp3-mRFP double reporter mice (control group, n=10 and OSM-treated group, n=8) were sacrificed and single cell suspensions were obtained from the spleen and the CNS. $CD45^+CD4^+TCR\beta^+$ T cells were analyzed by FACS for the expression of the pro-inflammatory cytokines IFN-γ and GM-CSF. Frequency of T cells expressing IFN-γ and GM-CSF in the spleen (A) and the CNS (B) are shown as a representative dot plot of each animal group and as mean ± S.E.M. Data are representative of 2 independent experiments. ***p<0,005 as calculated by unpaired Student's *t*-test. ns, not significant.

$IFN\text{-}\gamma^+IL\text{-}17A^+$-double producing cells are key drivers of MS and EAE *(22, 41, 45)*, among other autoimmune disorders. Similarly, production of GM-CSF by T_H17 cells has recently been associated with their pathogenicity in tissue-specific autoimmunity *(133, 134)*. FACS analysis comparing peripheral T_H17 cells in EAE mice treated or not with OSM yielded similar results. Although OSM-treated animals presented a tendency to reduced T_H17-derived IFN-γ levels, the differences were not significant, as they were not significant for GM-CSF production (Fig. 24A). On the contrary, in the CNS of OSM-treated mice levels of

IFN-γ secreted by T_H17 cells were significantly decreased compared to control mice and GM-CSF production in this specific T cell subset was also diminished (Fig. 24B). These data suggested that OSM regulates the inflammatory response in the CNS, by limiting the pathogenic capacity of infiltrating T cells, particularly of infiltrating T_H17 cells.

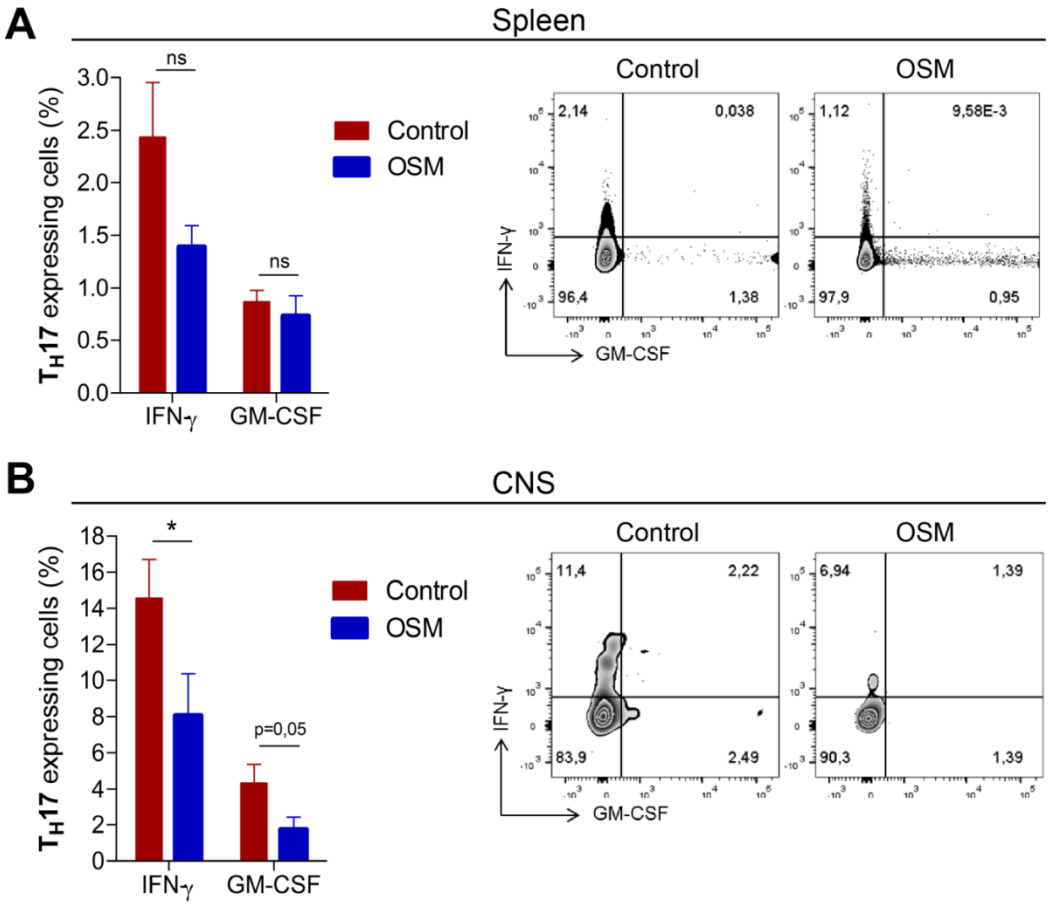

Figure 24. OSM treatment restrains the inflammatory capacity of T_H17 cells infiltrating the CNS. On day 21 post-immunization IL17A-eGFPxFoxp3-mRFP double reporter mice (control group, n=10 and OSM-treated group, n=8) were sacrificed and single cell suspensions were obtained from the spleen and the CNS. $CD45^+CD4^+TCR\beta^+$ IL-17A-$eGFP^+$ cells (T_H17 cells) were analyzed by FACS for the expression of the pro-inflammatory cytokines IFN-γ and GM-CSF. Frequency of T_H17 cells expressing IFN-γ and GM-CSF in the spleen (A) and the CNS (B) are shown as a representative dot plot of each animal group and as mean ± S.E.M. Data are representative of 2 independent experiments. *p<0,05 as calculated by unpaired Student's *t*-test. ns, not significant.

4 Discussion

By using the anti-CD3 model, but also in a model of sepsis and during influenza A viral infection (H1N1), it was recently demonstrated that the SI controls potentially inflammatory T_H17 cells in order to avoid exacerbated immune responses *(47)*. However, the underlying mechanisms governing this process are only partially understood. IL-10 *(49, 121)* and TGF-β *(48)* are two key immune-regulatory mediators known to limit T_H17 cell pathogenicity that are produced by a great range of cells and are not specifically induced in the SI. In recent years, elucidating local factors mediating T cell responses at the affected tissue has become an important topic in immunology. For example, similar to IL-33, IL-18 is an epithelial-derived IL-1 family member, that has been recently shown to be specifically produced in the intestine, where it controls differentiation of T_H17 cells and functionality of $Foxp3^+$ Tregs *(135)*. A proper understanding of local factors controlling T_H17 cells may help fighting chronic inflammatory processes and autoimmune diseases driven by this T-cell subset, such as MS *(136)*, rheumatoid arthritis *(34)* and IBD *(137)*.

4.1 IL-33 in control of T_H17 cells

In recent years, the IL-33/ST2 axis has emerged as a key modulator of inflammation in epithelial tissues *(112)*, particularly in the gut mucosa, where IL-33 seems to exert dichotomous roles *(138)*. Recently, the capacity of IL-33 to modulate $CD4^+$ T cell polarization to different phenotypes in favor of a healthy immunological state has become of great interest *(139)*.

In this study, IECs were shown to be the main source of IL-33 upon anti-CD3 treatment. Although IECs are $CD3^-$ and therefore cannot be directly activated by CD3-specific antibodies to release IL-33, several studies have shown that anti-CD3 treatment activates $CD3^+$ intestinal IELs, leading to the induction of cytotoxic pathways and consequently to tissue damage *(62, 70, 140–142)*. IL-33 is known to be released by epithelial cells upon tissue damage or infection and to function as an alarmin, alerting the immune system to mount an appropriate response *(82, 86, 143)*. It has recently been shown by Dr. Bayat Sarmadi from our group that $CD3^+$ IELs harbored granzyme-containing granules that were released upon administration of CD3-specific antibody. Apoptosis of IECs upon anti-CD3 treatment was mediated by IEL-derived, granzyme-dependent mechanisms *(62, 140, 142)* and by using $granzyme^{-/-}$ mice , Dr. Bayat Sarmadi showed that IL-33 up-regulation upon anti-CD3 administration was strongly abrogated in these mice, indicating that $granzyme^+$ IELs were in fact responsible for the induction of IL-33 in IECs *(144)*. However, since IL-33 expression was not completely abrogated in $granzyme^{-/-}$ mice, it could not be ruled out that other mechanisms also contribute to the induction of IEC-derived IL-33. Interestingly, these

granzyme bearing IELs are more abundant in the upper parts of the SI, which explains the specific localization of IL-33 up-regulation that coincides with the localization of granzyme$^+$ IELs (duodenum and jejunum). It has also been shown that IELs undergo apoptosis upon anti-CD3 treatment and can therefore degranulate only once *(140)*. This could explain that the peak of IL-33 was found after the first injection with CD3-specific antibody and less up-regulation was observed after each subsequent injection. Altogether, it suggests an indirect mechanism of IEC-derived IL-33 release mediated by CD3$^+$granzyme$^+$ IELs, which are indeed activated via administration of CD3-specific antibody. Therefore, IL-33 was identified here as a tissue-specific factor produced by IECs, specifically in the SI and the rapid and strong IL-33 response shown by epithelial cells in this study underlines previous reports describing the role of IL-33 as an alarmin *(113, 145)*.

Recently, it has been shown that IL-33 promotes resolution of inflammation by enhancing type 2 responses and by increasing ST2$^+$ regulatory T cells in intestinal epithelial sites *(118, 146)*. In this work, we describe ST2 expression in T_H17 cells *in vivo* for the first time. ST2$^+$ T_H17 cells were found to be specifically located in the spleen. Notably, IL-33 remained at low levels in the spleen during anti-CD3 treatment, comparable to untreated controls. However, around 90% of ST2$^+$ T_H17 cells co-expressed CCR6, a receptor known to direct these cells particularly to the proximal part of the SI, the region showing the strongest up-regulation of the CCR6-ligand CCL20 within the intestine *(47)*. Interestingly, the up-regulation of CCL20 by IECs upon anti-CD3 treatment, similar to IL-33, was also dependent on the activation of granzyme$^+$ IELs, as shown by Dr. Bayat Sarmadi *(144)*. This explains why IL-33 induction in the SI after anti-CD3 injection occurred in a gradient-like fashion from proximal to distal, similar to CCL20, coinciding with the spatial localization of T_H17 cells. Very low frequencies of ST2$^+$ T_H17 cells were detected in the SI. However, earlier studies showed that ST2 is internalized within 30 minutes upon IL-33 encounter *(92)*. Accordingly, it is likely that splenic ST2$^+$ T_H17 cells rapidly internalize ST2 after arrival in the SI, where IL-33 is abundantly expressed. In support of this notion, ST2 internalization was shown to be dependent on glycogen synthase kinase 3 beta activity *(92)*; which is known to be particularly high in differentiated pathogenic T_H17 cells when compared to naïve T cells or Tregs *(147)*. Further analyses of the T_H17 cell population in the SI at shorter time-points after CD3-specific antibody injection would be needed to find out whether ST2 is expressed by newly accumulated T_H17 cells. These findings suggest a spatial separation of ST2 induction in the spleen and the provision of IL-33 by the SI epithelium, which may be a mechanism to fine-tune the effects of IL-33 on T_H17 cells.

IL-17A has been shown to exert tissue-protective functions and to be a protective cytokine in models of intestinal inflammation *(20)*. T_H17 cells driving tissue inflammation express IL-17A

together with IFN-γ, TNF-α and/or GM-CSF and it is the expression of these cytokines and not of IL-17A that confers T_H17 cells pro-inflammatory abilities (*see section 1.1.3*). It has recently been published that ST2 deficiency led to an increased colitogenic potential of $CD4^+$ T cells *(114)* and T cells driving colitis are known to express high amounts the pro-inflammatory cytokines IFN-γ, TNF-α and GM-CSF *(36, 137, 148, 149)*. The results in our model of intestinal inflammation were in line with this observation. *St2*$^{-/-}$ mice showed a more severe clinical course during anti-CD3 treatment compared to WT mice, featured by a greater body weight loss, pronounced small intestinal injury with a higher degree of inflammation and increased *Il17a*, *Ifng* and *Tnf* levels in the duodenum. Remarkably, ST2 deficiency also led to a greater pathogenic phenotype of T_H17 cells accumulating in the SI, showing increased frequencies of both IL-$17A^+$IFN-γ^+ and IL-$17A^+$TNF-α^+ T cells. IL-$17A^+$IFN-γ^+ double producing T_H17 cells are pro-inflammatory cells that have been strongly linked to autoimmune diseases *(41, 150, 151)*. Schiering *et al*. showed that the increased pathogenic T-cell activity in the *St2*$^{-/-}$ mice was due to a reduced $Foxp3^+$ T cell population in the colon, unable to control the intestinal effector T-cell response. They concluded that the IL-33/ST2 axis promoted tissue-specific accumulation and maintenance of Treg cells in the intestine under inflammatory conditions. On the contrary, in the present study, equivalent frequencies of Foxp3-expressing cells were observed in *St2*$^{-/-}$ and WT mice in the SI upon inflammation. Also, a specific increase of T_H17 cells (ROR-γt^+ T cells and IL-$17A^+$ T cells), both in frequencies and absolute numbers, was observed in *St2*$^{-/-}$ compared to control littermates. Therefore, the elevated frequencies of intestinal T_H17 cells, which in turn showed and exacerbated pathogenic phenotype (depicted by increased frequencies of IFN-γ and TNF-α production) were not the result of a diminished Treg cell population in our model. These results suggested that IEC-derived IL-33 acts directly on T_H17 cells, at least in the SI, by restraining their pro-inflammatory capacity. It has been shown by others that Tregs are particularly abundant in the colon *(152)*. After anti-CD3 treatment, 75% of the T cells in the SI were T_H17 cells and only around 5% were Tregs. It might be that the IL-33/ST2 axis acts on the T cell subset prominently enriched in the specific condition under study, promoting regulatory functions in the intestine in a cell-intrinsic manner. The ST2 expression profile shown by Tregs and T_H17 cells during anti-CD3 treatment further supported this notion. While ST2 expression was maintained at around 10% in splenic $CCR6^-$ Tregs and went down from 20% to 5% in Tregs in the SI, ST2 expression was highly and specifically induced in splenic $CCR6^+$ T_H17 cells, reaching the 30% of the total T_H17 cell population. ST2 was expressed in the Treg cell population under homeostatic conditions, but it was only expressed under inflammatory settings in splenic $CCR6^+$ T_H17 cells. Together, our study complements previous findings by extending the role of IL-33 beyond the induction and

maintenance of Tregs in the colon *(118)* and in the visceral adipose tissue *(153)* to the conversion of pro-inflammatory T_H17 cells into rT_H17 cells in the SI.

IL-33 stimulation of splenic T_H17 cells isolated from anti-CD3-treated mice, with a significant frequency of the cells being $ST2^+CCR6^+$, led, indeed, to changes in the expression levels of two key cytokines modeling inflammation. A reduction in the *Ifng* levels expressed by T_H17 cells was observed, while *Il10* expression was significantly increased, in a dose-dependent manner, upon IL-33 stimulation. Of note, IL-10 is known to be one of the major players controlling homeostasis in the SI *(154)* and, specifically, controlling previously committed pathogenic T_H17 cells *(47, 49, 121)*.

A dose-dependent increase in IL-17A expression has already been described, when colitogenic T cells are IL-33 and TCR co-stimulated. *(155)*. We also observed an increase in *Il17a* expression when *in vitro* cultured T_H17 cells were stimulated with IL-33, which seemed contradictory to what we observed *in vivo* (increase of IL-17A production in the absence of IL-33/ST2 axis). We cannot rule out the contribution of other signals different from IL-33 or compensatory mechanisms to our *in vivo* observations regarding IL-17A expression. The level of complexity in an *in vivo* system cannot be properly addressed by using an *in vitro* approach. Nevertheless, T_H17 cells responded *in vitro* to IL-33 stimulation by down-regulating pro-inflammatory genes such as *Tbx21*, *Ifng* and *Csf2,* similar to what we observed *in vivo*. Importantly, stimulation of T_H17 cells with IL-33 led to an up-regulation of the anti-inflammatory gene *Il10*. Induction of *Il10* by IL-33 signaling in T_H17 cells was concurrent with the induction of a combination of transcription factors known to mediate IL-10 production in T cells. Among the transcripts positively regulated upon IL-33 stimulation, together with *Il10*, were *Ahr*, *Ikzf3*, *Irf4* and *Jun*. Moreover, *Ahr* expression significantly correlated with the expression of *Il10* in the cultures analyzed. Ahr has already been shown to mediate T_H17 cell plasticity, enhancing IL-10 production and being involved in the conversion of T_H17 into regulatory T cells *(48)*. Similarly, Aiolos, encoded by *Ikzf3,* has been recently reported to induce IL-10 expression in $CD4^+$ effector T cells, conferring them intrinsic regulatory abilities *(121)*. In another molecular approach, the transcription factor AP-1, encoded by *Jun*, has been shown to cooperate with IRF4, a T helper transcription factor, to promote the transcription of the *Il10* gene, which presents two IRF4 binding sites with associated AP-1 motifs *(122)*. In accordance with that, it was not only found an up-regulation of AP-1, but also an up-regulation of IRF4 in the T_H17 cultures upon IL-33 stimulation. AP-1 and IRF4 are also known to be downstream of the IL-33 signaling cascade *(153, 156, 157)*. The results shown here are of correlative nature and further experiments need to be done in order to provide strong evidence into the mechanisms by which IL-33 promotes IL-10 expression. We plan to address this by using KO mice for the transcription factors under

study. IL-33 stimulation of *Ahr*$^{-/-}$, *Ikzf3*$^{-/-}$, *Jun*$^{-/-}$ and *Irf4*$^{-/-}$ T_H17 cells would not lead to IL-10 up-regulation if the hypothesized mechanisms for IL-10 induction are indeed correct.

Importantly, in human T_H17 cells, *in vitro* IL-33 stimulation also promoted an increase in *IL17A* and *IL10* expression, an increase in IL-10 production, down-regulation of *TBX21* expression and reduction of GM-CSF secretion. GM-CSF has been shown to be a key cytokine for T helper cells involved in chronic immune disorders, as GM-CSF-producing T cells exert a pathogenic role in the inflamed brain of MS patients *(158)*. On a functional level, mouse T_H17 cells stimulated with IL-33 were able to partially suppress the proliferation of responder T cells *in vitro*, suggesting the acquisition of a regulatory phenotype. However, co-transfer experiments with pathogenic T_H7 cells (known to promote inflammation in hosts) together with IL-33-treated T_H17 cells in RAG$^{-/-}$ recipient mice (which lack mature lymphocytes) would be needed to test the *in vivo* suppressive functions of IL33-treated T_H17 cells.

In summary, our results extend the spectrum of IL-33 functions by showing that IEC-derived IL-33 acts on T_H17 cells via ST2, reprograms their cytokine profile and enables them to exert regulatory functions. Our *in vivo* studies performed with *St2*$^{-/-}$ mice suggest this novel role for the IL-33/ST2 axis in restraining the accumulation of pathogenic T_H17 cells in the SI during inflammation, with physiological implications in the clinical course observed in mice.

4.2 OSM in control of T_H17 cells

The normal development of an inflammatory response must be rapidly followed by the engagement of a feedback system to minimize adventitious tissue damage and regulate eventual return to homeostasis. Even though the discovery of OSM dates back 25 years, its involvement in inflammation and disease development is still incompletely understood. However, it has recently been associated to the wound healing process and attenuation of the inflammatory response *(102, 159)*, especially in the intestine *(100, 101)* and the CNS *(103–105)*.

In this study OSM was found to be specifically up-regulated in the duodenum upon repetitive anti-CD3 injections, reaching its highest values on day 5 of the treatment, during the phase that corresponds to the resolution of inflammation. Work done by Dr. Bayat Sarmadi in our group demonstrated that intestine-resident macrophages, but not DCs, completely disappeared from the SI shortly upon injection with CD3-specific antibody. This was due to cell apoptosis induced again by IELs-derived granzyme. Only during resolution of inflammation did CX_3CR1^+ monocytes start to repopulate the intestine and develop again

into sessile CX_3CR1^+ macrophages later on. Accordingly, the main sources of OSM were LP CX_3CR1^+ monocytes, which have also previously been shown to be able to suppress pro-inflammatory T cells and to have regulatory functions in the intestine *(160, 161)*. Again, similar to IL-33, the distinct parts of the intestine where T_H17 cells accumulate during CD3-specific antibody treatment coincide with the anatomical localization of the cytokine under study.

Interestingly, T_H17 cells were shown here to express the OSMRβ *in vitro*, suggesting that T_H17 cells could indeed respond to OSM. In fact, several studies showed the modulatory effects that OSM have on cytokine expression in several cell types *(96, 98, 99)*, but no reports explored the role of OSM signaling in T_H17 cells. The results depicted here show that OSM stimulation of *in vitro* cultured T_H17 cells led to a down-regulation of *Il17*, together with the pro-inflammatory genes *Tbx21* and *Csf2* (encoding for the proteins Tbet and GM-CSF, respectively). Interestingly, expression of Tbx21 by T_H17 cells has been linked to chronic inflammatory processes and tissue-specific auto-immunity *(41–43)* that stem from the increased pathogenic potential of double producing T_H17 cells (ROR-γt^+/$Tbx21^+$ that can therefore produce both IL-17A and IFN-γ). Similarly, expression of GM-CSF by T_H17 cells has also been linked to an exacerbated pro-inflammatory phenotype thereby contributing to autoimmune disorders *(130, 133)*. In addition to reducing the inflammatory capacity of T_H17 cells *in vitro*, OSM stimulation markedly increased the expression of *Il10*, which is, as already mentioned, a potent anti-inflammatory cytokine in control of tissue homeostasis. The data obtained from human T_H17 cell cultures was also in line with previous reports and emphasized the ability of OSM on limiting the secretion of pro-inflammatory cytokines while inducing those with anti-inflammatory properties *(98, 99)*. Human T_H17 cells responded to OSM stimulation by reducing the expression of *TBX21* and *IL17* and by increasing the expression of the anti-inflammatory gene *IL10*, resembling the effects of OSM on mouse T_H17 cells. Importantly, human T_H17 cells stimulated with OSM not only changed the gene expression profile in favor of anti-inflammatory settings, but also showed greater ability to produce IL-10 while producing impaired amounts of GM-CSF. GM-CSF has already been presented here as a key cytokine for T cells in mediating tissue inflammation and IL-10 over-expression in particular is a phenotypic feature linked to immune-suppressive functions. In this regard, mouse T_H17 cells stimulated with OSM were able to effectively suppress the proliferation of responder T cells *in vitro*, resembling the suppressive capacity attributed to professional Tregs and suggesting the acquisition of a proper regulatory phenotype also at the functional level. However, further studies will need to be performed in order to address if SI T_H17 cells express OSMRβ *in vivo* upon anti-CD3 treatment. In addition, similar to what has been proposed above for IL-33, co-transfer experiments with pathogenic T_H17 cells

together with OSM-treated T_H17 cells in $RAG^{-/-}$ recipient mice would be needed to test the *in vivo* suppressive functions of OSM-treated T_H17 cells.

Recent publications have highlighted the neuroprotective role of OSM *(103, 104)*. In line with this, OSM administration in EAE-induced mice resulted in an attenuated course of the disease. OSM-treated mice showed a significantly delayed-onset of EAE, with no weight loss associated to the onset, lower clinical scores and reduced incidence. Although the etiology of EAE is not completely understood, it is believed that myelin-specific $CD4^+$ T cells play a central role in initiating and orchestrating CNS inflammation. In this scenario, $CD4^+$T cells, activated in the periphery, infiltrate the CNS, where, by secreting pro-inflammatory cytokines they start an inflammatory cascade *(162)*. Interestingly, total $CD4^+$ T cell numbers were significantly reduced in the CNS of OSM-treated animals, but not in the periphery. This suggested that OSM restrained T cell infiltration, a key process in the initiation of EAE, and explained the reduced disease severity observed in the OSM-treated group.

T_H1 cells were thought originally to be the main pathogenic T cells in EAE and MS and the contribution of IFN- γ, a T_H1-derived cytokine, to CNS inflammation was well-stablished. However, activator of transcription-1 $(STAT1)^{-/-}$ mice lacking T_H1 cells were later found to develop more severe EAE *(163)*. Since the discovery of IL-23 , a cytokine promoting T_H17 expansion and acquisition of a pro-inflammatory phenotype, characterized by the expression of ROR-γt together with Tbx21 and secretion of IL-17A together with IFN-γ (T_H1/ T_H17 phenotype), a number of studies have highlighted the central role of T_H17 cells in the development and pathogenesis of EAE *(129, 136, 150, 162)*. In addition to the inflammation induced by antigen-specific T_H17 cells, also a disturbance in frequencies and/or functionality of Tregs contribute to disease severity *(129)*. Tregs have suppressor activities and play a critical role in the maintenance of self-tolerance. Tregs also assist in controlling the activation and expansion of auto-reactive T cells and protect against tissue injury via various mechanisms, such as cell contact-dependent processes and secretion of IL-10 and TGF-β, as previously mentioned. All this speaks for the importance of the dynamic T_H17/Treg balance in providing immunological mechanisms that induce and regulate autoimmunity. However, frequencies of T_H17 cells and Tregs in the CNS of OSM-treated mice did not differ from the control group, indicating that the mitigation of EAE observed upon OSM administration was not a consequence of an impaired T_H17/Treg ratio in the affected organ. In addition, while frequencies of T_H17 cells in the periphery did not change between groups, Treg percentages in the spleen of OSM-treated mice were found diminished and therefore the T_H17/Treg ratio impaired in favor of a T_H17 response. These results were presumably contradictory with the amelioration observed in the clinical course of the OSM-treated group,

but further analysis of the $CD4^+$ T cell population from control mice and from mice treated with OSM in terms of cytokine expression shed light into this apparent contradiction.

IFN-γ and GM-CSF are two pro-inflammatory cytokines secreted by T cells that have been strongly linked to CNS inflammation *(45, 127, 164)*. Normally, T cells do not traverse the blood-brain barrier at appreciable levels and, as such, IFN-γ and GM-CSF are generally undetectable within the CNS. Nevertheless, in EAE, T-cell traffic across the blood-brain barrier increases considerably, thereby exposing neuronal and glial cells to the potent effects of T cell-derived IFN-γ and GM-CSF. Anti-CD3 treatment has been shown to effectively limit T_H17 infiltration in the CNS during EAE by re-directing myelin-specific T_H17 cells to the SI *(47)*, attenuating thereby disease severity. OSM is presented here as a tissue-specific factor promoting the conversion from pathogenic T_H17 cells to rT_H17 cells, occurring in the SI upon anti-CD3 treatment. Consequently, OSM treatment in EAE-induced mice would not only be effective in attenuating the course of the disease, as it has been already discussed, but it would also specifically restrain T_H17 pathogenicity at the affected organ. Interestingly, OSM administration did not result in significant changes in the production of IFN-γ or GM-CSF by peripheral T cells, but T cell-derived IFN-γ levels were effectively reduced specifically in the CNS of OSM-treated mice. However, as previously mentioned, the main pathogenic T cell subset mediating EAE is the T_H17-cell subset. T_H17 cells are known to induce the disruption of the blood-brain barrier *(136)* and T_H17 cell-derived IFN-γ and GM-CSF have been reported to play an important role in the pathogenesis of these demyelinating disorder *(131, 133)*. Our *in vitro* results suggested that OSM limited the pro-inflammatory capacity of T_H17 cells. Accordingly, OSM-treated mice exhibited reduced frequencies of $IFN\text{-}\gamma^+$ and $GM\text{-}CSF^+$ T_H17 cells in the CNS, suggesting that OSM indeed restrained T_H17 pathogenicity at the affected tissue. However, no statistically significant differences were found comparing peripheral T_H17 cell population between control and OSM-treated groups.

Collectively, these data indicated that treatment with OSM alleviates the signs associated with EAE in mice by limiting the infiltration of $CD4^+$ T cells into the CNS and by suppressing T_H17 pro-inflammatory responses at the affected organ, which consequently limited the exposure to pro-inflammatory cytokines that mediate tissue damage. Although Treg numbers were not increased in the CNS of OSM-treated mice and, thus, a decrease in the T_H17/Treg ratio was not involved in the immunomodulatory role exerted by OSM, a deeper analysis of the Treg population in terms of functionality would be of great interest. Nevertheless, Tregs expressed negligible amounts of OSMRβ *in vitro* and therefore are not expected to respond to OSM. Also, it would be interesting to quantify IL-10 expression in T_H17 cells infiltrating the CNS in both control and OSM-treated animals and, so, test *in vivo* the ability to induce IL-10

production that OSM showed *in vitro*. It has not been assessed so far, because of the half-life and rapid secretion of IL-10 that make IL-10 detection difficult, especially *in vivo.* Nevertheless, we plan to do so by using a reporter mouse strain that couple IL-10 expression to GFP, so that IL-10 expression can be easily quantified by flow cytometry.

In summary, our results demonstrate that OSM is a tissue-specific factor expressed by tolerogenic monocytes in the LP during resolution of inflammation that acts on T_H17 cells via OSMRβ, reprograms their cytokine profile and enables them to exert regulatory functions. In addition, this study extends the spectrum of the neuroprotective functions that have been recently attributed to OSM by showing specific immunomodulatory effects in the CNS of EAE-induced mice. It is shown here for the first time that OSM treatment limits T_H17 pro-inflammatory capacity *in vivo*, leading to an attenuated clinical course of EAE.

4.3 Concluding remarks

The findings discussed in this study helped to identify two signals specifically expressed in the SI upon strong inflammation and that control T_H17 responses: IL-33, as a factor derived from the tissue itself and OSM, as a factor derived from hematopoietic LP cells. These findings highlight once more the role of the SI as an organ with systemic immune-regulatory functions and mechanistically explain the conversion of pro-inflammatory T_H17 into rT_H17 cells, occurring therein (Schema 7).

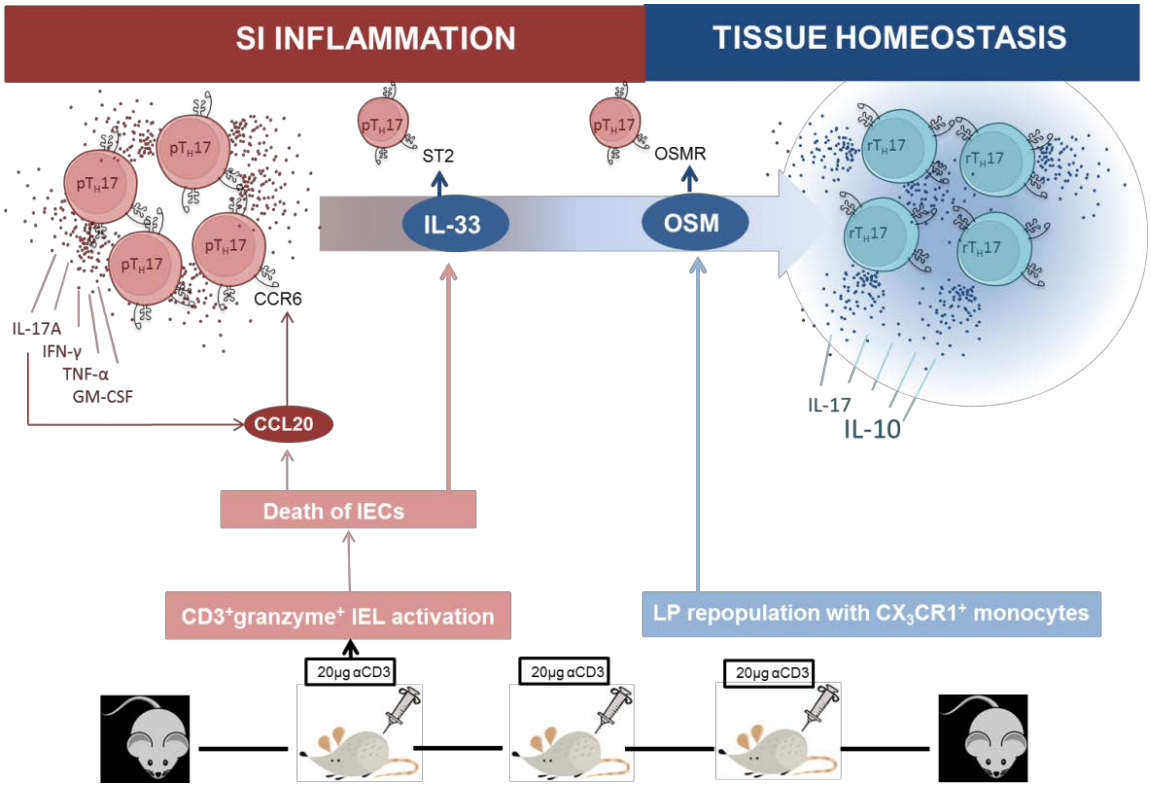

Schema 7. Proposed summary of the events that occur in the SI during anti-CD3 treatment and lead to the conversion of pro-inflammatory T_H17 cells to rT_H17 cells. Upon CD3-specific antibody injection $CD3^+$granzyme$^+$IELs are activated and release granzyme. IEC-derived granzyme damages IECs and induces an acute up-regulation of the chemokine CCL20 and the alarmin IL-33 in these cells. CCL20 expression promotes the recruitment of $CCR6^+$ pT_H17 cells from the periphery to the SI, where they actively proliferate. IL-17A expression by T_H17 cells further induces IEC-derived CCL20 expression, amplifying thereby T_H17 accumulation in the SI. Approximately 30-40% of peripheral $CCR6^+$ pT_H17 cells express ST2. Thus, $CCR6^+ST2^+$ T_H17 cells migrate to the SI, where they respond to IL-33. At later phases of the local inflammatory response CX_3CR1^+ monocytes with tolerogenic properties repopulate the LP and secrete OSM, a cytokine that also acts on T_H17 cells. IL-33 and OSM induce changes in the gene expression profile of pT_H17 cells, promoting a down-regulation of pro-inflammatory cytokines and an up-regulation of the anti-inflammatory cytokine IL-10. By doing so, IEC-derived IL-33 and monocyte-derived OSM control the pro-inflammatory phenotype of T_H17 cells that shift towards rT_H17 cells with immune-suppressive functions. The alarmin IL-33, which increases shortly after every injection is given but especially at day 1, would be part of a first line of defense counteracting the exacerbated acute inflammatory response in the SI. OSM, which increases during the treatment reaching its highest value at day 5, would be part of a fine-tuned mechanism that acts in advanced phases of the course of SI inflammation. Both mechanisms would synergize to push the system back to homeostasis by inducing tolerance in activated T_H17 cells.

The active cell-renewal that constantly takes place in the SI makes of it a well-suited tissue for dealing with the accumulation of pro-inflammatory, pathogenic T_H17 cells, which initially cause local inflammation and tissue damage. The existence of specialized hematopoietic cells with tolerogenic properties that home to the SI also helps to prevent further tissue damage and to counteract inflammation. The outcome of all this is the local restoration of tissue that leads to homeostasis, having an impact on immune responses on a systemic level. The gastrointestinal tract harbors the largest number of immune cells in the body, which shape the gut-associated lymphoid tissue. Both system are highly interrelated and, thus, intestinal cues may be transported via lymphatics and eventually enter the bloodstream with the subsequent systemic manifestations. Nevertheless, expression of IL-33 and OSM is not restricted to the SI. High levels of the alarmin IL-33 have also been described in the lungs during allergic reactions or in the spinal cord of MS patients. Similarly, high levels of OSM have been found in the joints of RA patients and in the CNS of MS patients, as it has been previously discussed in this study. Thus, both signals may be involved in several tissue-specific responses to local inflammatory conditions.

A better knowledge of these tissue-derived and local factors in control of inflammatory and regulatory T cells might open the door for targeted immune-modulation at the affected organ, avoiding thereby an unfavorable systemic immune suppression. The challenge is to extend this knowledge and translate it into new therapeutic approaches for the treatment of autoimmune diseases driven by T_H17 cells, such as IBD, RA, psoriasis and MS. Treatments for such disorders currently focus on eliminating pathogenic T_H17 cells or on inducing regulatory T cells. But what if new strategies that combine both outcomes could be developed? IL-33 and Osm may be promising candidates to work with in this field.

5 Bibliography

1. D. R. Littman, A. Y. Rudensky, Th17 and regulatory T cells in mediating and restraining inflammation, *Cell* **140**, 845–58 (2010).

2. D. Masopust, J. M. Schenkel, The integration of T cell migration, differentiation and function, *Nat Rev Immunol* **13**, 309–320 (2013).

3. A. Habtezion, L. P. Nguyen, H. Hadeiba, E. C. Butcher, Leukocyte trafficking to the Small Intestine and Colon, *Gastroenterology* , 1–15 (2015).

4. A. K. Abbas, K. M. Murphy, A. Sher, Functional diversity of helper T lymphocytes.*Nature* **383**, 787–793 (1996).

5. T. R. Mosmann, H. Cherwinski, M. W. Bond, M. a Giedlin, R. L. Coffman, Two types of murine helper T cell clone. I. Definition according to profiles of lymphokine activities and secreted proteins., *J. Immunol.* **136**, 2348–2357 (1986).

6. S. J. Szabo, S. T. Kim, G. L. Costa, X. Zhang, C. G. Fathman, L. H. Glimcher, A novel transcription factor, T-bet, directs Th1 lineage commitment., *Cell* **100**, 655–669 (2000).

7. W. Zheng, R. a Flavell, The transcription factor GATA-3 is necessary and sufficient for Th2 cytokine gene expression in CD4 T cells., *Cell* **89**, 587–596 (1997).

8. D. F. Fiorentino, M. W. Bond, T. R. Mosmann, Two types of mouse T helper cell. IV. Th2 clones secrete a factor that inhibits cytokine production by Th1 clones., *J. Exp. Med.* **170**, 2081–95 (1989).

9. A. Rao, O. Avni, Molecular aspects of T-cell differentiation., *Br. Med. Bull.* **56**, 969–84 (2000).

10. S. Romagnani, Th1/Th2 cells., *Inflamm. Bowel Dis.* **5**, 285–94 (1999).

11. S. Z. Josefowicz, A. Rudensky, Control of Regulatory T Cell Lineage Commitment and Maintenance*Immunity* **30**, 616–625 (2009).

12. C. L. Maynard, L. E. Harrington, K. M. Janowski, J. R. Oliver, C. L. Zindl, A. Y. Rudensky, C. T. Weaver, Regulatory T cells expressing interleukin 10 develop from Foxp3+ and Foxp3- precursor cells in the absence of interleukin 10., *Nat. Immunol.* **8**, 931–41 (2007).

13. T. Caza, S. Landas, Functional and Phenotypic Plasticity of CD4+ T Cell Subsets*Biomed Res. Int.* **2015** (2015), doi:10.1155/2015/521957.

14. M. Lochner, Z. Wang, T. Sparwasser, *The Special Relationship in the Development and Function of T Helper 17 and Regulatory T Cells.* (Elsevier Inc., ed. 1, 2015; http://www.sciencedirect.com/science/article/pii/S1877117315001453).

15. L. E. Harrington, R. D. Hatton, P. R. Mangan, H. Turner, T. L. Murphy, K. M. Murphy, C. T. Weaver, Interleukin 17–producing CD4+ effector T cells develop via a lineage distinct from the T helper type 1 and 2 lineages, *Nat. Immunol.* **6**, 1123–1132 (2005).

16. H. Park, Z. Li, X. O. Yang, S. H. Chang, R. Nurieva, Y. Y.-H. Wang, Y. Y.-H. Wang, L. Hood, Z. Zhu, Q. Tian, C. Dong, A distinct lineage of CD4 T cells regulates tissue inflammation by producing interleukin 17., *Nat. Immunol.* **6**, 1133–1141 (2005).

17. C. L. Langrish, Y. Chen, W. M. Blumenschein, J. Mattson, B. Basham, J. D. Sedgwick, T. McClanahan, R. A. Kastelein, D. J. Cua, IL-23 drives a pathogenic T cell population that induces autoimmune inflammation., *J. Exp. Med.* **201**, 233–40 (2005).

18. S. C. Liang, A. J. Long, F. Bennett, M. J. Whitters, R. Karim, M. Collins, S. J. Goldman, K. Dunussi-Joannopoulos, C. M. M. Williams, J. F. Wright, L. A. Fouser, An IL-17F/A Heterodimer Protein Is Produced by Mouse Th17 Cells and Induces Airway Neutrophil Recruitment, *J. Immunol.* **179**, 7791–7799 (2007).

19. S. C. Liang, X.-Y. Tan, D. P. Luxenberg, R. Karim, K. Dunussi-Joannopoulos, M. Collins, L. A. Fouser, Interleukin (IL)-22 and IL-17 are coexpressed by Th17 cells and cooperatively enhance expression of antimicrobial peptides, *J. Exp. Med.* **203**, 2271–2279 (2006).

20. W. O'Connor, M. Kamanaka, C. J. Booth, T. Town, S. Nakae, Y. Iwakura, J. K. Kolls, R. a Flavell, A protective function for interleukin 17A in T cell-mediated intestinal inflammation., *Nat. Immunol.* **10**, 603–9 (2009).

21. N. Manel, D. Unutmaz, D. R. Littman, The differentiation of human T(H)-17 cells requires transforming growth factor-beta and induction of the nuclear receptor RORgammat., *Nat. Immunol.* **9**, 641–9 (2008).

22. N. Garrido-Mesa, F. Algieri, A. Rodríguez Nogales, J. Gálvez, Functional Plasticity of Th17 Cells: Implications in Gastrointestinal Tract Function, *Int. Rev. Immunol.* **32**, 493–510 (2013).

23. C. T. Weaver, R. D. Hatton, P. R. Mangan, L. E. Harrington, IL-17 family cytokines and the expanding diversity of effector T cell lineages., *Annu. Rev. Immunol.* **25**, 821–852 (2007).

24. C. T. Weaver, L. E. Harrington, P. R. Mangan, M. Gavrieli, K. M. Murphy, Th17: An Effector CD4 T Cell Lineage with Regulatory T Cell Ties*Immunity* **24**, 677–688 (2006).

25. Y. K. Lee, S. K. Mazmanian, Microbial learning lessons: SFB educate the immune system*Immunity* **40**, 457–459 (2014).

26. Y. Goto, C. Panea, G. Nakato, A. Cebula, C. Lee, M. G. Diez, T. M. Laufer, L. Ignatowicz, I. I. Ivanov, Segmented filamentous bacteria antigens presented by intestinal dendritic cells drive mucosal Th17 cell differentiation, *Immunity* **40**, 594–607 (2014).

27. C. Panea, A. M. Farkas, Y. Goto, S. Abdollahi-Roodsaz, C. Lee, B. Koscsó, K. Gowda, T. M. Hohl, M. Bogunovic, I. I. Ivanov, Intestinal Monocyte-Derived Macrophages Control Commensal-Specific Th17 Responses, *Cell Rep.* **12**, 1314–1324 (2015).

28. M. N. Lee, C. Ye, A. Villani, T. Raj, W. Li, T. M. Eisenhaure, S. H. Imboywa, P. I. Chipendo, F. A. Ran, L. D. Ward, K. Raddassi, C. Mccabe, M. H. Lee, I. Y. Frohlich, D. A. Hafler, M. Kellis, S. Raychaudhuri, Focused Specificity of Intestinal Th17 Cells towards Commensal Bacterial Antigens, *Nature* **343**, 1–19 (2014).

29. M.-L. Cho, J.-W. Kang, Y.-M. Moon, H.-J. Nam, J.-Y. Jhun, S.-B. Heo, H.-T. Jin, S.-Y. Min, J.-H. Ju, K.-S. Park, Y.-G. Cho, C.-H. Yoon, S.-H. Park, Y.-C. Sung, H.-Y. Kim, STAT3 and NF- B Signal Pathway Is Required for IL-23-Mediated IL-17 Production in Spontaneous Arthritis Animal Model IL-1 Receptor Antagonist-Deficient Mice, *J. Immunol.* **176**, 5652–5661 (2006).

30. M. Veldhoen, R. J. Hocking, C. J. Atkins, R. M. Locksley, B. Stockinger, TGF?? in the context of an inflammatory cytokine milieu supports de novo differentiation of IL-17-producing T cells, *Immunity* **24**, 179–189 (2006).

31. E. Bettelli, Y. Carrier, W. Gao, T. Korn, T. B. Strom, M. Oukka, H. L. Weiner, V. K. Kuchroo, Reciprocal developmental pathways for the generation of pathogenic effector TH17 and regulatory T cells, *Nature* **441**, 235–238 (2006).

32. E. Volpe, N. Servant, R. Zollinger, S. I. Bogiatzi, P. Hupé, E. Barillot, V. Soumelis, A critical function for transforming growth factor-beta, interleukin 23 and proinflammatory cytokines in driving and modulating human T(H)-17 responses., *Nat. Immunol.* **9**, 650–657 (2008).

33. A. Rostami, B. Ciric, Role of Th17 cells in the pathogenesis of CNS inflammatory demyelination., *J. Neurol. Sci.* **333**, 76–87 (2013).

34. K. Hirota, M. Hashimoto, H. Yoshitomi, S. Tanaka, T. Nomura, T. Yamaguchi, Y. Iwakura, N. Sakaguchi, S. Sakaguchi, T cell self-reactivity forms a cytokine milieu for spontaneous development of IL-17+ Th cells that cause autoimmune arthritis, *J. Exp. Med.*

204, 41–47 (2007).

35. J. Li, X. Chen, Z. Liu, Q. Yue, H. Liu, Expression of Th17 cytokines in skin lesions of patients with psoriasis., *J. Huazhong Univ. Sci. Technolog. Med. Sci.* **27**, 330–2 (2007).

36. C. O. Elson, Y. Cong, C. T. Weaver, T. R. Schoeb, T. K. McClanahan, R. B. Fick, R. a. Kastelein, Monoclonal Anti–Interleukin 23 Reverses Active Colitis in a T Cell–Mediated Model in Mice, *Gastroenterology* **132**, 2359–2370 (2007).

37. P. Miossec, T. Korn, V. K. Kuchroo, Interleukin-17 and type 17 helper T cells., *N. Engl. J. Med.* **361**, 888–98 (2009).

38. J. A. Bluestone, C. R. Mackay, J. J. O'Shea, B. Stockinger, The functional plasticity of T cell subsets, *Nat Rev Immunol* **9**, 811–816 (2009).

39. L. M. Hegazy AN, Peine M, Helmstetter C, Panse I, Fröhlich A, Bergthaler A, Flatz L, Pinschewer DD, Radbruch A, Interferons direct Th2 cell reprogramming to generate a stable GATA-3(+)T-bet(+) cell subset with combined Th2 and Th1 cell functions., *Immunity* **32**, 116–128 (2010).

40. F. T. Hakim, S. A. Memon, R. Cepeda, E. C. Jones, C. K. Chow, C. Kasten-Sportes, J. Odom, B. A. Vance, B. L. Christensen, C. L. Mackall, R. E. Gress, Age-dependent incidence, time course, and consequences of thymic renewal in adults, *J. Clin. Invest.* **115**, 930–939 (2005).

41. F. Annunziato, L. Cosmi, V. Santarlasci, L. Maggi, F. Liotta, B. Mazzinghi, E. Parente, L. Filì, S. Ferri, F. Frosali, F. Giudici, P. Romagnani, P. Parronchi, F. Tonelli, E. Maggi, S. Romagnani, Phenotypic and functional features of human Th17 cells., *J. Exp. Med.* **204**, 1849–61 (2007).

42. L. Reinert-Hartwall, J. Honkanen, H. M. Salo, Th1/Th17 plasticity is a marker of advanced β cell autoimmunity and impaired glucose tolerance in humans, *J. Immunol.* **194**, 68–75 (2014).

43. K. Nistala, S. Adams, H. Cambrook, S. Ursu, B. Olivito, W. de Jager, J. G. Evans, R. Cimaz, M. Bajaj-Elliott, L. R. Wedderburn, Th17 plasticity in human autoimmune arthritis is driven by the inflammatory environment., *Proc. Natl. Acad. Sci. U. S. A.* **107**, 14751–6 (2010).

44. K. Ghoreschi, a Laurence, X. P. Yang, C. M. Tato, M. J. McGeachy, J. E. Konkel, H. L. Ramos, L. Wei, T. S. Davidson, N. Bouladoux, J. R. Grainger, Q. Chen, Y. Kanno, W. T. Watford, H. W. Sun, G. Eberl, E. M. Shevach, Y. Belkaid, D. J. Cua, W. Chen, J. J. O'Shea, Generation of pathogenic T(H)17 cells in the absence of TGF-beta signalling, *Nature* **467**, 967–971 (2010).

45. K. Hirota, J. H. Duarte, M. Veldhoen, E. Hornsby, Y. Li, D. J. Cua, H. Ahlfors, C. Wilhelm, M. Tolaini, U. Menzel, A. Garefalaki, A. J. Potocnik, B. Stockinger, Fate mapping of IL-17-producing T cells in inflammatory responses, *Nat. Publ. Gr.* **12**, 255–263 (2011).

46. D. Bending, H. De La Peña, M. Veldhoen, J. M. Phillips, C. Uyttenhove, B. Stockinger, A. Cooke, Highly purified Th17 cells from BDC2.5NOD mice convert into Th1-like cells in NOD/SCID recipient mice, *J. Clin. Invest.* **119**, 565–572 (2009).

47. E. Esplugues, S. Huber, N. Gagliani, A. E. Hauser, T. Town, Y. Y. Wan, W. O'Connor, A. Rongvaux, N. Van Rooijen, A. M. Haberman, Y. Iwakura, V. K. Kuchroo, J. K. Kolls, J. A. Bluestone, K. C. Herold, R. A. Flavell, Control of TH17 cells occurs in the small intestine., *Nature* **475**, 514–8 (2011).

48. N. Gagliani, M. C. A. Vesely, A. Iseppon, L. Brockmann, H. Xu, N. W. Palm, M. R. de Zoete, P. Licona-Limon, R. S. Paiva, T. Ching, C. Weaver, X. Zi, X. Pan, R. Fan, L. X. Garmire, M. J. Cotton, Y. Drier, B. Bernstein, J. Geginat, B. Stockinger, E. Esplugues, S. Huber, R. A. Flavell, Th17 cells transdifferentiate into regulatory T cells during resolution of inflammation, *Nature* **523**, 221–225 (2015).

49. S. Huber, N. Gagliani, E. Esplugues, W. O'Connor, F. J. Huber, A. Chaudhry, M. Kamanaka, Y. Kobayashi, C. J. Booth, A. Y. Rudensky, M. G. Roncarolo, M. Battaglia, R. A. Flavell, Th17 cells express interleukin-10 receptor and are controlled by Foxp3$^-$ and Foxp3+ regulatory CD4+ T cells in an interleukin-10-dependent manner., *Immunity* **34**, 554–65 (2011).

50. F. J. Quintana, A. S. Basso, A. H. Iglesias, T. Korn, M. F. Farez, E. Bettelli, M. Caccamo, M. Oukka, H. L. Weiner, Control of T(reg) and T(H)17 cell differentiation by the aryl hydrocarbon receptor., *Nature* **453**, 65–71 (2008).

51. K. S. Voo, Y.-H. Wang, F. R. Santori, C. Boggiano, Y.-H. Wang, K. Arima, L. Bover, S. Hanabuchi, J. Khalili, E. Marinova, B. Zheng, D. R. Littman, Y.-J. Liu, Identification of IL-17-producing FOXP3+ regulatory T cells in humans., *Proc. Natl. Acad. Sci. U. S. A.* **106**, 4793–4798 (2009).

52. M. Lochner, L. Peduto, M. Cherrier, S. Sawa, F. Langa, R. Varona, D. Riethmacher, M. Si-Tahar, J. P. Di Santo, G. Eberl, In vivo equilibrium of proinflammatory IL-17+ and regulatory IL-10+ Foxp3+ RORgamma t+ T cells., *J. Exp. Med.* **205**, 1381–93 (2008).

53. A. Ueno, A. Ghosh, D. Hung, J. Li, H. Jijon, Th17 plasticity and its changes associated with inflammatory bowel disease*World J. Gastroenterol.* **21**, 12283–12295 (2015).

54. R. Basu, R. D. Hatton, C. T. Weaver, The Th17 family: flexibility follows function, *Immunol. Rev.* **252**, 89–103 (2013).

55. L. W. Peterson, D. Artis, Intestinal epithelial cells: regulators of barrier function and immune homeostasis., *Nat. Rev. Immunol.* **14**, 141–53 (2014).

56. A. M. Mowat, Anatomical basis of tolerance and immunity to intestinal antigens., *Nat. Rev. Immunol.* **3**, 331–341 (2003).

57. C. Varol, A. Vallon-Eberhard, E. Elinav, T. Aychek, Y. Shapira, H. Luche, H. J. Fehling, W. D. Hardt, G. Shakhar, S. Jung, Intestinal Lamina Propria Dendritic Cell Subsets Have Different Origin and Functions, *Immunity* **31**, 502–512 (2009).

58. E. Zigmond, S. Jung, Intestinal macrophages: Well educated exceptions from the rule*Trends Immunol.* **34**, 162–168 (2013).

59. U. Hadis, B. Wahl, O. Schulz, M. Hardtke-Wolenski, A. Schippers, N. Wagner, W. M??ller, T. Sparwasser, R. F??rster, O. Pabst, Intestinal Tolerance Requires Gut Homing and Expansion of FoxP3+ Regulatory T Cells in the Lamina Propria, *Immunity* **34**, 237–246 (2011).

60. H. Cheroutre, F. Lambolez, D. Mucida, The light and dark sides of intestinal intraepithelial lymphocytes., *Nat. Rev. Immunol.* **11**, 445–56 (2011).

61. a Hayday, E. Theodoridis, E. Ramsburg, J. Shires, Intraepithelial lymphocytes: exploring the Third Way in immunology., *Nat. Immunol.* **2**, 997–1003 (2001).

62. M. Swamy, L. Abeler-Dörner, J. Chettle, T. Mahlakõiv, D. Goubau, P. Chakravarty, G. Ramsay, C. Reis E Sousa, P. Staeheli, B. a Blacklaws, J. L. Heeney, A. C. Hayday, Intestinal intraepithelial lymphocyte activation promotes innate antiviral resistance., *Nat. Commun.* **6**, 7090 (2015).

63. K.-J. Lou, Gutsy call on Th17 cells, *SciBX* .

64. J. Wang, F. Li, H. Wei, Z.-X. Lian, R. Sun, Z. Tian, Respiratory influenza virus infection induces intestinal immune injury via microbiota-mediated Th17 cell-dependent inflammation, *J. Exp. Med.* **211**, 2397–2410 (2014).

65. B. Zygmunt, M. Veldhoen, T helper cell differentiation more than just cytokines., *Adv. Immunol.* **109**, 159–96 (2011).

66. V. Brucklacher-Waldert, E. J. Carr, M. A. Linterman, M. Veldhoen, Cellular Plasticity of CD4+ T Cells in the Intestine., *Front. Immunol.* (2014), doi:10.3389/fimmu.2014.00488.

67. L. Chatenoud, CD3-specific antibody-induced active tolerance: from bench to bedside., *Nat. Rev. Immunol.* **3**, 123–132 (2003).

68. L. Chatenoud, J. A. Bluestone, CD3-specific antibodies: a portal to the treatment of autoimmunity., *Nat. Rev. Immunol.* **7**, 622–632 (2007).

69. C. Penaranda, Q. Tang, J. A. Bluestone, Anti-CD3 Therapy Promotes Tolerance by Selectively Depleting Pathogenic Cells while Preserving Regulatory T Cells, *J. Immunol.* **187**, 2015–2022 (2011).

70. M. Merger, J. L. Viney, R. Borojevic, D. Steele-Norwood, P. Zhou, D. A. Clark, R. Riddell, R. Maric, E. R. Podack, K. Croitoru, Defining the roles of perforin, Fas/FasL, and tumour necrosis factor alpha in T cell induced mucosal damage in the mouse intestine., *Gut* **51**, 155–163 (2002).

71. N. Ueno, T. Hasebe, A. Kaneko, M. Yamamoto, M. Fujiya, Y. Kohgo, T. Kono, C. Z. Wang, C. S. Yuan, M. Bissonnette, E. B. Chang, M. W. Musch, TU-100 (Daikenchuto) and ginger ameliorate anti-CD3 antibody induced T cell-mediated murine enteritis: Microbe-independent effects involving Akt and NF-kB suppression, *PLoS One* **9**, 1–9 (2014).

72. F. Balzola, C. Bernstein, G. T. Ho, C. Lees, Persistent gut motor dysfunction in a murine model of T-cell-induced enteropathy: Commentary*Inflamm. Bowel Dis. Monit.* **10**, 145–146 (2010).

73. H. Zhang, N. Ameen, J. E. Melvin, S. Vidyasagar, Acute inflammation alters bicarbonate transport in mouse ileum., *J. Physiol.* **581**, 1221–1233 (2007).

74. M. W. Musch, L. L. Clarke, D. Mamah, L. R. Gawenis, Z. Zhang, W. Ellsworth, D. Shalowitz, N. Mittal, P. Efthimiou, Z. Alnadjim, S. D. Hurst, E. B. Chang, T. a. Barrett, T cell activation causes diarrhea by increasing intestinal permeability and inhibiting epithelial Na+/K+-ATPase, *J. Clin. Invest.* **110**, 1739–1747 (2002).

75. L. Chatenoud, J.-F. O. Bach, S. Sakaguchi, CD3-specific antibodies restore self-tolerance: mechanisms and clinical applications This review comes from a themed issue on Autoimmunity Edited, *Curr. Opin. Immunol.* **17**, 632–637 (2005).

76. L. Chatenoud, CD3-specific antibodies restore self-tolerance: Mechanisms and clinical applications*Curr. Opin. Immunol.* (2005), doi:10.1016/j.coi.2005.09.011.

77. L. Chatenoud, E. Thervet, J. Primo, J. F. Bach, Anti-CD3 antibody induces long-term remission of overt autoimmunity in nonobese diabetic mice., *Proc. Natl. Acad. Sci. U. S. A.* **91**, 123–127 (1994).

78. C. A. Notley, F. E. McCann, J. J. Inglis, R. O. Williams, Anti-CD3 therapy expands the numbers of CD4+ and CD8+ Treg cells and induces sustained amelioration of collagen-induced arthritis, *Arthritis Rheum.* **62**, 171–178 (2010).

79. J. L. Zhang, D. J. Sun, C. M. Hou, Y. L. Wei, X. Y. Li, Z. Y. Yu, J. N. Feng, B. F. Shen, Y. Li, H. Xiao, CD3 mAb treatment ameliorated the severity of the cGVHD-induced lupus nephritis in mice by up-regulation of Foxp3 + regulatory T cells in the target tissue: Kidney, *Transpl. Immunol.* **24**, 17–25 (2010).

80. J. Schmitz, A. Owyang, E. Oldham, Y. Song, E. Murphy, T. K. McClanahan, G. Zurawski, M. Moshrefi, J. Qin, X. Li, D. M. Gorman, J. F. Bazan, R. A. Kastelein, IL-33, an interleukin-1-like cytokine that signals via the IL-1 receptor-related protein ST2 and induces T helper type 2-associated cytokines, *Immunity* **23**, 479–490 (2005).

81. V. Carriere, L. Roussel, N. Ortega, D.-A. Lacorre, L. Americh, L. Aguilar, G. Bouche, J.-P. Girard, IL-33, the IL-1-like cytokine ligand for ST2 receptor, is a chromatin-associated nuclear factor in vivo., *Proc. Natl. Acad. Sci.* **104**, 282–287 (2007).

82. C. Moussion, N. Ortega, J.-P. Girard, D. Unutmaz, Ed. The IL-1-Like Cytokine IL-33 Is Constitutively Expressed in the Nucleus of Endothelial Cells and Epithelial Cells In Vivo: A Novel “Alarmin”?, *PLoS One* **3**, e3331 (2008).

83. M. Pichery, E. Mirey, P. Mercier, E. Lefrancais, a. Dujardin, N. Ortega, J.-P. Girard, Endogenous IL-33 Is Highly Expressed in Mouse Epithelial Barrier Tissues, Lymphoid Organs, Brain, Embryos, and Inflamed Tissues: In Situ Analysis Using a Novel Il-33-LacZ Gene Trap Reporter Strain, *J. Immunol.* **188**, 3488–3495 (2012).

84. N. T. Martin, M. U. Martin, Interleukin 33 is a guardian of barriers and a local alarmin, *Nat. Immunol.* **17**, 122–131 (2016).

85. G. Haraldsen, J. Balogh, J. Pollheimer, J. Sponheim, A. M. Küchler, Interleukin-33 – cytokine of dual function or novel alarmin?, *Trends Immunol.* **30**, 227–233 (2009).

86. W. V. Bonilla, A. Frohlich, K. Senn, S. Kallert, M. Fernandez, S. Johnson, M. Kreutzfeldt, A. N. Hegazy, C. Schrick, P. G. Fallon, R. Klemenz, S. Nakae, H. Adler, D. Merkler, M. Lohning, D. D. Pinschewer, The Alarmin Interleukin-33 Drives Protective Antiviral CD8+ T Cell Responses, *Science (80-.).* **335**, 984–989 (2012).

87. C. Baumann, W. V. Bonilla, A. Fröhlich, C. Helmstetter, M. Peine, A. N. Hegazy, D. D. Pinschewer, M. Löhning, T-bet– and STAT4–dependent IL-33 receptor expression directly promotes antiviral Th1 cell responses, *Proc. Natl. Acad. Sci.* , 201418549 (2015).

88. D. Xu, H.-R. Jiang, Y. Li, P. N. Pushparaj, M. Kurowska-Stolarska, B. P. Leung, R. Mu, H. K. Tay, A. N. J. McKenzie, I. B. McInnes, A. J. Melendez, F. Y. Liew, IL-33 exacerbates autoantibody-induced arthritis., *J. Immunol.* **184**, 2620–2626 (2010).

89. M. a K. Sedhom, M. Pichery, J. R. Murdoch, B. Foligné, N. Ortega, S. Normand, K. Mertz, D. Sanmugalingam, L. Brault, T. Grandjean, E. Lefrancais, P. G. Fallon, V. Quesniaux, L. Peyrin-biroulet, G. Cathomas, T. Junt, M. Chamaillard, J.-P. Girard, B. Ryffel, Neutralisation of the interleukin-33/ST2 pathway ameliorates experimental colitis through enhancement of mucosal healing in mice., *Gut* **62**, 1714–23 (2013).

90. A. B. Molofsky, A. K. Savage, R. M. Locksley, Interleukin-33 in Tissue Homeostasis, Injury, and Inflammation, *Immunity* **42**, 1005–1019 (2015).

91. F. Y. Liew, N. I. Pitman, I. B. McInnes, Disease-associated functions of IL-33: the new kid in the IL-1 family., *Nat. Rev. Immunol.* **10**, 103–10 (2010).

92. J. Zhao, J. Wei, R. K. Bowser, R. S. Traister, M.-H. Fan, Y. Zhao, Focal Adhesion Kinase-Mediated Activation of Glycogen Synthase Kinase 3 Regulates IL-33 Receptor Internalization and IL-33 Signaling, *J. Immunol.* **194**, 795–802 (2014).

93. T. Gajardo Carrasco, R. A. Morales, F. Pérez, C. Terraza, L. Yáñez, M. Campos-Mora, K. Pino-Lagos, Alarmin' Immunologists: IL-33 as a Putative Target for Modulating T Cell-Dependent Responses., *Front. Immunol.* **6**, 232 (2015).

94. M. Tanaka, A. Miyajima, Oncostatin M, a multifunctional cytokine., *Rev. Physiol. Biochem. Pharmacol.* **149**, 39–52 (2003).

95. C. D. Richards, The Enigmatic Cytokine Oncostatin M and Roles in Disease., *ISRN Inflamm.* **2013**, 512103 (2013).

96. K. Boniface, C. Diveu, F. Morel, N. Pedretti, J. Froger, E. Ravon, M. Garcia, E. Venereau, L. Preisser, E. Guignouard, G. Guillet, G. Dagregorio, J. Pène, J.-P. Moles, H. Yssel, S. Chevalier, F.-X. Bernard, H. Gascan, J.-C. Lecron, Oncostatin M secreted by skin infiltrating T lymphocytes is a potent keratinocyte activator involved in skin inflammation., *J. Immunol.* **178**, 4615–4622 (2007).

97. H.-J. Tu, T.-H. Lin, Y.-C. Chiu, C.-H. Tang, R.-S. Yang, W.-M. Fu, Enhancement of placenta growth factor expression by oncostatin M in human rheumatoid arthritis synovial fibroblasts., *J. Cell. Physiol.* , 1–33 (2012).

98. J. K. Loy, T. J. Davidson, K. K. Berry, J. F. Macmaster, B. Danle, S. K. Durham, Oncostatin M: development of a pleiotropic cytokine, *Toxicol Pathol* **27**, 151–155 (1999).

99. P. M. Wallace, J. F. MacMaster, K. a Rouleau, T. J. Brown, J. K. Loy, K. L. Donaldson, a

F. Wahl, Regulation of inflammatory responses by oncostatin M., *J. Immunol.* **162**, 5547–5555 (1999).

100. A. Sanchez, C. Langdon, M. Akhtar, J. Lu, C. Richards, P. Bercik, D. McKay, Adenoviral transfer of the murine oncostatin M gene suppresses dextran-sodium sulfate-induced colitis, *J Interf. Cytokine Res* **23**, 193–201 (2003).

101. F. Beigel, M. Friedrich, C. Probst, K. Sotlar, B. Göke, J. Diegelmann, S. Brand, Oncostatin M mediates STAT3-dependent intestinal epithelial restitution via increased cell proliferation, decreased apoptosis and upregulation of SERPIN family members., *PLoS One* **9**, e93498 (2014).

102. A. Dumas, S. Lagarde, C. Laflamme, M. Pouliot, Oncostatin M decreases interleukin-1 β secretion by human synovial fibroblasts and attenuates an acute inflammatory reaction in vivo., *J. Cell. Mol. Med.* **16**, 1274–85 (2012).

103. K. Janssens, A. Maheshwari, C. Van den Haute, V. Baekelandt, P. Stinissen, J. J. a. Hendriks, H. Slaets, N. Hellings, Oncostatin M protects against demyelination by inducing a protective microglial phenotype, *Glia* , n/a–n/a (2015).

104. H. Slaets, S. Nelissen, K. Janssens, P. M. Vidal, E. Lemmens, P. Stinissen, S. Hendrix, N. Hellings, Oncostatin M reduces lesion size and promotes functional recovery and neurite outgrowth after spinal cord injury., *Mol. Neurobiol.* **50**, 1142–51 (2014).

105. S. Moidunny, R. B. Dias, E. Wesseling, Y. Sekino, H. W. G. M. Boddeke, A. M. Sebasti??o, K. Biber, Interleukin-6-type cytokines in neuroprotection and neuromodulation: Oncostatin M, but not leukemia inhibitory factor, requires neuronal adenosine A1 receptor function, *J. Neurochem.* **114**, 1667–1677 (2010).

106. J. H. Chewning, C. T. Weaver, Development and Survival of Th17 Cells within the Intestines: The Influence of Microbiome- and Diet-Derived Signals, *J. Immunol.* **193**, 4769–4777 (2014).

107. C. Ohnmacht, J.-H. Park, S. Cording, J. B. Wing, K. Atarashi, Y. Obata, V. Gaboriau-Routhiau, R. Marques, S. Dulauroy, M. Fedoseeva, M. Busslinger, N. Cerf-Bensussan, I. G. Boneca, D. Voehringer, K. Hase, K. Honda, S. Sakaguchi, G. Eberl, The microbiota regulates type 2 immunity through ROR t+ T cells, *Science (80-.).* **349**, 989–93 (2015).

108. E. Sefik, N. Geva-Zatorsky, S. Oh, L. Konnikova, D. Zemmour, A. M. McGuire, D. Burzyn, A. Ortiz-Lopez, M. Lobera, J. Yang, S. Ghosh, A. Earl, S. B. Snapper, R. Jupp, D. Kasper, D. Mathis, C. Benoist, Individual intestinal symbionts induce a distinct population of RORγ+ regulatory T cells., *Science* **349**, 993–7 (2015).

109. M. J. Townsend, P. G. Fallon, D. J. Matthews, H. E. Jolin, A. N. McKenzie, T1/ST2-deficient mice demonstrate the importance of T1/ST2 in developing primary T helper cell type 2 responses., *J. Exp. Med.* **191**, 1069–76 (2000).

110. C. E. Zielinski, F. Mele, D. Aschenbrenner, D. Jarrossay, F. Ronchi, M. Gattorno, S. Monticelli, A. Lanzavecchia, F. Sallusto, Pathogen-induced human TH17 cells produce IFN-γ or IL-10 and are regulated by IL-1β*Nature* **484**, 514–518 (2012).

111. C. Asseman, S. Mauze, M. W. Leach, R. L. Coffman, F. Powrie, An essential role for interleukin 10 in the function of regulatory T cells that inhibit intestinal inflammation., *J. Exp. Med.* **190**, 995–1004 (1999).

112. M. García-miguel, M. J. González, R. Quera, M. a Hermoso, Innate Immunity Modulation by the IL-33 / ST2 System in Intestinal Mucosa, **2013** (2013).

113. L. Pastorelli, C. De Salvo, M. Vecchi, T. T. GvPizarro, The role of IL-33 in gut mucosal inflammation, *Mediators Inflamm.* **2013** (2013), doi:10.1155/2013/608187.

114. C. Schiering, T. Krausgruber, A. Chomka, A. Fröhlich, K. Adelmann, E. a Wohlfert, J. Pott, T. Griseri, J. Bollrath, A. N. Hegazy, O. J. Harrison, B. M. J. Owens, M. Löhning, Y. Belkaid, P. G. Fallon, F. Powrie, The alarmin IL-33 promotes regulatory T-cell function in the

intestine., *Nature* **513**, 564–8 (2014).

115. A. Kobori, Y. Yagi, H. Imaeda, H. Ban, S. Bamba, T. Tsujikawa, Y. Saito, Y. Fujiyama, A. Andoh, Interleukin-33 expression is specifically enhanced in inflamed mucosa of ulcerative colitis, *J. Gastroenterol.* **45**, 999–1007 (2010).

116. J. B. Seidelin, J. T. Bjerrum, M. Coskun, B. Widjaya, B. Vainer, O. H. Nielsen, IL-33 is upregulated in colonocytes of ulcerative colitis., *Immunol. Lett.* **128**, 80–5 (2010).

117. M. Löhning, A. Stroehmann, A. J. Coyle, J. L. Grogan, S. Lin, J. C. Gutierrez-Ramos, D. Levinson, A. Radbruch, T. Kamradt, T1/ST2 is preferentially expressed on murine Th2 cells, independent of interleukin 4, interleukin 5, and interleukin 10, and important for Th2 effector function., *Proc. Natl. Acad. Sci. U. S. A.* **95**, 6930–5 (1998).

118. C. Schiering, T. Krausgruber, A. Chomka, A. Fröhlich, K. Adelmann, E. a. Wohlfert, J. Pott, T. Griseri, J. Bollrath, A. N. Hegazy, O. J. Harrison, B. M. J. Owens, M. Löhning, Y. Belkaid, P. G. Fallon, F. Powrie, The alarmin IL-33 promotes regulatory T-cell function in the intestine, *Nature* (2014), doi:10.1038/nature13577.

119. N. Murakami-Satsutani, T. Ito, T. Nakanishi, N. Inagaki, A. Tanaka, P. T. X. Vien, K. Kibata, M. Inaba, S. Nomura, IL-33 Promotes the Induction and Maintenance of Th2 Immune Responses by Enhancing the Function of OX40 Ligand, *Allergol. Int.* **63**, 443–455 (2014).

120. J. S. Stumhofer, J. S. Silver, A. Laurence, P. M. Porrett, T. H. Harris, L. a Turka, M. Ernst, C. J. M. Saris, J. J. O'Shea, C. a Hunter, Interleukins 27 and 6 induce STAT3-mediated T cell production of interleukin 10, *Nat. Immunol.* **8**, 1363–1371 (2007).

121. H. G. Evans, U. Roostalu, G. J. Walter, N. J. Gullick, K. S. Frederiksen, C. A. Roberts, J. Sumner, D. L. Baeten, J. G. Gerwien, A. P. Cope, F. Geissmann, B. W. Kirkham, L. S. Taams, TNF-α blockade induces IL-10 expression in human CD4+ T cells, *Nat. Commun.* **5** (2014), doi:10.1038/ncomms4199.

122. P. Li, R. Spolski, W. Liao, L. Wang, T. L. Murphy, K. M. Murphy, W. J. Leonard, BATF-JUN is critical for IRF4-mediated transcription in T cells., *Nature* **490**, 543–6 (2012).

123. J. Xu, Y. Yang, G. Qiu, G. Lal, Z. Wu, D. E. Levy, J. C. Ochando, J. S. Bromberg, Y. Ding, c-Maf regulates IL-10 expression during Th17 polarization., *J. Immunol.* **182**, 6226–36 (2009).

124. N. Malik, J. C. Kallestad, N. L. Gunderson, S. D. Austin, M. G. Neubauer, V. Ochs, H. Marquardt, J. M. Zarling, M. Shoyab, C. M. Wei, Molecular cloning, sequence analysis, and functional expression of a novel growth regulator, oncostatin M., *Mol. Cell. Biol.* **9**, 2847–53 (1989).

125. J. M. Zarling, M. Shoyab, H. Marquardt, M. B. Hanson, M. N. Lioubin, G. J. Todaro, Oncostatin M: a growth regulator produced by differentiated histiocytic lymphoma cells., *Proc. Natl. Acad. Sci. U. S. A.* **83**, 9739–43 (1986).

126. C. D. Richards, C. Langdon, F. Botelho, T. J. Brown, A. Agro, Oncostatin M inhibits IL-1-induced expression of IL-8 and granulocyte-macrophage colony-stimulating factor by synovial and lung fibroblasts., *J. Immunol.* **156**, 343–9 (1996).

127. ??ine C. Murphy, S. J. Lalor, M. A. Lynch, K. H. G. Mills, Infiltration of Th1 and Th17 cells and activation of microglia in the CNS during the course of experimental autoimmune encephalomyelitis, *Brain. Behav. Immun.* **24**, 641–651 (2010).

128. I. M. Stromnes, L. M. Cerretti, D. Liggitt, R. A. Harris, J. M. Goverman, Differential regulation of central nervous system autoimmunity by T(H)1 and T(H)17 cells., *Nat. Med.* **14**, 337–42 (2008).

129. Y. Sun, T. Tian, J. Gao, X. Liu, H. Hou, R. Cao, B. Li, M. Quan, L. Guo, Metformin ameliorates the development of experimental autoimmune encephalomyelitis by regulating T helper 17 and regulatory T cells in mice, *J. Neuroimmunol.* **292**, 58–67 (2016).

130. A. L. Croxford, S. Spath, B. Becher, GM-CSF in Neuroinflammation: Licensing Myeloid Cells for Tissue Damage*Trends Immunol.* **36**, 651–662 (2015).

131. G. A. Popko B1, Corbin JG, Baerwald KD, Dupree J, The effects of interferon-gamma on the central nervous system., *Mol. Neurobiol.* **14**, 19–35 (1997).

132. J. Goverman, Autoimmune T cell responses in the central nervous system., *Nat. Rev. Immunol.* **9**, 393–407 (2009).

133. M. J. McGeachy, GM-CSF: the secret weapon in the T(H)17 arsenal., *Nat. Immunol.* **12**, 521–522 (2011).

134. R. Noster, R. Riedel, M.-F. Mashreghi, H. Radbruch, L. Harms, C. Haftmann, H.-D. Chang, A. Radbruch, C. E. Zielinski, IL-17 and GM-CSF expression are antagonistically regulated by human T helper cells., *Sci. Transl. Med.* **6**, 241ra80 (2014).

135. O. Harrison, N. Srinivasan, J. Pott, C. Schiering, T. Krausgruber, N. Ilott, K. Maloy, Epithelial-derived IL-18 regulates Th17 cell differentiation and Foxp3+ Treg cell function in the intestine, (2015), doi:10.1038/mi.2015.13.

136. H. Kebir, K. Kreymborg, I. Ifergan, A. Dodelet-Devillers, R. Cayrol, M. Bernard, F. Giuliani, N. Arbour, B. Becher, A. Prat, Human TH17 lymphocytes promote blood-brain barrier disruption and central nervous system inflammation., *Nat. Med.* **13**, 1173–5 (2007).

137. J. Stallhofer, M. Friedrich, A. Konrad-Zerna, M. Wetzke, P. Lohse, J. Glas, C. Tillack-Schreiber, F. Schnitzler, F. Beigel, S. Brand, Lipocalin-2 Is a Disease Activity Marker in Inflammatory Bowel Disease Regulated by IL-17A, IL-22, and TNF-α and Modulated by IL23R Genotype Status., *Inflamm. Bowel Dis.* **21**, 2327–40 (2015).

138. L. R. Lopetuso, F. Scaldaferri, T. T. Pizarro, Emerging role of the interleukin (IL)-33/ST2 axis in gut mucosal wound healing and fibrosis, *Fibrogenesis Tissue Repair* **5**, 18 (2012).

139. T. Gajardo Carrasco, R. a. Morales, F. Pérez, C. Terraza, L. Yáñez, M. Campos-Mora, K. Pino-Lagos, Alarmin' Immunologists: IL-33 as a Putative Target for Modulating T Cell-Dependent Responses, *Front. Immunol.* **6**, 4–11 (2015).

140. M. Ogata, T. Oomori, H. Soga, Y. Ota, A. Itoh, T. Matsutani, M. Nanno, R. Suzuki, T. Itoh, DNA repair after DNA fragmentation in mouse small intestinal epithelial cells., *Cell Tissue Res.* **335**, 371–82 (2009).

141. K. Yaguchi, S. Kayaba, H. Soga, M. Yamagishi, A. Tamura, S. Kasahara, S. Ohara, J. Satoh, Y. Oka, T. Toyota, T. Itoh, DNA fragmentation and detachment of enterocytes induced by anti-CD3 mAb-activated intraepithelial lymphocytes, *Cell Tissue Res.* **315**, 71–84 (2004).

142. M. Ogata, Y. Ota, M. Nanno, R. Suzuki, T. Itoh, Activation of intra-epithelial lymphocytes; their morphology, marker expression and ultimate fate, *Cell Tissue Res.* **356**, 217–230 (2014).

143. K. Oboki, T. Ohno, N. Kajiwara, K. Arae, H. Morita, A. Ishii, A. Nambu, T. Abe, H. Kiyonari, K. Matsumoto, K. Sudo, K. Okumura, H. Saito, S. Nakae, IL-33 is a crucial amplifier of innate rather than acquired immunity., *Proc. Natl. Acad. Sci. U. S. A.* **107**, 18581–18586 (2010).

144. J. Bayat Sarmadi, thesis, Freie Universität Berlin (2016).

145. C. Moussion, N. Ortega, J.-P. Girard, D. Unutmaz, Ed. The IL-1-Like Cytokine IL-33 Is Constitutively Expressed in the Nucleus of Endothelial Cells and Epithelial Cells In Vivo: A Novel "Alarmin"?, *PLoS One* **3**, e3331 (2008).

146. L. Duan, J. Chen, H. Zhang, H. Yang, P. Zhu, A. Xiong, Q. Xia, F. Zheng, Z. Tan, F. Gong, M. Fang, Interleukin-33 ameliorates experimental colitis through promoting Th2/Foxp3$^+$ regulatory T-cell responses in mice., *Mol. Med.* **18**, 753–61 (2012).

147. E. Beurel, W.-I. Yeh, S. M. Michalek, L. E. Harrington, R. S. Jope, Glycogen Synthase

Kinase-3 Is an Early Determinant in the Differentiation of Pathogenic Th17 Cells, **186**, 1391–1398 (2011).

148. A. Di Sabatino, M. V. Lenti, P. Giuffrida, A. Vanoli, G. R. Corazza, New insights into immune mechanisms underlying autoimmune diseases of the gastrointestinal tract, *Autoimmun. Rev.* (2015), doi:10.1016/j.autrev.2015.08.004.

149. T. Griseri, I. C. Arnold, C. Pearson, T. Krausgruber, C. Schiering, F. Franchini, J. Schulthess, B. S. McKenzie, P. R. Crocker, F. Powrie, Granulocyte Macrophage Colony-Stimulating Factor-Activated Eosinophils Promote Interleukin-23 Driven Chronic Colitis, *Immunity* **43**, 187–199 (2015).

150. H. Kebir, I. Ifergan, J. I. Alvarez, M. Bernard, J. Poirier, N. Arbour, P. Duquette, A. Prat, Preferential recruitment of interferon-γ-expressing T $_H$ 17 cells in multiple sclerosis, *Ann. Neurol.* **66**, 390–402 (2009).

151. S. N. Harbour, C. L. Maynard, C. L. Zindl, T. R. Schoeb, C. T. Weaver, Th17 cells give rise to Th1 cells that are required for the pathogenesis of colitis, *Proc. Natl. Acad. Sci.* **112**, 201415675 (2015).

152. T. L. Ai, B. D. Solomon, C.-S. Hsieh, T-cell selection and intestinal homeostasis., *Immunol. Rev.* **259**, 60–74 (2014).

153. A. Vasanthakumar, K. Moro, A. Xin, Y. Liao, R. Gloury, S. Kawamoto, S. Fagarasan, L. A. Mielke, S. Afshar-Sterle, S. L. Masters, S. Nakae, H. Saito, J. M. Wentworth, P. Li, W. Liao, W. J. Leonard, G. K. Smyth, W. Shi, S. L. Nutt, S. Koyasu, A. Kallies, The transcriptional regulators IRF4, BATF and IL-33 orchestrate development and maintenance of adipose tissue-resident regulatory T cells., *Nat. Immunol.* **16**, 276–85 (2015).

154. A. Kole, K. J. Maloy, Interleukin-10 in Health and Disease, **380**, 19–38 (2014).

155. J. B. Seidelin, M. Coskun, P. H. Kvist, T. L. Holm, K. Holgersen, O. H. Nielsen, IL-33 promotes GATA-3 polarization of gut-derived T cells in experimental and ulcerative colitis, *J. Gastroenterol.* **50**, 180–190 (2015).

156. E. K. Brint, K. a Fitzgerald, P. Smith, A. J. Coyle, P. G. Fallon, L. a J. O. Neill, Characterization of Signaling Pathways Activated by the Interleukin 1 (IL-1) Receptor Homologue T1 / ST2, *Biochemistry* **277**, 49205–49211 (2002).

157. R. Kakkar, R. T. Lee, The IL-33/ST2 pathway: therapeutic target and novel biomarker, *Nat. Rev. Drug Discov.* **7**, 827–840 (2008).

158. R. Noster, R. Riedel, M.-F. Mashreghi, H. Radbruch, L. Harms, C. Haftmann, H.-D. Chang, A. Radbruch, C. E. Zielinski, IL-17 and GM-CSF Expression Are Antagonistically Regulated by Human T Helper Cells, *Sci. Transl. Med.* **6**, 241ra80–241ra80 (2014).

159. T. Komori, M. Tanaka, E. Senba, A. Miyajima, Y. Morikawa, Lack of oncostatin M receptor β leads to adipose tissue inflammation and insulin resistance by switching macrophage phenotype., *J. Biol. Chem.* **288**, 21861–75 (2013).

160. E. Kurmaeva, D. Bhattacharya, W. Goodman, S. Omenetti, A. Merendino, S. Berney, T. Pizarro, D. V Ostanin, Immunosuppressive monocytes: possible homeostatic mechanism to restrain chronic intestinal inflammation., *J. Leukoc. Biol.* **96**, 1–13 (2014).

161. K. Nishikawa, N. Seo, M. Torii, N. Ma, D. Muraoka, I. Tawara, M. Masuya, K. Tanaka, Y. Takei, H. Shiku, N. Katayama, T. Kato, Interleukin-17 induces an atypical M2-Like macrophage subpopulation that regulates intestinal inflammation, *PLoS One* **9** (2014), doi:10.1371/journal.pone.0108494.

162. A. Rostami, B. Ciric, Role of Th17 cells in the pathogenesis of CNS inflammatory demyelination, *J. Neurol. Sci.* **333**, 76–87 (2013).

163. J. M. Fletcher, S. J. Lalor, C. M. Sweeney, N. Tubridy, K. H. G. Mills, T cells in multiple sclerosis and experimental autoimmune encephalomyelitis*Clin. Exp. Immunol.* **162**, 1–11

(2010).
164. O. Leavy, T cells: Plastic TH17 cells., *Nat. Rev. Immunol.* **11**, 160 (2011).

6 Table of schemas

7 Table of figures

8 List of publications

Pascual-Reguant *et al*., T_H17 cells express ST2 and are controlled by the alarmin IL-33 in the small intestine. *Manuscript under revision*. ID# MI-16-006.